AFCRC-TN-60-426

IMPERIAL COLLEGE OF SCIENCE & TECHNOLOGY
LONDON
DEPARTMENT OF METEOROLOGY

RADAR ANALYSIS OF A HAILSTORM

by

K. A. Browning and F. H. Ludlam

TECHNICAL (SCIENTIFIC) NOTE No. 5
Contract No. AF 61 (052)—254

JULY 1960

The research reported in this document has been sponsored in part by the Geophysics Research Directorate, Air Force Cambridge Research Center of the AIR RESEARCH AND DEVELOPMENT COMMAND, UNITED STATES AIR FORCE, through its European Office.

RADAR ANALYSIS OF A HAILSTORM

by

K. A. Browning and F. H. Ludlam

CONTENTS

Abstract

Observations of a summer hailstorm which travelled across England from the SW were made with five radars and a dense network of ground observers. It is shown that in the intense phase of the storm, when 2-inch hailstones fell, the radar echoes persistently showed some features from which the pattern of the air flow in the storm can be deduced. According to the analysis the updraught was composed of air which entered the storm at low levels in a NE'ly current and left it at high levels in a SW'ly current. Strong wind shear caused the updraught to be tilted at an angle of about 45° to the horizontal. Precipitation from the updraught induced a downdraught in the region beneath it; air entered the rear of the storm in the middle troposphere, descended in the downdraught and left the storm near the ground as a NE'ly current. It is suggested that in the presence of wind shear the downdraught is essential for the maintenance of organised convection, and often also for its establishment when the instability is latent. The tilted intense updraught is favourable if not essential for the growth of large hailstones, for the small stones which are carried forward from the cloud tops descend and re enter the updraught at low levels; in this way some cloud particles can pass through the updraught twice or more, until they reach the largest size which it can support. The kind of organisation inferred for the hailstorm studied is regarded as representative of severe travelling storms; it is only less completely attained in many cumulonimbus and is responsible for the generally greater energy of precipitating clouds as opposed to ordinary cumulus.

1. Introduction

A severe storm travelled NE across S.E.England on 9 July, 1959, passing inland across the Dorset coast at about 1030 and reaching E.Anglia about 1500[1]. About noon it became intense and discharged hailstones of diameter up to about 2 inches. It was observed by radar from the Meteorological Office station at East Hill, near Dunstable. Five radars were used: two 3.5 cm RHI radars, one 4.7 cm PPI radar, and 10 cm PPI and RHI radars; their characteristics and mode of operation are given in Appendix 1.

Besides the radar and routine synoptic data, special pilot balloon soundings were made at 31 stations in England between 1400 and 1500, and three afternoon reconnaissances were made by the Meteorological Research Flight. About 1500 voluntary observers, mostly within 100 miles of East Hill, reported whether or not hail fell and about 100 gave rather detailed accounts of surface weather. A further 400 reports were obtained by interrogating people living in the storm path, and from 13 of these people samples of hailstones were collected for examination. From all this material a detailed, though still not fully comprehensive picture of the storm can be drawn. This report exposes the radar data and uses them to construct a dynamical model of the storm in its intense phase.

---

1 All times are in British Summer Time, one hour ahead of G.M.T.

2. General behaviour and intensity of the storms of 9 July 1959

Early on 8 July a cold front lay through the Irish Sea to just west of Portugal. It advanced slowly eastwards, and on the morning of the 9th extended from the central North Sea, across S.E.England and N.W.France into Spain. Figs.1(a and b) show that at mid day a cool NE'ly surface wind over S.E.England and N.W.France was replaced already at 5,000 ft by a S to SW current; this increased with height, and reached a speed of about 75 mi/hr at the 300 mb level (fig 1c) and a maximum speed of 80 mi/hr at 36-37,000 ft, the level of the tropopause.

The sferic observations of the British C.R.D.F. network show that during the 8th, thunderstorms spread from the west into the Bay of Biscay, and were again active there on the morning of the 9th (fig.2) The activity declined after 0900, but at 0800 a storm was located over the Brest peninsula, and in contrast to the previous storm groups this seemed to travel rather rapidly N and then NE across the English Channel, being plotted at 0900 and 1000 as compact clusters of sferic fixes. At 0830 an air observer over Bristol saw developing cumulonimbus tops reaching 32,000 ft south of the Dorset coast, with anvil tops to 40,000 ft farther southwest, and at 0920 the storm was observed as an intense echo about 60 miles SW of Hurn airport radar, directly on the path shown by the sferics (fig.2) Fig 3 shows its progress across England after 1030, as seen on the East Hill 10 cm PPI display.

The echo mass[1] of this main storm (1) was followed by another (2); subsequently the development of echoes which formed between them led to the merging of these echo masses At 1200 some sferics were located over the

---

1 Echo nomenclature is specified in Appendix 2.

Channel near the Isle of Wight, and soon afterwards a cluster of small echoes (3) appeared in the south of the display. At 1430 (after a power failure had interrupted the radar observations) they and similar groups (4,5) lay in a belt extending southward from the main storm, while two others (6,7) had appeared to the NW of East Hill. Judging by the sferics observations, some thundery activity persisted during the afternoon near the W coast of France, (intensifying off shore in the evening) and also near the NE coast of France, but after 1530 the storms over England began to die out. A member of the group 4 became a more severe thunderstorm for a while after 1600; the sferics at this time (fig. 2) located it accurately over the sea near the coast of E. Anglia Between 1700 and 1800 there was a severe storm on the Dutch coast, but by then all the echoes over England had disappeared.

As might have been expected from the times and places of formation of the storms, they were not directly dependent upon solar heating of the ground Over England the air in the lowest 4,000 ft was stably stratified (fig 1e), while on the neighbouring Continent only in the extreme NE of France was the ground heating sufficient to produce cumulus clouds All the storms appeared in areas where there were extensive altocumulus, and evidently originated as showers from cumuliform developments in these medium level clouds

Throughout the day measurements of echo intensity were made at all three wavelengths. On the 3.3 cm and 4.7 cm radars attention was concentrated on the main storm, and so the evolution in the intensity of the other storms has been derived from the 10 cm PPI records, which include frequent series of photographs in which the gain was reduced in a series of steps Corrections for incomplete filling of the beam were made; these are detailed in Appendix 3 Unfortunately this radar was liable to drift off tune and was less readily set

to a standard brightness, so that the further adjustments specified in Appendix 4 were made to ensure that the measurements were consistent with those of the other, more strictly controlled radars. The final values are displayed in fig.4 in the manner previously recommended[1]. The figure in each 10 km square represents the greatest echo intensity present over any area of at least 4 km^2, according to the code of Table 1. This table includes the

Table 1. Code for maximum echo intensity, expressed as equivalent Z (mm^6/m^3), and probable associated rainfall rate R, hail size H (at the ground) and frequency F of lightning discharges.

Code figure	10 log Z	F no/hr	R mm/hr	H
0	< 25		< 1	slight rain, drizzle
1	26 - 35		1 - 5	moderate rain; slight shower
2	36 - 45		5 - 20	heavy rain; moderate shower
3	46 - 50	1 - 5	20 - 40	heavy shower
4	51 - 55	5 - 20	40 - 100	thunder shower
5	56 - 60	20 - 100	100 - 200	thunderstorm
6	61 - 65	100 - 500	> 200	hailstorm (max. stone diameter < $\frac{3}{4}$")
7	66 - 70	500 - 1500	> 200	large hail (diameter $\frac{3}{4}$" - $1\frac{1}{2}$")
8	71 - 75	1500 - 3000	> 200	giant hail ($1\frac{5}{8}$" - $2\frac{1}{2}$"); tornado
9	> 76	> 3000	> 200	giant hail (> $2\frac{1}{2}$"); tornado

1 See Tech. Note No.3 under the present contract, "The role of radar in rainstorm forecasting".

probable rate of rainfall and lightning discharge, and the probable hail size at the ground, to be associated with the given echo intensities[1].

Fig. 5 shows the trend with time of the maximum intensity in each of the storms; the individual measurements have smoothed curves drawn through them, which are dotted during periods when the storms were over the sea. There are some interesting features; in particular

(i) storm 1 was the most persistently intense as well as the largest storm;

(ii) there is no obvious relation between intensity and location over sea or land;

(iii) while over the Channel storm 2 was as intense as storm 1 ahead of it but subsequently it weakened greatly while the other was intensifying;

(iv) after 1530 all the storms declined, with the notable exception of storm 4, whose intensification was also indicated by the sferics observations (fig. 2);

(v) the storms of groups 3, 5, 6 and 7, and storm 2 while overland, had intensities which usually were too low to be associated with the occurrence of thunder. By comparison storms 1 and 4 became very severe.

From the ground observations, mostly from the network of about 1500 volunteers, it appears that only storm 1 produced significant hail inland. Storm 2 also traversed the area which experienced hail, but in view of its comparatively low intensity it is unlikely to have discharged any hail.

---

1 See Tech. Note No. 3 under the present contract, "The role of radar in rainstorm forecasting".

The isopleths of maximum hail size at the ground (fig. 6, a and b), which indicate size according to the code of Table 2, can therefore be associated with the passage of the main storm. Figs. 6a and b include the path of the right-hand edge of the 10 cm PPI full gain echo of this storm; it has a number of bulges due to the intermittent formation of new echoes on this flank. The large hail occurred in a rather narrow strip near this path (within 3 - 8 miles), and both the path and the strip are very nearly straight over the whole distance of about 200 miles between the south and east coasts. Near the south coast the direction of the path was approximately from 220°, whereas the upper winds (fig. 10) were from between 190 and 200° at Larkhill, and from between 200 and 210° at Crawley on the other side of the path: over this part the motion of the storm was about 20° to the right of the upper winds. Near the east coast the storm was weakening, and the direction of its path (from about 230°) was more nearly that of the upper winds (210 to 220° at Hemsby), but the deviation still amounted to more than 10°. This behaviour is typical of severe storms (Newton, 1960).

Table 2. Scale of hailstone size

Code figure	Diameter in inches			Description
0	-			No hail
1		$\frac{1}{4}$	Hail	Grain; small pea
2	$\frac{1}{4}$	$\frac{3}{8}$	Hail	Pea
3	$\frac{3}{8}$	$\frac{1}{2}$	Hail	Mothball, small marble
4	$\frac{1}{2}$	$\frac{3}{4}$	Hail	Cherry, marble
5	$\frac{3}{4}$	1	Large hail	Large marble
6	1	$1\frac{1}{4}$	Large hail	Walnut
7	$1\frac{1}{4}$	$1\frac{5}{8}$	Large hail	Golf ball
8	$1\frac{5}{8}$	2	Giant hail	Small egg
9	2	$2\frac{1}{2}$	Giant hail	Egg
10	$2\frac{1}{2}$	3	Giant hail	Tennis ball

Fig.7 shows the smoothed pattern of the total rainfall, in the 24 hours beginning at 1000 on 9 July, over the track of the main storm and in a surrounding area. Other storms made an unknown but probably unimportant contribution. The reports of rainfall are more sparse than those of hail size, but it is clear that most places in the path of the intense part of the storm received between $\frac{1}{4}$ and $\frac{3}{4}$ in of rain. This is only about one quarter of the fall in the similar but more severe Horsham storm in S.E.England on 5 September, 1958 (Ludlam and Macklin, 1959); on that occasion the speed of travel was less (about 25 mi/hr compared with 40 mi/hr), and the direction of motion veered by as much as 30-40° from the observed winds.

Fig.6a shows that 1-inch hail (size 6) occurred just inland of the south coast; it appears that this fell from an echo at the rear of the cluster which then composed storm 1; its maximum echo height was 40,000 ft and the maximum intensity was [63][1]. Afterwards this particular echo decayed remarkably quickly; during a period of 10 minutes its leading edge remained stationary, while the rear continued to advance until the echo disappeared. Almost certainly the cloud producing this echo had previously discharged hail over the sea, since hail of size 5 was reported only 1 mile from the coast (at the habitation nearest to the coast in this vicinity).

While this echo was decaying others within the cluster but a few miles farther east were moving inland; subsequently fresh echoes formed on their flanks in a manner discussed in detail later. These intensified as they moved farther inland and came within range of the 3.3 cm radars. In contrast, the

---

1 Echo intensity is written as 10 log Z_e, where Z_e is the equivalent radar reflectivity in mm^6/m^3; the figures are given alone, in ordinary brackets, or in square brackets, according as they are obtained from the 3.3 cm, 4.7 cm or 10 cm radar, respectively.

echoes composing storm 2 became weak overland. Over the sea at extreme range the main echo of this storm had a high intensity, and a motion from 209°, as shown in fig. 13. As the storm came inland a number of new echoes formed, aligned approximately at a right angle to their motion, which was from about 190°, the wind direction in the medium levels. The most intense echoes occurred near the right-hand end of the line, but none had an intensity within an order of magnitude of that of the first echo. Their motion confirms the wind direction in this region, and shows that the previous intense echo had moved noticeably to the right of this direction, although not so markedly as was found for the main storm in its intense phase.

The paths of the individual echoes of storm 3 show that they formed and dissipated in an unsystematic manner near the south coast. The early history of the later storms (4 - 7) is unknown, because they formed during the power failure.

3. The intensification of the main storm

The intensification of the main storm is illustrated by figs. 8, 11a and 11b, which contain radar data mainly from the 3.3 cm sets. These were operated manually, one to locate and follow the tops of individual echo columns (with the aim of measuring their rates of rise), and the other to locate and measure the maximum echo intensities by reducing the gain until the echoes almost faded from the display. Fig. 8 shows where intensities exceeding 65 and 70 were found, and where column tops were observed above 40,000 and 43,000 ft (when a top above 40,000 ft was followed for some time, only the position at which it reached its peak height is plotted). Because the sets were not operated systematically the monitoring of the storm was not perfect; nevertheless the diagram shows that it reached its greatest intensity, with tops above 43,000 ft, over a rather broad front (about 8 miles across) at ranges between 55 and 40 miles, where the largest hailstones fell. Afterwards the storm weakened some what and the hail size diminished, apart from a temporary intensification about 20 miles east of the radars which was associated with another increase in hail stone size.

Figs. 11a and 11b show the trends in the intensity and height of the strongest echoes, in the maximum echo height, and in the maximum hailstone size. In the first the intensity of the storm core is plotted against time; at any given time the observations from the several radars refer to the same part of the storm core, and the intensity measurements have been adjusted for beam width effects (Appendix 3) so that they can properly be compared. The figure contains an approximate range scale, by which the maximum hailstone size at the ground can be included. It can be seen that during the fall of the large hail there was a noticeable increase, on all the radars, of the

peak heights and intensities of the echoes. Fig. 11b shows that there was also an increase in the heights at which the maximum intensities were observed, to about 25,000 ft at the time of the largest hail[1]. After 1220 there was a sudden decrease in the height of the peak intensities and of the echo tops; this was closely followed by a prolonged fall of large hail in the Wokingham area, after which the maximum hail size decreased.

The general structure of the storm at 1200 is shown in fig. 12 by contours of the height of the full-gain echo base, obtained from a series of 13 3.3 cm RHI sections. It is clear that hail reached the ground over an area (deduced from surface observations) which was only a small part of that covered by the echo mass. Most of the echo came from the cumulonimbus anvil, and was not seen on the 10 cm PPI display at short ranges, since there it lay above the beam.

The detailed structure of the radar echoes during the most intense phase of the storm will be examined later with the aim of deducing the kind of air motion inside it.

---

1 The maximum intensity and the height at which it occurred have values similar to those of echoes accompanied by tornadoes in the U.S.A. We have no definite evidence of a tornado in this storm, although five eye-witnesses reported 'whirlwinds', and some characteristic damage (trunk-snapping and twisting) to individual trees was found.

4. The row structure of the main storm echo

The echo mass of the main storm appeared to be built of several parallel rows of columns. These were most apparent in the afternoon when the storm was receding, but following a description based on the records from this period, it will be shown that the same structure could be traced in the morning, before the most intense phase.

Fig. 14(a) has been drawn from a series of 10 cm PPI photographs taken between 1422 and 1516. Five or six intensity contours are available, but for clarity only one is shown on each diagram. The full gain PPI pictures taken regularly at 3-minute intervals show that throughout this period initially separate echoes formed intermittently a mile or two to the right of and behind the main echo mass. Once a new echo disappeared while remaining separate, but otherwise the new echoes moved towards 040°, lengthened in this direction, broadened and merged with the main echo After the amalgamation their position in the echo mass can be inferred from indentations in the several intensity contours: they can be traced for some time, as indicated in the figure. Consequently, the echo mass can be regarded as a composition of several parallel rows. This view can hardly be justified solely on the basis of the single intensity contour shown in the figure, but is clearer when several contours are examined, as demonstrated in fig. 14(b), which contains four contours for 1458. It is strongly supported by the disposition of the consecutive positions of each particular row along a straight line towards 040°, as shown in fig. 14(c).[1] The formation of new echoes at the right flank of the storm, and their eventual decay on the left flank, is shown schemati-

---

1 The behaviour of the shaded row is complicated by amalgamation with a smaller echo which it overtakes.

cally in fig. 15; it causes the movement of the echo mass as a whole to the right of the winds, which has already been noted. A similar process can be inferred where this deviation is evident, even though the resolution of the radar is too poor to distinguish the freshly formed parts of the echo, as in the instance of the intense echo in the early history of storm 2.

The development of a row by the elongation of an originally small echo is attributed to two processes: first, the formation and spreading forward of an anvil 'cloud'[1] from an echo column, and secondly, the formation of new columns at the rear of the echo, (evidence for this process is given in the next section). If there is a considerable change of wind direction with height then the separation of any rows which have been formed is likely to become blurred beyond recognition. The wind sounding made at Hemsby (fig 10) is probably representative of the environment of the storm during the afternoon; it shows that from near the ground to 35,000 ft the wind direction was almost constant (the directions determined over 1 minute intervals varied irregularly by up to 7° on either side of the average of 214°, in reasonable agreement with the row orientation of 220-040°). This approximate uniformity is probably responsible for the readiness with which the row structure can be detected at this time. On the other hand the soundings made at Crawley and Larkhill are likely to be more representative of the winds around the storm in the morning; on them the winds at medium levels are backed by as much as 20° from those in the high troposphere, and this may be the reason why the row structure is more difficult to discern when the storm was near the south coast.

---

1 The particles of an anvil cloud decrease in size towards its tip and upper surface, but at moderate ranges are mostly sufficiently large to produce a detectable radar echo.

Nevertheless, row formation can be detected in the period 1110 to 1145, before the storm reached its peak intensity. This is illustrated in fig. 16a, where, again for clarity, only the full-gain contours are drawn, although in the analysis several gain contours were used. The echo structure deduced is supported by the 3.3 cm RHI observations discussed in the next section, for with the narrow beams of these radars it was possible to recognise new rows of columns growing on the right flank of the echo mass. Furthermore, soon after 1220, for example, the structure typified by fig. 17 was evident in a series of 3.3 cm RHI sections in which the radar beams were directed obliquely across the leading edge of the echo mass, as shown in fig. 18, in order to examine the rise of columns in the most recently formed row on its right flank. It can be seen in fig. 17 that as the range increases the base of the echo descends in well-defined steps. Occasionally the steps were distinctly separated by spaces, evidently corresponding to the rows and gaps between them. From 13 such RHI sections it was possible to obtain the paths of several rows having a width and orientation (fig. 19) closely resembling that deduced for the earlier period (fig. 16a).

It is striking that in the period 1147 to 1220, when the storm attained its peak intensity, it was not possible to distinguish a row structure in the echo mass. This could have been due partly to an increased change of wind direction with height immediately in front of the storm[1], leading to a greater merging of the rows of echo, particularly in the broad vertical beam of the 10 cm PPI radar. At the same time, however, there was established a more uniform organisation over a front of several miles, in which the air motion

---

1 As indicated by the sounding at Silwood, made just before the onset of the storm (fig. 10).

and the echo structure was in virtually a steady state, at least in so far as could be seen with radars with the present powers of resolution. In this phase the precipitation was suspended aloft long enough to be displaced well across the front of the storm and obliterate the previous row structure.

The new organisation is discussed in section 6, after the description in the following section of the behaviour of the echoes in the rows recognised before its establishment.

5. The behaviour of echoes in individual rows

It was not possible to find a row structure in the PPI observation of the storm at 1109 (fig. 16a), when the echo mass was an amalgamation of a cluster of echoes which earlier had crossed the coast, but by 1124 two rows (A and B) had formed on the right flank, and at 1133 a third (C) was appearing.

Fig. 20 shows the range of the rear and leading edges of the echo of row A as a function of time, determined from the full gain 10 cm PPI photographs taken at 3 minute intervals. It indicates that the row was developed by the appearance of 8 echoes successively during a 25-minute period within a strip 5 miles long, strongly suggesting the triggering of convection (in the medium levels[1]) by a ground feature some 10 to 20 miles upwind, in this case probably the coast line. Accordingly, most of the columns appeared at the rear of the row. The first three were short lived, but others persisted to produce a row which was 13 miles long by 1130.

At this time the axis of the rows lay along the beams of the RHI radars, so that they displayed sections along the whole length of the rows. It is interesting to compare that given by the 10 cm RHI set at 1130 (fig. 16b) with the 10 cm PPI picture for 1133 (fig. 16a), which shows that this particular row had been extended rearwards more than its neighbours by the formation of new columns. Accordingly, even though the beam of the RHI set is very broad horizontally at this range, we can be confident that the succession of columns which it shows at the rear of the echo mass, with tops lowering rearward, are actually those inferred to exist in the row from the PPI records (fig. 20). During the subsequent 10 minutes (1130 to 1140) the rear edge of row A advanced

---

1 Since the stability of the lowest layers precluded the formation of large clouds by convection from the ground.

steadily at 50 mi/hr (fig 20), indicating that no new columns formed at the rear during this period The history of this row is continued in fig 21, a series of 3 3 cm RHI photographs Two particular column tops, marked T_1 and T_2, can be followed throughout this series, and can be seen to move through the row, demonstrating it to have consisted of columns which grew at the rear, reached a peak development in the middle, and eventually emerged at the front as decaying, tilted columns of particles falling freely since they were no longer in an updraught

The 3 3 cm radar beam was carefully centred on the top T_2 for several minutes From the pictures taken it is possible to make reasonable estimates of its rate of rise and horizontal speed, with the results which are shown in Fig 22 At first the rising speed was nearly 20 m/sec and the forward horizontal speed was less than 30 mi/hr, at a level where the representative wind in the environment had a speed of about 70 mi/hr (fig 23); a little previously, when the top rose through the level of strongest winds at about 35,000 ft the difference in speeds must have been about 60 mi/hr While the rising speed diminished rapidly as the top rose above the tropopause level at 37,000 ft it was accelerated forward by about 40 mi/hr in less than 3 minutes As the tower was sinking back again its forward speed appeared to be several mi/hr greater than that of the wind in the environment It seems possible that this was due to a divergent outflow from the column T_3 (fig 21) which rose about 3 mi to the rear[1] The high forward speed persisted in the echo

---

1 If the divergence was produced by the reduction of average rising speed from 20 m/sec to zero over the area of a cylinder 2 miles across between the levels 32,000 and 40,000 ft, the average speed of outflow 3 miles from the axis of the updraught would have been 5 mi/hr Divergence of this magnitude is also implied by the rate of increase of echo width at a particular level as an echo column rose through it, since the echoing particles at the edges of the column can be regarded as transported with only small fall speeds relative to the air Typically, the columns at the 30,000 ft level had a width of about 2 miles when the tops were at 36,000 ft If the rate of rise of the column top was 20 m/sec (4,000 ft/min) and the column had a circular cross-section, then an echo at the 30,000 ft level had a radius which increased at the rate 1 mi/1½ min while the column was rising The resulting divergence is such that 3 miles from the column axis the outward velocity would again have been about 5 mi/hr

at lower levels, but this may simply be because the particles were falling from the spreading tops at about 35,000 ft, so that this was their effective 'generating level'.

While row A was appearing, another (B) was forming in a similar way $2\frac{1}{2}$ mi to its right. Fig. 24 shows the range of the rear and leading edges of this row as a function of time. It suggests that it too was initiated by some topographical disturbance near the Hampshire coastline. The 3.3 cm RHI pictures of fig. 25 show the columns in this row, and include the tops of the columns in row A, which lay in the edge of the beam: the lower parts of these columns do not appear, their particles having been carried sideways out of the beam by the cross-wind. Fig. 26 shows RHI sections of the next row (C), which formed $2\frac{1}{2}$ mi to the right of row B; again the highest tops faintly shown on the pictures are the more strongly developed columns of the previous row (B) which lay in the edge of the beam.

6. The radar echo of the storm in the intense phase

a) The distribution of echo intensity

The marked change in the structure of the echo mass occurred between 1145 and 1150; it became impossible to discern a row structure, and the rear edges of the echo in the positions where previously rows A and B had been identified now advanced steadily at a noticeably reduced speed (figs. 20, 24). At the same time a distinctive structure became apparent on the 3.3 cm RHI sections. Whereas formerly there were growing columns at the rears of the rows (fig. 16b, and first five photographs of fig. 21, in respect of row A; first four photographs of fig. 25, in respect of row B), now the tallest, most intense column was found at the rear of the echo (last photographs of figs. 21 and 25). It also became difficult for the operator to find rising tops, although the maximum echo heights increased steadily, and reached a peak value of 45,000 ft at 1159 (figs. 11a and 29).

The interpretation of the storm structure is greatly assisted by the systematic survey of the distribution of echo intensity which was made with the 4.7 cm radar. Photographs were taken of the PPI display at different gain settings on a succession of elevations. The entire storm could be examined once in this way in 12 minutes. This period is normally much too long for a successful reconstruction of an instantaneous 3 dimensional model, but during this intense phase of the storm all the radar records show that there was no very marked variation in the echo characteristics, and that the echo mass moved with a uniform velocity of 210° 40 mi/hr. Consequently although in each scanning cycle the top of the storm was examined as much as 12 minutes later than its base, it has been possible to construct representative instantaneous vertical sections by displacing the almost horizontal

sections according to this velocity[1].

Figs. 27(a)-(c) show these sections, which represent the storm in the three periods 1137-1149 (during the development of the new organisation), 1156-1208, and 1213-1225. Their general appearance is similar to the instantaneous 3.3 cm RHI displays, typical examples of which are given in fig. 29. From the same data vertical sections can be made across the direction of motion of the storm; these have been used to construct figs. 28(a)-(c), which clearly show the tendency for the precipitation carried forward of the storm to fall towards its left flank (right of diagrams).

b) The 'wall'

A striking feature of the storm in this phase was that in its right-hand and central parts the leading precipitation which approached the ground formed a 'wall' which had a sharply defined and upright front face, orientated perpendicularly to the direction of movement of the storm. It became as long as 7 miles at 1158 (figs. 28b and 28d), and extended above 13,000 ft over much of its length. The wall was first observed at a range of nearly 61 miles (RHI section for 1146.50 in fig. 21) and it is significant that the width of the hail swath suddenly increased twofold at 60 miles range (fig 6b and fig. 34). Its rate of advance after its appearance is indicated on figs. 20 and 24, from which it is clear that it lay at greater ranges than the leading edge of the echo mass as shown on the 10 cm PPI display. This is because the broad vertical beam of this radar included nearer echoes at higher levels. The steadiness of

---

1 In future studies of convective storms it would be better to make the scanning cycle with an RHI display; on the present radar this was not preferred because it involved restricting the survey to a small sector of the sky.

the echo structure during the intense phase of the storm is illustrated in fig. 32, which shows that the wall advanced uniformly at 40 mi/hr, and that the highest top was always located at a range within $1\frac{1}{2}$ miles of that of the wall. Before the wall had formed (at 1147) an individual top (such as T_1, T_2, or T_3 in fig. 21) could be identified as the highest for about 10 minutes before it was succeeded by another in a position up to 5 miles to the rear; this behaviour caused the spread in the ranges of the highest tops which is shown in the lower part of fig. 32. The sudden change in behaviour is clear evidence for the transition from the previous intermittent updraughts to one persistent updraught. Accordingly, after the transition there were hardly any rising columns to be found by the radar operator briefed to locate and follow them[1]. Small echo turrets occasionally penetrated a few thousand feet above the top of the main echo mass, indicating that the continuous updraught was not quite steady, at least at high levels a fact reflected in the somewhat irregular distribution of the largest hail at the ground during the intense phase of the storm.

Figs. 27(b) and (c) show that an echo intensity of (50) was attained practically at the edge of the wall, and this is confirmed by the 3.3 cm intensity contours in fig. 30b. Further confirmation is supplied by the full gain 3.3 cm RHI pictures (fig. 29) which illustrate the echo extending farthest below the radar horizon very near the leading edge, showing that the most intense echo was also in this position[2].

---

1 Cunningham (1960) has described the appearance of a 'self-propagating' hailstorm, with splendid pictures which graphically portray the kind of structure which will be deduced from our data; in particular he notes that there were no distinct individual turrets at the storm top, 'suggesting that it was characterised by a large region of fairly continuous upward velocity'.

2 Echo displayed at elevations between 0^0 and the radar horizon at $1\frac{1}{4}^0$ is a side-lobe effect. The first side-lobe of the 3.3 cm radar lies 1.1^0 from the beam axis; consequently the distance which the echo extends below the radar horizon is a measure of the echo intensity just above the horizon.

In the path of this part of the storm the first precipitation was large hail; typically it fell alone or with hardly any rain for several minutes before giving way to a similar period of heavy rain. This is shown by the observations listed in Appendix 5 and figs. 33, 34 and 35. Fig. 33 shows that the time of onset of the hail at the ground was within 3 minutes of the time of arrival of the wall at about 8,000 ft, as determined from the radar records. Fig. 34 contains echo intensity contours at heights around 14,000 ft at the three times 1141 (before the appearance of an extensive wall), 1158 and 1218, and the locations of the observations given in Appendix 5. At 1158 the position of the wall was along the rear side of the deep notch which enters the outline of the echo from the right, approximately along the line OQ. The path of the left end of the wall is drawn, and lies from south of O to near H; the largest hail fell near this line (fig. 37c). To the left of the wall precipitation reached the ground several miles ahead of it, and characteristically began as rain which intensified and later fell with hail; far to the left and on the extreme right of the storm there was only rain. Fig. 35 is a graphical representation of observations which illustrate these sequences and also shows that about 10 minutes before the arrival of the large hail there was a squall in which the NE'ly winds were replaced by a SW wind flowing out of the storm. A dark arch cloud heralding the storm passed over at about the time of the squall at the ground.

c) The forward overhang and echo-free vault

Another feature of the radar echo was the 'forward overhang', echo which reached down to about 12,000 ft along the length of the wall and one to three or more miles ahead of it. Nearer to the wall the base of the overhang rose,

forming the 'echo-free vault' whose ceiling extended upwards to nearly 15,000 ft close to the wall (the conventional RHI display gives a poor impression of the horizontal extent of such a feature). It too extended several miles across the storm; on PPI presentations which intersect the storm at heights between 12,000 and 15,000 ft the echo free vault appears as the echo-free wedge or notch which has already been pointed out in fig. 34, of which a part is reproduced separately in fig. 28d to show it more clearly.

d) The interpretation of the echo intensity distribution

Fig. 30b shows the intensity contours for 18 and 53, determined by the 3.3 cm radar at 1203, superimposed upon contours determined at about the same time by the 4 7 cm radar, extracted from fig 27b. The structure shown is regarded as characteristic of the storm in its intense phase.

Its implications have been discussed in detail by Atlas and Ludlam (1960). They show that the similarity and absolute intensity of the strongest echo at all three wavelengths (about 69 at 1203, after tentative corrections for attenuation) indicate that large hail, in a narrow size range about a diameter of 4.6 cm and in a concentration of about 6 8 g/m^3, was predominantly responsible for the echo. This estimate of hail size is supported by the maximum diameter (5cm) of the stones observed at the ground at this time (fig 11a). Hail of this size was observed over areas only about 1 km across, and evidently the excessive attenuation which it would cause (10 db/km at 4.7 cm) precludes its extent in the cloud being much greater. On the other hand an echo intensity of (58) occurred over a range interval of several miles, and if due to hail in a broader range of sizes up to a diameter of 2 to 3 cm implies an attenuation of 1 to 2 db/km,

or a total of about 15 db through the whole storm. This estimate is supported by the intensity recorded for the following storm (2), which appears to be about 15 db too low when the 4.7 cm observations are compared with those at 10 cm, which are subject to negligible attenuation. Accordingly we suppose that the contour for the intensity (58), and hail of diameter up to 2.3 cm, actually extended towards the rear of the storm at levels between about 20,000 and 30,000 ft so as to lie between those drawn on fig. 30b for (38) and (49).

The decrease of intensity downwards below the most intense echo is attributed by Atlas and Ludlam to the combined effects of wetting and decrease of concentration (due to falling out of a strong updraught) of the large hailstones, and possibly also to the destruction of numbers of them by thunder. On the 3.3 cm RHI sections (fig. 30b, for example) a secondary echo intensity maximum appears below the 0°C level at about 1 mile behind the wall; this is thought to be produced by the wetting of small hail, of diameters up to about 1 cm, which began to arrive at the ground several minutes after the onset of the large hail. This echo maximum has an intensity of about 60 at 3.3 cm, corresponding to hail of diameters 0.5 to 1 cm in concentrations of 1 to 3 g/m^3. Hail in this size range may melt completely before reaching the ground, and can thus produce rainfall at a rate of 35 to 150 mm/hr, which in a zone 5 miles across travelling at a rate of 40 mi/hr implies a total fall of 1/5 to 3/4 inch. This corresponds well to the reported amounts of around 1/2 inch which occurred in less than 15 minutes (fig. 7). The attenuation of the 3.3 cm beam in such rainfall is severe, amounting to 2 to 9 db/km, and causes a marked tapering downwards of the echo intensity contours below the 0°C level. This is also a feature of the sections made with the 4.7 cm radar,

on which the attenuation is only about half as great; in contrast the rear edge of the echo mass at 10 cm is vertical until it meets the radar horizon (fig.31). A few timed observations by volunteers show that the rain ceased 1 - 2 miles behind the rear edge of the echo shown on the 10 cm PPI, presumably because below the radar horizon the rain was displaced by the winds diverging from the rear of the storm.

7. The dynamical structure of the storm in the intense phase

a) The form of the updraught

On this day we have seen that echoes formed over the sea as well as over the land, and that they were not produced by cumulus convection beginning at the ground, since in the lowest few thousand feet the air was stably stratified (fig. 1e). Rather, the echoes formed at places within an altocumulus system, probably chiefly where topographical disturbances stimulated convective growths. Subsequently the precipitation into the unsaturated lower layers seems to have produced a cool downdraught which allowed the convective clouds to gain access to a layer between about 3,000 and 7,000 ft in which there was a rather high wet bulb potential temperature (fig. 1e). The downdraught can be regarded as producing a circulation in the lower layers or as acting as a scoop there to lift this potentially warm air to about 9,000 ft, above which level it began to acquire an excess temperature. Its upward motion would then continue under a buoyancy which could reach a value much exceeding any which had previously been associated with convection beginning in the medium levels. In this way precipitation from cumuliform developments in the altocumulus system could stimulate the production of vigorous cumulo nimbus.

The updraught can be expected to have originated near the ground above the cold downdraught, which we have seen was encountered at the surface several miles ahead of the precipitation wall; condensation in it produced the arch cloud which heralded the storm. The strongest updraught can be expected to have passed through the heart of the storm, where the maximum echo intensity and hailstones of diameter about 5 cm occurred. In theory (Ludlam, 1958) the fall speeds of large hailstones are unlikely to exceed by more than 20 to 30% the speeds of the updraughts in which they are grown.

At 25,000 ft the fall speed of a spherical stone of drag coefficient 0.6 (Macklin and Ludlam, 1960), density 0.9 g/cm^3 and diameter 5 cm is about 45 m/sec. Accordingly 35 m/sec is a reasonable estimate of the maximum updraught speed[1]. It is likely to have been attained over a region not more than about 1 mile across in the direction of advance of the storm, since the large hail probably had only about this extent (section 6(d)). On the other hand a less strong updraught must have extended at least 5 miles farther to the rear, because between 20,000 and 30,000 ft echo is found over the whole of this distance (fig. 30b). This is still likely to have been a part of the same continuous updraught which rose ahead of the wall, because the rear of the full gain 10 cm PPI echo due to it travelled very uniformly at a speed close to that of the wall (figs. 20 and 24).

Above 25,000 ft the echo intensity diminished and the updraught must have decelerated, rapidly where it passed above the level of the tropopause at 37,000 ft. The updraught must then have been almost upright, since the highest echo tops were found almost vertically above the region of maximum echo intensity (fig. 30b). These considerations roughly fix the form of the updraught and its maximum speed: it was strongly inclined in the lower troposphere and more nearly upright in the high troposphere.

On its path from near the ground well ahead of the storm to the region of strongest echo it passed through the base of the forward overhang. Here the pattern and intensity of the echo allow us to estimate the updraught speed. The particles present in the anvil 'cloud' and the forward overhang

---

1 The maximum observed rate of rise of an isolated echo column top was the 20 m/sec already mentioned in the discussion of the top T_2 (section 5). If such a top is associated with a large cloud tower having a circulation like that of a thermal, the rising speed of the air over a substantial part of its interior is likely to have reached 40 m/sec (Ludlam, 1958). In the intense phase of the storm, however, when the updraught was steadier, its structure was no longer like that of a thermal.

were carried forward from the region of strong updraught not having attained a size and fall speed which would allow them to descend through it As the air of the updraught lost its rising speed and took up the speed of the environment winds at these levels the particles poured from it, falling into the region ahead of the strong updraught The smaller particles, with fall speeds less than 1 m/sec, were carried far forward as the spreading anvil cloud Progressively larger particles, with greater fall speeds, were encountered nearer the updraught, and it was these which composed the forward overhang. As the particles descended they approached the forward part of the updraught where it was strongly inclined beneath them, and at some level between about 15,000 and 10,000 ft they re entered the updraught

In figs. 27(b)(and 30b) the intensity contours (29) and (49) in the forward overhang at these levels turn upwards towards the echo wall evidently the updraught sweeps up the particles and carries them towards the heart of the storm once more At the tip of the contours the updraught speed must have been at least equal to the fall speed of the largest particles which were present and this can be estimated in the following ways

First, neglecting the size sorting during the fall of the particles from high levels into the base of the overhang, we can assume that they had a size distribution similar to that found by Jones (1960) for the ice particles in the dense anvil clouds of the tropics

$$N_D = 10^3/D^3$$

where $N_D \delta D$ is the concentration (no/m^3) of particles with diameters between D and D + δ D mm Assuming that they behaved like dry spheres of ice, that D/λ was small and therefore that the scattering was in the Rayleigh regime,

$$Z_e = 0.21 \Sigma ND^6$$
$$= 0.21 \int_{D_o}^{D_1} 10^3 D^3 dD$$
$$\approx 50 D_1^4$$

where D_1 is the diameter of the largest particles present. Accordingly this diameter is 2.0 and 6.3 mm where 10 log Z_e is (29) and (49) respectively. Assuming a drag coefficient of 0.6 (Macklin and Ludlam, 1960) and a mean density of 0.8 g/cm^3, the corresponding fall speeds at the base of the overhang (about 12,000 ft) are 6.5 and 11.5 m/sec.

Because the dominant contribution to the echo was made by the largest particles, the estimate of their size is not much affected by the particular form assumed for the spectrum; for example, if it is alternatively assumed that the echo of intensity (49) was produced by particles of uniform size present in a concentration of 1 g/m^3, their diameter is again found to be about 6 mm.

However, on entering the updraught near the 0°C level and presumably renewing their growth, it is possible that particles of about this size quickly became so wetted that their radar cross sections increased to the values appropriate to water spheres (Atlas and others, 1960). The diameter of the largest particles where the intensity reached (49) then decreases to about 4 mm, but the fall speed (assuming now a mean density of 0.9 g/cm^3), is reduced only to about 10 m/sec.

Consequently we can rather confidently infer that in the neighbourhood of the base of the overhang, at about 12,000 ft, particles of diameter up to about 6 mm re entered the updraught, and that here it had already an upward speed of at least 10 m/sec. That this was not an intermittent updraught has already been established (section 6(b) and fig. 32): it is confirmed by the

persistence of the overhang with its base always above 12,000 ft, as shown by fig 36. Here the lowest extent of the (28) intensity contour within the over hang at 1158 and 1218 is plotted as a function of distance across the storm from the intersection with the azimuth marker for 210° [1]. The overhang contained particles with fall speeds of up to about 10 m/sec (2000ft/min) but it nowhere lowered by as much as 5,000 ft during the whole period of 20 minutes (the maximum cross wind was about 17 mi/hr between 5,000 ft and 8,000 ft (fig 9b); in the absence of an updraught one of about 80 mi/hr would have been needed if the particles were to have moved downward and to the left along the slope of the intensity contours in fig 36). The position and extent of the overhang are also important in showing the unusually great horizontal dimensions of the updraught in the middle levels: two miles or more from front to back and several miles across the line of advance of the storm.

b) The rain area and the downdraught

Figures 28(a)-(c) show that the instantaneous echo intensity contours slope downwards to the left of the storm (the right of the diagrams) in the same way as the tip of the overhang. In figures 28 (b and c) the wall can be seen on the right hand side of the storm at the farthest indicated ranges, with the overhang above and ahead of it. On the left of the storm there was neither wall nor overhang, the contour intensity (29) sloping directly downwards and reaching the ground up to six or seven miles ahead of the wall (figs 27b and c). Since the diameter of the largest ice particles where the echo has this intensity is only about 2 mm, it is to be anticipated that on

---

1 During this period the storm advanced with the practically uniform velocity of 40 mi/hr from about 210°.

this flank of the storm the first precipitation to reach the ground was rain. Only 2 miles nearer the plane of the wall the echo intensity at a beam width above the radar horizon exceeded (50), and small hail was thus to be expected with the rain at the ground. The duration of the precipitation (and hail) on this side of the storm was in fact often double that on the other flank (fig. 37a).

In the central parts of the storm, where the strongest updraughts occurred and the tops were highest, small particles of fall speed up to several m/sec (echo intensity about (29)) were not released until the updraught had been greatly decelerated at levels as high as 40,000 ft (see, for example, the height of the tops on azimuth 209° in fig. 27b). In falling from this height, where the wind relative to the storm was over 40 mi/hr (fig 9a), down to about 20,000 ft, where the relative wind was nearly zero, it is reasonable to assume that the largest particles were subjected to an average relative wind of 20 mi/hr. Their fall speeds have already been deduced as about 6 5 m/sec (20 ft/sec); the period of fall was thus about 1000 sec and the forward displacement about 5 miles. The mean cross wind was only about 8 mi/hr (fig. 9b) but this was sufficient to displace the particles sideways by about 2 miles, that is, to increase their azimuth at a range of 50 miles by a little over 2°. Consequently, on the section along the azimuth 211° in fig 27(b) the intensity contour (29) at 20,000 ft is found at a range of 45 mi, about 5 mi ahead of its leading edge at 40,000 ft on the azimuth 209°. Below 20,000 ft this intensity contour slopes inwards towards the storm, since here the particles encountered relative winds in that direction; also the cross wind increased, its mean from 20,000 ft to the ground being about 17 mi/hr (fig 9b). Consequently particles found at about 20,000 ft on the intensity contour (29)

and the azimuth 211° reached the radar horizon on azimuths of 213° and higher, and well ahead of the wall. The manner in which the fall-out from the highest towers arrived at low levels ahead of and to the left of the wall is further illustrated in fig. 28d. Particles released from the lower tops farther to the right were carried a smaller distance ahead with the result that they were prevented from reaching the ground by the updraught; it was these that comprised the overhang.

The descent and partial evaporation of precipitation into the rather dry air in the medium levels generates a downdraught which spreads out from the precipitation area near the ground. Although the main downdraught can be expected in the region of intense rain behind the wall, it must be considered that the chute of small hail and rain which descended from high levels to the ground some distance ahead of and to the left of the wall may not have been much less efficient in generating a downdraught, since although the concentration of fall out water may be less, the evaporation is more rapid when it is distributed into smaller particles. Consequently a cool current spread out near the ground not only from behind the wall, but also from a region to the left of the wall and ahead of it. Since the low level NE'ly winds entered the storm rapidly and with a cross component directed from its right flank, it is reasonable to expect the low level updraught to have been generated predominantly in the region lying between the wall and the arm of precipitation reaching forward on its left. If the air which flowed into this region is regarded as all having risen through a lid to the rectangular box two of whose sides were formed by precipitation walls, as shown in fig. 38, we can make a rough estimate of the speed of the updraught which was generated. We suppose that the sides have an extent of 6 miles across the storm front and 3 miles

perpendicular to it. If $\bar{u}_x$ and $\bar{u}_y$ are respectively the mean components of the wind normal and parallel to the wall, and $u_z(z)$ is the mean updraught at the height z, we have in the lower troposphere, neglecting the variation of air density with height

$$\bar{u}_z = z\,(6\,\bar{u}_x + 3\,\bar{u}_y)/18$$

Using appropriate values of $\bar{u}_x$ and $\bar{u}_y$ we have calculated that $\bar{u}_z$ reaches about 8 m/sec at a height of 1 mile[1] and about 12 m/sec at a height of 2 miles. The latter value is quite close to that previously inferred to have existed near the base of the overhang. Above this level the updraught can be assumed to continue accelerating under its buoyancy. The strongest updraughts appear to have occurred above a position near the left-hand end of the wall; fig. 37c shows that all 13 reports of giant hail (diameter $\geq 1\frac{5}{8}$ in) were from places close to the line along which the top of the echo free vault had sunk to 10,000 ft at the left end of the wall. (The horizontal displacement of hail of this size after leaving the updraught is negligible.)

In view of the steadiness and the great extent of the updraught it is reasonable to suppose that in its interior the air temperature could not have been much affected by mixing processes, and can thus be calculated by assuming adiabatic ascent from low levels. According to the sounding made at Crawley (fig 1e) the maximum difference of temperature between the updraught and the undisturbed environment increased from zero at about 9,000 ft to about 1.5°C between 12,000 and 20,000 ft, and then decreased to zero again near 25,000 ft. According to the parcel theory, air accelerating under the buoyancy produced by these temperature excesses could attain a speed of about

---

1 That updraughts of this strength exist at low levels near shower squall-fronts is known by glider pilots. For example, Reitsch (1956) gives an interesting account of a flight along such a front, in which a persistent steady updraught was experienced at levels a little below that of the cloud base (at 1 km); its speed was 2 - 3 m/sec about 3 miles ahead of the wall of precipitation, and 6 - 7 m/sec close to it.

25 m/sec at the 25,000 ft level; unfortunately this calculation cannot be regarded as realistic, because the buoyancy can be affected seriously by the weight of the condensed cloud water and of the precipitation, and by the release of latent heat of fusion during hail growth (Saunders, 1957). Never theless the maximum speed of 35 m/sec previously inferred (section 7a) does not seem unreasonable.

A rather better estimate can be made of the excess density which may have been attained in the downdraught. This is based upon the wet-bulb potential temperature observed in the rain area at the ground. Unfortunately we have no screen temperature observations beneath the storm in its intense phase; however, at Greenham Common (223°, 50 mi) the wet-bulb potential temperature in the rain area fell to 14.6°C (at 1156), and at White Waltham (202°, 31 mi) it fell to 14.9°C (at 1250). According to the soundings from Crawley and Hemsby (fig. 1e) air with a wet-bulb potential temperature below 15°C could be found before the storm only at heights between about 9,000 and 16,000 ft. If it is assumed that the evaporation of precipitation caused air from these levels to descend to the ground practically undiluted, it appears from the soundings that it would have been colder than the environment by about 3°C at 12,000 ft and 9°C at 3,000 ft (fig. 1d). Its excess density would have been further increased by the presence of rain water, whose concentration can be assumed to have been about 2 g/kg, sufficient to produce a rainfall of the observed magnitude (fig. 7). According to the parcel theory the downward acceleration is then sufficient to produce a speed of about 35 m/sec at 3,000 ft. No great reliance can be placed on this particular value, but nevertheless it is clear that the downdraught could attain a speed as great as that found in the updraught. It is interesting that the descent

of air from the medium levels to near the ground involved the evaporation of about 8 g of rain water into each kg of air (fig 1d) On the other hand each kg of air moving through the updraught condensed only about the same amount; a part of this eventually evaporated in the anvil, and another part reached the ground as precipitation. Consequently the mass of air involved in the downdraught can have been only a fraction of that composing the updraught, although the energy released was comparable It appears that for each 5 unit masses which ascended about 1 unit mass descended, consuming about one fifth of the condensed vapour during the evaporation of precipitation and develop ing a kinetic energy which was used mainly to lift the 5 unit masses to the level above which they accelerated upwards under buoyancy forces.

c) A model of the storm

A tentative model can now be constructed of the air flow in the storm during its intense phase

First, we consider the horizontal speed of the air within the updraught We have no direct evidence of this, but it has been possible to measure the horizontal speed of turrets reaching the tops of the storm In one instance (column T_2, fig 23) the motion first observed at a height of 39,000 ft was only 30 mi/hr along 210°, at a level where the wind in the environment was moving in the same direction at about 70 mi/hr Later, a column top reaching 41,000 ft was found moving with a component velocity along 210° of only 15 mi/hr (fig 39). In both instances the column top was accelerated forward rapidly as its rising speed diminished; however, it is reasonable to assume that in the intense phase of the storm the forward speed of the air in the larger and more rapidly rising updraught was less than 15 mi/hr at 41,000 ft.

It follows that the air in it must have been derived from levels below 15,000 ft (fig. 9a); since the air of highest potential temperature occurred below about 8,000 ft (fig. 1e) it can be supposed that the mean forward speed of the updraught air was initially only about 5 mi/hr, and had barely increased to 15 mi/hr when the air had reached 40,000 ft. Relative to the storm these speeds imply motions at about 35 mi/hr at low levels and about 25 mi/hr at 40,000 ft, still towards the rear of the storm. Above this level the updraught rapidly acquired a forward relative speed, so that the axis of the updraught first became upright, and then sloped forward until it passed through the level of the highest tops (44,000 ft) almost vertically above the position of the wall. In the heart of the storm the strong inclination of the axis of the updraught towards the rear must be consistent with the deduced upward speeds of at least 10 m/sec at 12,000 ft and about 35 m/sec at 25,000 ft; it is implied that the axis will have penetrated about 3 miles rearwards through the storm in rising from the ceiling of the echo free vault to the 35,000 ft level, a distance sufficient to account for the full width of the echo at this level.

In respect of the downdraught we have already seen (last section) that it must have been derived from medium levels; it now further seems reasonable to suppose that its efficient maintenance demands that air should have entered the storm and flowed through the downdraught region continuously. Now the light winds experienced in the area of heavy precipitation and the restoration of a light NE'ly wind at the ground behind it imply that the downdraught air left the storm rearward with a relative speed of fully 40 mi/hr; even if it was limited to a shallow layer some 2,000 ft deep, we must suppose that it was derived from a much thicker layer in the middle

levels, say between 13,000[1] and 23,000 ft, in which the air had a mean relative speed into the storm of a little less than 15 mi/hr. We know little about the downward speed of the cold draught except that it may have reached 35 m/sec before it decelerated near the ground.

These considerations impose some limiting conditions for the horizontal and vertical velocities within both updraught and downdraught, which have been taken into account in drawing fig. 40, which shows the air flow in the storm during its intense phase. The diagram contains an RHI section based on fig. 27(b), isopleths of vertical velocity and schematic trajectories of air. A striking feature, which would be even more apparent if the vertical and horizontal scales of the diagram were the same, is the strong inclination of the updraught throughout the bulk of the storm; this can be regarded as a consequence of the pronounced wind shear in the general airstream. It had the important effect of permitting the precipitation to fall clear of the updraught without interfering with the continued rise of potentially warm air, and indeed to generate a strong downdraught in the potentially cold air in the middle levels. A part of the downdraught spread forward to maintain the squall front in advance of the storm and may mostly have left the plane of the diagram sideways, since the squall front does not appear to have advanced steadily relative to the storm. Air travelled through both updraught and downdraught in a period (about 12 minutes) which was rather short compared with the 32 minutes during which the radar data show that this organised structure persisted, and it is natural to suspect that the storm was in a virtually steady state in which the condensation and precipitation processes

---

1 The environmental wind speeds below 13,000 ft were less than the speed of the storm (fig. 9a).

and the dynamics of the air flow were rather stably linked The horizontal acceleration of the updraught air at the storm tops required a pressure gradient which probably was produced by the density excess which arose beneath the cloud top where it penetrated into the stratosphere and became a cold dome. The acceleration of the downdraught air in the reverse direction was associated with a pressure gradient set up beneath the area of intense precipitation by its weight and the chilling due to its partial evaporation. The magnitude of the gradient may have set some limit upon the relative speed with which air could enter the top of the downdraught region, since the maintenance of a downdraught requires that air should pass continuously through it and be removed at low levels. Consequently the speed of advance of the storm was a little less than the speed of the wind at the mid-troposphere level where air entered the storm beneath the precipitating shelf of the updraught and began to sink into the downdraught region. On this occasion the speed of the storm was 40 mi/hr in the intense phase, increasing to about 45 mi/hr as it weakened in the afternoon[1]. The details of the manner in which the storm was organised and its speed was determined will not be clear until a quantitative dynamical analysis is made.

Fig 41 shows a schematic 3 dimensional representation of the storm. In this diagram the outline of the volume in which the echo intensity exceeded about 10^3 mm^6/m^3 is drawn, indicating the position of the wall, the echo free vault and the forward overhang. Arrows show the trajectories of air in the updraughts and downdraughts. The component of the wind across the storm,

---

1 The speed of travel of the echoes in the early history of the storm was 50 mi/hr (figs 20 and 24), which is significantly greater. At this stage the echoes were produced by precipitation from clouds grown in the medium levels, and travelled with about the speed of the wind at a generating level at about 20,000 ft. It is characteristic that as the convection begins from lower levels and intensifies, the velocity of a storm is more affected by propagation: the speed decreases, and the direction of advance veers to the right.

which was most marked at the lower levels, is implied by the twist of the arrows denoting the updraught below the overhang. The downdraught spread out in all directions near the ground, and was strongly opposed to the general low level wind at the front and right-hand flanks of the precipitation region. Consequently the updraught was concentrated in these sectors, and in particular became extended towards the right rather than towards the left of the storm. The propagation of the storm to the right is implied in the model by the new precipitation column which has not yet reached the level of the main tops.

d) The growth of hail in the storm

Ludlam (1958) showed that in a model cloud in which supercooled water occurs between the 0°C and -40°C levels, only a very restricted growth of cloud particles can occur when the updraught between these levels has speeds comparable with the fall speeds of large hailstones. It was concluded that when large stones are grown some unsteadiness of the updraught prolongs the period spent by cloud particles in the region of supercooling. For example stones might fall from one thermal and enter another near the 0°C level. The tilted steady updraught of our storm model is a more efficient means to the same end, permitting embryo stones to descend from the cloud tops and re-enter the updraught near the 0°C level. In this way they may be recycled several times through the region of updraught maximum before finally attaining a size and fall speed which permits them to fall out beneath this region. Tentative calculations show that if the fall-speed of the embryos is very nearly equal to the updraught speed at the point of re-entry, then stones of about the largest possible size can be grown during the second ascent into the updraught maximum.

We have already estimated (section 7) that in the lowest part of the forward overhang, where the echo intensity was approximately 29. particles of radius up to about 1 mm were re-entering the updraught. At ranges 50 to 70 miles the minimum detectable intensity on the 10 cm PPI radar was about [24]. On the basis of a similar calculation it can therefore be supposed that particles of radius about 1 mm were present when echo appeared along the line which represents the path of the extreme right-hand edge of the echo mass. The history of the proportion of those particles which first reached the ground as large hailstones can be divided into three stages. In the first the particles fell without growth from some level between about 20,000 and 35,000 ft to the level of their re-entry into the updraught, at about 15,000 ft. Their rate of descent was probably increased by a slight down draught, and was about 10 m/sec (2000 ft/min), so that the period of descent was between about 3 and 10 minutes. During the second stage growth was renewed in the updraught, at levels where the concentration of condensed water, m, varied between about 4.8 and 5.4 g/m^3. Assuming an average value, $\bar{m}$, of 5 g/m^3, and taking unity for the efficiency of catch, E, of a particle of radius R, fall speed V, and mean density δ of 0.9 g/cm^3, we have

$$dR/dt = E\,\bar{m}\,V/4\delta$$

or $$dR/dt = 5 \times 10^{-6} V/3.6$$

If, further, the fall speed is determined by a mean drag coefficient C of 0.6 and a mean air density ρ of 6×10^{-4} g/cm^3, then

$$V^2 = 8\,g\,R\,\delta / 3\,\rho\,C$$

or $$V = 25.5 \times 10^2 R^{\frac{1}{2}}$$

Thus $$dt = 3.6\,dR/(R^{\frac{1}{2}} \times 5 \times 10^{-6} \times 25.5 \times 10^2)$$

$$= 2.8 \times 10^2\,dR/R^{\frac{1}{2}}$$

Integrating, $t = 5.6 \times 10^2 (R_1^{\frac{1}{2}} - 0.32)$

where t is the period during which the radius increased from 0.1 cm to R_1.

In the third stage the particles left the updraught at about 12,000 ft and fell to the ground with a fall speed which was probably somewhat increased by a downdraught and therefore can with negligible error be taken as the value of V used above. We therefore estimate the total time between the detection of echo on the extreme right of the storm and the arrival of some of the echoing particles at the ground as large hail of radius R_1 as

$T = (200 \text{ to } 600) + 5.6 \times 10^2 (R_1^{\frac{1}{2}} - 0.3) + (4 \times 10^5/V)$ sec

Accordingly if $R_1 = 1.25$ cm (size 6), T = 800 to 1200 sec,

and if $R_1 = 2.2$ cm (size 8), T = 1000 to 1400 sec.

These periods can be compared with values independently deduced from the distribution of hail at the ground and the winds. Since the early echoes at the extreme right of the storm appeared at practically the same range as the wall (see the section along 203° in fig.27b, for example), and since the large hail fell immediately behind the wall, it is reasonable to assume that the hail particles moved with a component velocity along 210° (towards the radar) which was the same as the speed of the wall, that is 40 mi/hr. The average speed of the wind between the ground and 35,000 ft carrying the hail across this direction was about 11 mi/hr (fig.9b), so that individual stones could be expected to have travelled at slightly more than 40 mi/hr along paths directed from about 195°. It is striking that there is some tendency for the isopleths of maximum hail size at the ground to be orientated in this direction[1] particularly in the swath at ranges between about 50 and 60 miles (fig.6b), where the

---

1 A similar tendency for the isopleths to be elongated to the left of the storm track was noticed in a severe storm in S.E.England the previous year (Ludlam and Macklin 1959).

the first hail of size 8 occurred. If a line is drawn extending from this swath towards 195° it meets the path of the edge of the 10 cm echo where a slight bulge to the right (marked X in fig.6b) suggests an intensification of the storm. The length of the line between the bulge and the isopleth of hail of size 6 implies a growth period of 20 minutes, or 1200 sec. A shorter period of about 760 sec found at a later stage is about the minimum which can be inferred (see line leading to Y in fig.6b). In both localities hail of size 8 occurred about $2\frac{1}{2}$ miles farther along the hail path, implying an additional growth period of about 200 sec. These times are as nearly in agreement with the previous estimates as could be expected, and support our view of the history of the hailstones within the storm.

We have considered the growth of large stones during a single traverse of the updraught after the re-entry of small embryos in the lower part of the overhang. Stones grown in this manner could be expected to have a small core (diameter less than a few mm) which is opaque or clear according to whether the re-entry was effected above the 0°C level or considerably below it: in the latter event the embryo might have melted into a raindrop before freezing again when lifted back above the 0°C level. It does not seem important whether or not the embryo in its early history is regarded as a small hailstone (graupel) or a small raindrop, and the supply of embryos from the cloud tops was probably abundant and not sensitively related to the properties or concentrations of freezing nuclei present in the updraught. Embryos which on the first re-entry into the updraught had fall-speeds too small to ensure that they attained the largest size on the second traverse probably again passed through the updraught maximum and were released ahead of it; they then re-entered the updraught a second time, or perhaps again

and again at successively higher levels, since each successive time they were carried forward a smaller distance near the cloud tops. Wherever an embryo entered the updraught with too great a fall-speed and grew too rapidly to be lifted into the updraught maximum, it would have moved towards the rear of the storm and fallen out of the updraught behind the wall without attaining the largest possible size.

8. The decline of the intense phase

At ranges of about 40 miles, in the Wokingham area, it appears that the forward overhang collapsed, and the duration of the hail increased within ½ mile from 5 minutes to about 15 minutes (fig. 37a). In Wokingham, where the particles from the descending overhang first reached the ground, hailstones of 1 in diameter (size 6) fell from both the region where the overhang had existed and the part of the storm behind the wall, arriving at the ground (according to reports, without much rain) for a period of 15 minutes in perhaps the most memorable fall of the storm (see observation E in figs 34 and 35, and Appendix 5), although larger stones fell elsewhere. The descent of the overhang is illustrated in the 3.3 cm RHI pictures of fig. 42; its great forward extent (over 5 miles from the wall) just before the collapse can be seen in both figs. 42 and 27c. The vertical sections in fig. 27c also show that echo of high intensity had begun to extend into the lower part of the forward overhang, and it seems probable that hailstones of diameter about 1 inch and fall-speeds of about 25 m/sec had arrived in this region. We are not able to account satisfactorily for the marked forward extention and collapse of the overhang. It seems possible that the particles spreading forward from the storm tops and descending into the upper part of the overhang encountered near the Chiltern hills extensive layers of altocumulus in which their evaporation was halted and some growth occurred. This is suggested by a forward extension of the 10 cm PPI echo in a manner which indicates that particles were entering the beam from above but not from any fresh columnar echo. It is also suggested by the first two 3.3 cm RHI pictures of fig. 42. On these pictures it can be seen that the echo from the anvil extending forward from the storm increases near its base, at heights

between 20,000 and 25,000 ft and ranges between about 28 and 38 miles; on the first picture echo descending below 15,000 ft at 35 to 38 miles is too low and too near the radar to have been derived directly from columns at the range of the wall (45 miles) and on smaller azimuths than that of this section. The intensification of the anvil echo towards its base can still be traced on the last two pictures of fig. 42, and was accompanied by a great increase in the extent of the echo at 20,000 ft.

The effect of the extending forward and lowering of the overhang would be to interfere with the updraught, since the particles would enter it at a level and distance forward from the wall where it was comparatively weak and unable to support them. Following the diminution or cessation of the updraught the particles of the main echo would also collapse to the ground, so that the hail size at the ground would diminish progressively along a swath orientated from about 195° in the manner observed (fig. 6b): hail production evidently had ceased, but the arrival at the ground of the smaller stones was delayed on account of their smaller fall-speeds and the greater heights from which they fell. Stones of size 2 were observed at the ground up to a point about 15 miles in advance of the rear of the storm tops at the range 40 miles when the overhang had collapsed (figs. 42 and 6b). These stones have diameters and fall-speeds of about 7 mm and 12 m/sec below the 0°C level, and 12 mm and 20 m/sec above the 0°C level, and so the time of freefall from 40,000 ft to the ground would have been about 12 min and their forward displacement about 10 mi. Since an updraught could be expected to persist in the upper part of the cloud for several minutes after it had ceased at low levels it appears reasonable that the whole of the hail swath at ranges closer than 40 miles was produced by fall-out after the interruption of the updraught.

The fall out from a large part of the storm probably led to a downdraught reaching the ground over a large area and displacing the region of updraught generation well to the right. Soon after the collapse of the overhang fresh echoes formed in this position and are responsible for the pronounced bulge in the track of the right hand edge of the echo mass which can be seen at a range of about 44 miles in figs. 6a and 6b. After a period in which only rain reached the ground the development of convection continued and the storm became re-organised; 1 inch hail was again produced 30 to 60 miles further along the storm track. The storm was moving into a more unfavourable environment, however (fig. 1e), and probably for this reason did not attain its former intensity. Later it died out near the east coast.

The structure of the storm during the early afternoon could not be examined in the same detail as before, mainly because of the power failure. However, sixteen 3.3 cm RHI photographs taken between 1330 and 1400 show the presence of a wall and forward overhang (and occasionally an echo free vault) during probably the whole of this period. An example is given in fig. 43a[1], taken at a time a little before the fall of 1 inch hail at Horseheath. During this period the wall increased its range from 18 to 38 miles, moving at the same speed (40 mi/hr) as during the earlier intense phase. As the storm moved beyond 40 miles range it weakened; probably the updraught became intermittent, for on the 3.3 cm RHI display the distinctive features of the echo disappeared and separate rising columns appeared at the rear (fig. 43b) in the same manner as before the intense phase (fig. 21).

---

1 Notice that now that the radar examines the storm from the rear, a distinct rearward tilt of the sharply-defined back edge can be seen from about 22,000 to 32,000 ft; attenuation when the storm was viewed from the front had previously made the tilt appear always in the opposite sense.

9. The generality of the storm model

A survey of the literature shows that many of the characteristics of the storm which we have studied in detail are typical of severe hailstorms in this part of the world.

Thus Gibson (1863) says, "In Europe hailstorms usually travel in straight bands of great length but small breadth, and travel very rapidly.... A hailstorm of 13 July, 1788 began in the morning in the southwest of France, and reached Holland in a few hours, destroying a narrow line of country in its path. It moved in two columns twelve miles apart, the one on the west ten miles broad, and the other five miles broad, the one extending nearly 500 and the other 440 miles." Marriott (1892), who studied British thunder storms with the help of about 200 voluntary observers, called such storms 'line thunderstorms'. He gives two examples (fig.44) in which storms "were tracked across England in a direct line from south to north for over 400 miles, the rate of progression being 50 miles an hour. These thunderstorms occurred during the night and early morning." Prohaska (1907), who investigated storms with a network of several hundred observers in Austria, also showed that hailstorms affected bands of country some hundreds of km long but less than 20 km across, usually moving at a speed of about 30 mi/hr from some westerly or southwesterly point, often against a cool surface wind.

In New England travelling storms which produce falls of hail over a long track are distinguished from local hailstorms by Donaldson, and called 'hail repeaters'. Well developed downdraughts in these storms are implied by the finding that damaging winds are associated only with hail repeaters, and not with the local storms (Donaldson, Chmela and Shackford, 1960).

The frequency of such severe travelling storms in England is about one each year, so that at most places they are experienced only once in a lifetime and are popularly described as 'freak' storms. They are, however, not at all capricious, but regularly occur in situations where a marked instability arises by differential advection in or just ahead of a cold trough advancing into the Continent after a hot spell. These situations are characterised by a large wind shear associated with the strong horizontal temperature gradient, and an upper SW'ly current lying above an E'ly or NE'ly surface flow across England on the north side of shallow low pressure systems over western France. The storms are also often described as being of "tropical" severity, which may be a further misjudgement, since although the same rain intensity may more often be encountered in the tropics, hailstorms of equal intensity are there limited to particular regions. The severe travelling storms of mid-latitudes are manifestations of the most intense convection which occurs in the terrestrial atmosphere. They often occur at night and give spectacular lightning displays in which the discharges occur at the rate of 1/sec or more (Vonnegut and Moore (1959) very appropriately name such storms "giant electrical storms"), and are sometimes accompanied by tornadoes. In S.E.England the frequency of destructive tornadoes is comparable to that in Kansas (Lamb, 1957). A famous storm with tornadoes moved northward across Wales and western England in 1913, along a path which is shown in fig.45. The distribution of the rainfall in this diagram indicates that this was a typical travelling storm; characteristically the tornadoes occurred on the right flank. A tornado also occurred on the right flank of the Horsham storm in S.E.England in 1958 (Ludlam and Macklin, 1959), whose behaviour was very similar to that of the Wokingham storm, but which was even more severe (fig.46).

We think that the Wokingham storm and the structure we have inferred for it are typical of severe extra tropical hailstorms. That the form of storm draughts, though not their intensity, and in particular the essential role of the downdraught, is also typical of many lesser storms is suggested by the marked invigoration of cumulus which become cumulonimbus.

Ludlam (1957a, b), on the basis of experience in Sweden and England, drew attention to a frequent surge in the growth of convective clouds which occurs soon after the onset of precipitation and the first appearance of glaciation in the cloud tops. This surge commonly leads to the production of clouds whose tops are about twice as high as the general level of the tops of the biggest non precipitating clouds: it appears that in these latter the convective currents have difficulty in penetrating into the upper troposphere, whereas in the maturing cumulonimbus they readily reach the tropopause or even penetrate into the stratosphere. This surge in the growth was previously associated with a new source of buoyancy in the upper levels, the heat of fusion released during extensive glaciation. While this source is often important (for example, in the Wokingham storm), it now seems more reasonable to regard the growth surge as an effect of the establishment of a downdraught.

This view has been expressed by other writers, for example by Thorkelsson in 1946 on the basis of his observations in Iceland[1], and more recently by Howell (1960), who has described the growth surge in tropical clouds[2]. Our interpretation of the difference in the character between the cumulus and the cumulonimbus is that the precipitation from the cumulonimbus causes a change

---

1 "When rain begins to fall the cumulus growth is accelerated, their development enters a new phase, and the rain area spreads rapidly and moves."

2 "It is hard to avoid the impression that a marked increase in the rate of growth of the cloud is often connected with the onset of precipitation ... new towers rise from the top of the precipitating cloud to much greater heights than formerly ... the impression of rolling, tumbling growth-and-dissipation activity is replaced by one of swift organisation of a large-scale convective cell." Craddock (1949) writes very similarly of clouds observed at Singapore.

in the scale and organisation of the convection. In cumulus convection buoyant air ascends intermittently in thermals of restricted volume, which are released following a convective overturning within a superadiabatic layer at the ground which is only about 100 m deep[1]. On the other hand precipitation leads to the formation of a cold downdraught and strong horizontal temperature differences throughout the lower troposphere, and an overturning commences in a layer which is kilometres deep. In the presence of a wind shear and the ground, which causes a spreading of the downdraught, the overturning becomes organised in such a manner that the cloud is fed by a much larger updraught in which conditions are closer to adiabatic. In the severe storms the updraught is vast, almost continuous and practically adiabatic. In these circumstances the dimension and duration of the updraught and its precipitation system are such that its main features, such as the echo wall and forward overhang, are likely to be readily discernible with radars of conventional resolution. In less severe storms the updraught has a smaller extent, is intermittent and only occasionally or locally supports an overhang, so that these features are not detectable. Nevertheless, many such storms, and even showers, persist for an hour or more, which is long compared with the time taken for rain or small hail in their upper parts to fall to the ground. Evidently the precipitation is renewed by some mechanism related to the cloud itself, even though the details of the mechanism are unlikely to be revealed by a conventional radar, which may show merely a persistent echo column of practically unchanging appearance. Equally the downdraught

---

1 Anabatic winds over hills and sea breeze fronts have a marked influence on cumulus growth by concentrating and enhancing updraughts in particular localities, but their importance is limited because in a general wind the cumulus which are produced drift away from these places.

mechanism is implied whenever showers occur with stably stratified air in the lower layers, particularly when they travel long distances or when they occur over the ocean (in returning polar air) where there are no topographical disturbances to release or maintain the convection.

In recent years a number of writers have commented upon the strong wind shears in which severe convective storms occur. Dessens (1960), for example, has shown that hailstorm situations in southwest France are characterised by very strong upper winds, and Ramaswamy (1956) has pointed out that severe convective storms in India and elsewhere in the sub-tropics are associated with the presence of a jet stream in the upper troposphere. In particular Newton (1960) has summarised several stimulating papers in which he has attributed the marked tendency of severe storms to propagate on the downshear side and on the right flank to the dynamical effects of the increase and veer of wind with height which is characteristic of the weather in which the storms occur in the United States. He has also emphasised that downdraughts may originate outside the thunderstorm cloud and play an essential part in releasing latent instability (Newton, 1950). Their role in the maintenance of squall-lines was suggested by Harrison and Orendorff (1941).

It is because of this general association of severe storms with a strong wind shear and sometimes also with a stable stratification near the ground, that we regard our model of the airflow in the Wokingham storm as representative of the organisation of intense hailstorms. We believe that a similar kind of organisation, though more intermittent and less well developed, is typical of all travelling cumulonimbus. Their cold downdraught is a vital part, as envisaged by Sir Charles Normand (1946): "It is well to keep in mind the possibility that cumulonimbus is a cloud that takes advantage of the

energy available from moist descending currents, that it is organised to take in potentially cool air at the higher levels as well as potentially warm air at the lower levels."

ACKNOWLEDGEMENTS

We are pleased to thank the Director-General of the British Meteorological Office for the provision of staff and facilities at the East Hill Radar Station, from which the observations were made. The research on severe storms of which this work has been a part, is also supported by the Geophysics Research Directorate, Air Force Cambridge Research Center of the Air Research and Development Command, United States Air Force. The British Rainfall Organisation kindly provided data from their observers, and we are very grateful for the many painstaking records provided by a large number of voluntary hail observers. Messrs. W.C.Macklin and D.A.Rogers of Imperial College undertook most of the work of interrogation in the area severely affected by the storm. Other personnel who made indispensable contributions to the observations programme were Messrs. W.G.Harper (Officer in Charge), N.Coupe, A.Denham and J.Beimers of the Radar Station; Dr. David Atlas, Messrs. P.J.Harney and P.Petrocchi of the Geophysics Research Directorate, U.S.A.F.; and Dr. and Mrs. S.C.Mossop of the South African Council for Scientific and Industrial Research.

We have been greatly helped by long discussions with Dr. Atlas. Miss Maureen Squires drew many of the diagrams.

REFERENCES

Atlas, D., Harper, W.G., Ludlam F.H. and W.C.Macklin	1960	Radar scatter by large hail, Quart. J. R. Met. Soc., to be published
Atlas, D. and F.H.Ludlam	1960	Multiwavelength radar reflectivity of hailstorms, Tech. Note 4, Contract AF 61(052)-254, Dept. of Met., Imperial College, London
Craddock, J.M.	1949	The development of cumulus cloud Quart. J. R. Met. Soc., **75**, p.147
Cunningham, R.M.	1960	Hailstorm structure viewed from 32,000 ft, Geophys. Monograph No.5, Amer. Geophys. Un., Washington, D.C.
Dessens, H.	1960	Severe hailstorms are associated with very strong winds between 6,000 and 12,000 m, Geophys. Monograph No.5, Amer. Geophys. Un., Washington, D.C.
Donaldson, R.J., Jr., A.C.Chmela, and C.R.Shackford	1960	Some behaviour patterns of New England hailstorms, Geophys. Monograph No.5, Amer. Geophys. Un., Washington, D.C.
Gibson, W.S.	1863	Hailstorms and their Phenomena, in Miscellanies, Longman, Green, Longman, Roberts and Green, London.
Harrison, H.T. and W.K.Orendorff	1941	Pre-cold frontal squall lines, United Air Lines Transport Corp. meteor. circ. No.106 (quoted by Newton, 1950)
Howell, W.E.	1960	Cloud seeding in the American Tropics, Geophys. Monograph No.5, Amer. Geophys. Un., Washington, D.C.
Jones, R.F.	1960	Size-distribution of ice crystals in cumulonimbus clouds, Quart. J. R Met. Soc., **86**, p.187
Lamb, H.H.	1957	Tornadoes in England, May 21, 1950, Geophys. Mem. 99, Met. Office, London
Ludlam, F.H.	1957a	Cumulonimbus, O.S.T.I.V. section, Swiss Aero-Review, April.
	1957b	New concepts of cumulonimbus, The Aeroplane, May 10; London
	1958	The hail problem, Nubila, **1**, p.12

Ludlam, F.H.	1959	Hailstorm studies, 1958, Nubila, 2, p.7
	1960	The role of radar in rainstorm forecasting, Tech. Note 3, Contract AF 61(052)-254, Dept. of Met., Imperial College, London
Ludlam, F.H. and W.C.Macklin	1959	Some aspects of a severe storm in S.E. England, Nubila, 2, p.38
Macklin, W.C. and F.H.Ludlam	1960	The fallspeeds of hailstones, Tech. Note 6, Contract AF 61(052)-254, Dept. of Met., Imperial College, London
Marriott, W.	1892	Report on the thunderstorms of 1888 and 1889, Quart. J. R. Met. Soc., 18, p.23
Newton, C.W.	1950	Structure and mechanism of the pre-frontal squall line, J.Met., 7, p.210
	1960	Morphology of thunderstorms and hailstorms as affected by vertical wind shear, Geophys. Monograph No.5, Amer. Geophys. Un., Washington, D.C.
Normand, Sir Charles	1946	Energy in the atmosphere, Quart. J.R. Met. Soc., 72, p.145
Prohaska, K.	1907	The hail fall of 6 July, 1905 in the east Alps, Met. Zeit, 24, p.193
Ramaswamy, C.	1956	On the sub-tropical jet stream and its role in the development of large scale convection, Tellus, 8, p.26
Reitsch, H.	1956	Observations during a soaring flight along a squall line, Publication IV, O.S.T.I.V. (from Swiss Aero-Review)
Saunders, P.M.	1957	The thermodynamics of saturated air: a contribution to the classical theory, Quart. J.R. Met. Soc, 83, p.342
Thorkelsson, T.	1946	Cloud and shower, Quart. J.R. Met. Soc., 72, p.332
Vonnegut, B. and C.B.Moore	1958	Giant Electrical Storms, Recent Advances in Atmospheric Electricity, Pergamon Press

Appendix 1. Characteristics and mode of operation of radars on 9 July 1959 at East Hill (51°55'N 00°30'W; National Grid Reference 52(TL) 028 248)

Type	Wave-length cm	Beam-width, degrees Hor.	Vert.	Max. display range (statute mi.)	Sweep period sec.	Mode of operation
AN/TPS-10	3.3	2.0	0.7	70	1	Set A: manual following of echo column tops, to obtain their rate of rise. Set B: manual location of most intense echoes, and intensity measurement by reduction of gain
MPS-4	4.7	4.0	0.8	140	12	Stepwise gain reduction during PPI sweeps at successive fixed elevations (complete cycle time 20 min)
A.M.E.S. Type 13	10 (RHI)	7½	1½	75	10	Manual search for maximum echo heights; intensity measurement by reduction of gain.
Type 14	(PPI)	1¼	6 (centred at 2° elevation)	120	15	Automatic full-gain photograph every 3 min; intermittent stepwise gain reduction

Records were made by photographing the displays, and have been analysed with the help of the written notes and tape-recorded comments of the radar operators.

Appendix 2. Echo nomenclature.

	Name	Description	Typical dimensions
1.	Column	An echo appearing as an upright column on the usual kind of RHI display, probably associated with a single updraught.	Diameter about 1 mile, increasing to 3 miles for the tallest columns
2.	Row	A group of columns arranged in a straight line	1 - 3 miles wide, and up to 10 miles long.
3.	Cluster of Echoes	A fairly compact group of separate echoes	10 - 30 or more miles across
4.	Echo Mass	A large region of echo containing some columns at least partly embedded in more diffuse and weaker echo which may be the residue of previous columns	10 - 50 or more miles across
5.	Core	The most intense part of an echo mass, containing recently formed columns	Usually less than 10 miles across

Appendix 3. Corrections for beam-width.

The RHI sets have beams which are broader in the horizontal, being filled in the vertical at all working ranges. Intensity measurements have been adjusted for horizontal beam-widths on the assumption that the intense echoes have a width of 2 miles at right angles to the beam axis, and that where the beam-width is greater the excess contains negligible echo. Accordingly, the apparent intensities are increased as a function of range by the amounts given in Table 1.

The 10 cm PPI set has a beam which is broad in the vertical. One correction to observed intensities is necessary because a part of the beam lies below the radar horizon. Another was made on the assumption that strong echoes (apparent intensity ≥ [60]) occur only between 15,000 and 30,000 ft., and weaker echoes from the ground up to 30,000 ft., with negligible echo outside these limits. These assumptions involve adjustments which are included in Table 1.

Table 1. Beam-width adjustments to apparent echo intensities

Range (mi)	Increment of 10 log Z				
	3.3 cm	4.7 cm	10 cm RHI	10 cm PPI	
				strong echoes	weak echoes
26 - 30	0	-	2½	12*	2
31 - 35	0	-	2½	10*	2
36 - 45	0	1½	4	7	2
46 - 55	0	2½	5	5	2
56 - 65	0	3	6	3½	2
66 - 75	0	-	6½	4½	3
76 - 85	-	-	7	5	4
86 - 95	-	-	7½	5½	5½
96 - 105	-	-	8	6	6
106 - 115	-	-	8½	7	7

* Arbitrary correction

Appendix 4. Corrections to intensity measurements of the 10 cm PPI to allow for drifting off tune.

During the period 1030 to 1650 19 3 cm and 11 10 cm RHI intensity measurements were made within 3 minutes of gain reduction series on the 10 cm PPI. The intensity measurements have been compared after correction for beam width according to Table 1 in Appendix 3. The resulting differences are plotted in fig. 1 as a function of time, and on the basis of these, corrections of + 11 db before 1210 and + 6 db after 1210 have been added to the 10 cm PPI values to make them consistent with the intensity measurements of the other radars.

Figs. 8, 11a, and 11b indicate that the maximum hailstone size increases with the maximum radar intensity of the echo, and so, in order to make the trend in the intensity of the core of the main storm consistent with this, further corrections were added to 5 particular gain reduction series on the 10 cm PPI. The resulting amended corrections are listed in Table 1.

Table 1.

Time	Correction (db)
1030 - 1155	+ 11
1155 - 1205	+ 12
1205 - 1210	+ 19
1210 - 1300	+ 6
1422 - 1442	+ 3
1442 - 1650	+ 6

Appendix 5. Summary of timed observations in path of storm 1 during its most intense phase

Times followed by 1 exclamation mark are reported as reliable to the nearest 3 minutes.
Times followed by 2 exclamation marks are reported as reliable to the nearest 1 minute.
When the code letter is enclosed in brackets there was definitely no rain prior to the onset of the hail

	Position Grid E	Position Ref N	Max. size	Hail Duration From	Hail Duration To	Rain Duration From	Rain Duration To
A	763	819	0	-	-	1230	1255
B[1]	851	778	6	1234!!	1240!!	1230!!	1250!!
C	722	722	2	1224!!	1228	1218!!	1230!!
(D)	794	697	6	1223!!	1227!!	1227	
(D)[2]	795	697	6	1223½!!	1227½!!	1227½!! (1232½)!!	1232½!! (1241½)!!
(E)	798	680	7	1220!!			
(E)	802	683	6 4	1225 1231!	1231 1234!	1234!	1255!
(E)[3]	805	675	7	x	x + 15 min	x + 14 min	
F	732	683	6	1220!	1230!		
(G)	757	667	7	1210		1225	
(H)[4]	795	645	7 6 decreasing	y + 8 y + 9	y + 9 y + 13	y + 13!!	y + 23!!
(J)	792	632	4	1220	1224	1224	
(K)[3]	752	564	7 decreasing	x	x + 4 min	x + 4 min	
L[5]	612	621	2 -	1207! 1214!!	1208! 1217!!	1205	1221!
M[6]	622	551	2	1205!	1215	1205	1215
N	619	532	2	1205!!	1210!!	1200!	1215!
N	620	622	4	1202!!	1210!!	1140!	1230!
N	637	528	4	1201!!	1204!!		
O	613	517	6	1158!!	1210!!		
P	583	525	4	1155	1215		
Q	682	437	0	-	-	5 mins	

Supplementary information:
1. First hail size 4, then size 6, then sizes 2 - 6 inclusive Highest recorded gusts at 42ft above ground: 21 mi/hr at 1229; 23 mi/hr at 1229½; 33 mi/hr at 1232; 40 mi/hr at 1232½; 43 mi/hr at 1233
2. Bracketed times refer to light rain; wind violent and gusty before and during hail
3. x = time of onset of hail
4. y = time of arrival of main gust front; wind subsequently 30 mi/hr dropping to 6 mi/hr in hail
5. Total rainfall due to storm 1 at this position = 0.6"
6. Main gust front passed at 1145

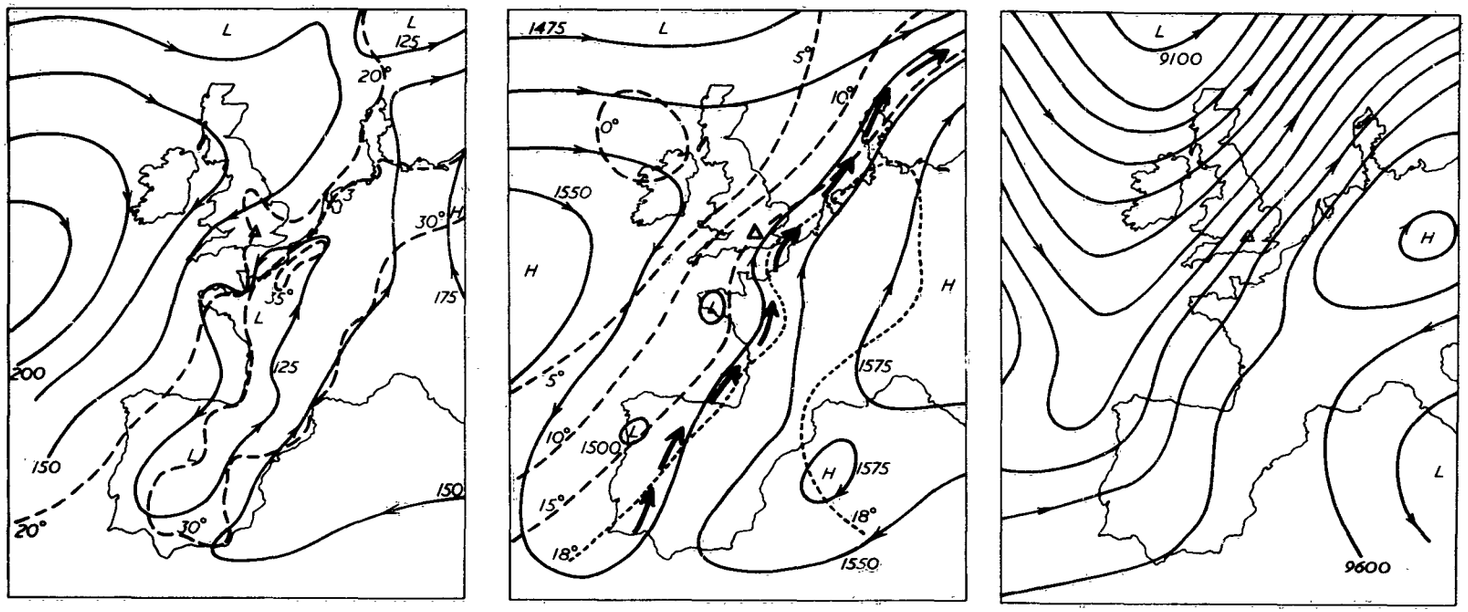

FIGS. 1(a, b & c) Contours (at 25 m intervals) of the 1000, 850 and 300 mb pressure surfaces, 1200 9 July 1959. Arrows show the direction of flow of the geostrophic wind and pecked lines are isotherms (of screen-level temperature on the 1000 mb chart). On the 850 mb chart a chain of black arrows shows a belt in which the wind speed reached or exceeded 20 kt.

The position of the hailstorm over England is shown by the triangular hail symbol.

Figs. 1(d & e)

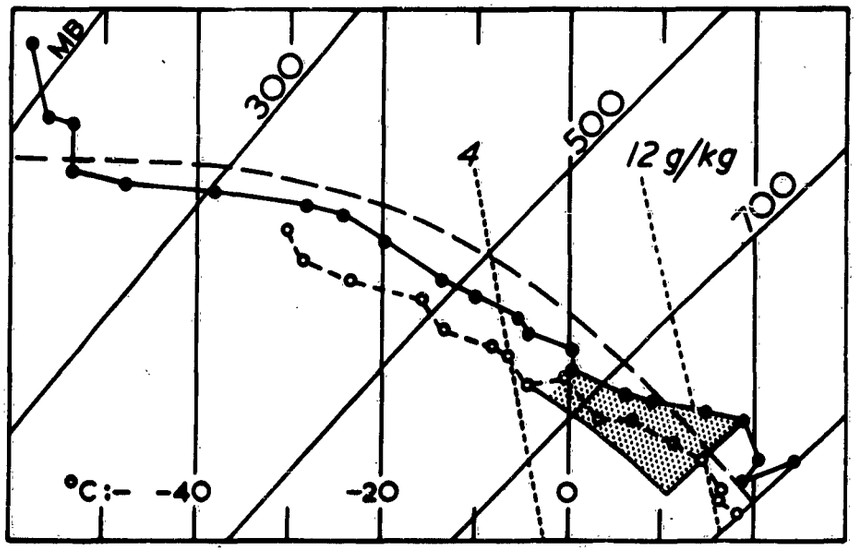

FIG. 1(d) Dry- and wet-bulb temperature sounding at Crawley, 1200 9 July 1959, represented on a tephigram. Two (dashed) lines of saturation mixing ratio and the wet adiabatic (pecked) for θ_w of 20°C are included. The energy of air descending in the downdraught from medium levels is derived mainly from the stippled area.

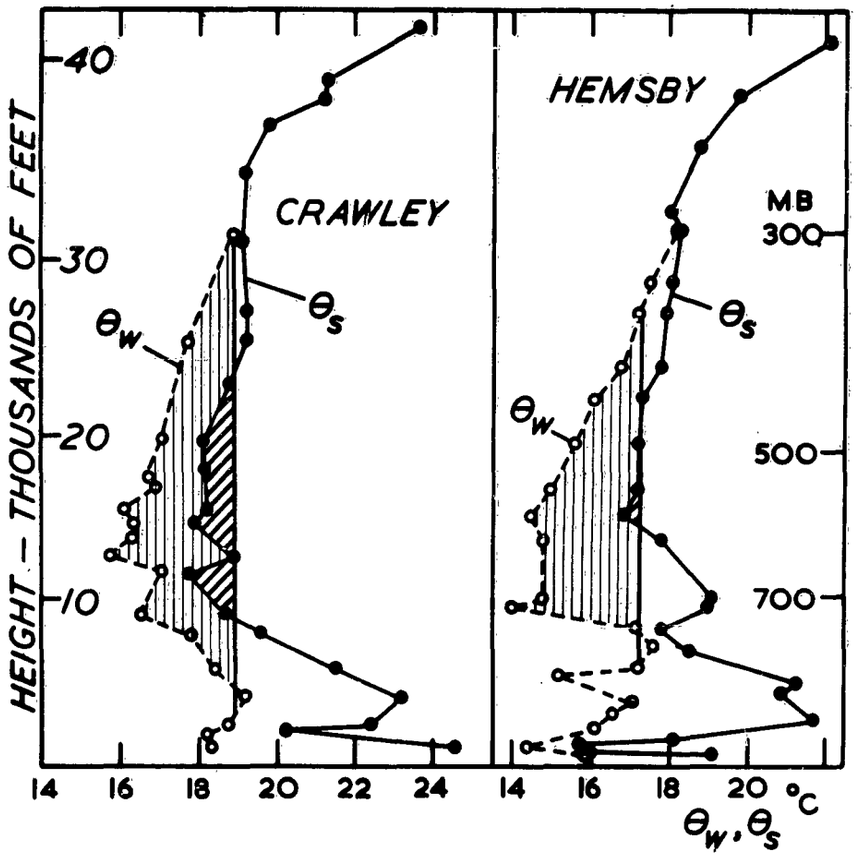

FIG. 1(e) Distribution with height of θ_w, the wet-bulb potential temperature, and θ_s, the wet-bulb potential temperature if the air were saturated; from soundings at Crawley and Hemsby, 1200 9 July 1959.

Rising air can become warmer than its environment only if it has become saturated and where its θ_w exceeds θ_s at the new level. Air which has risen from near the ground at Crawley acquires an excess potential temperature of about 1°C between about 9,000 and 23,000 ft on the unmodified sounding (obliquely hatched area), or a maximum of 1 to 3°C if the environment has been cooled and brought to saturation by a general lifting (vertically shaded area). At Hemsby, near the locality in which the storm died out, the possible temperature excess on the unmodified sounding is negligible.

Fig. 2

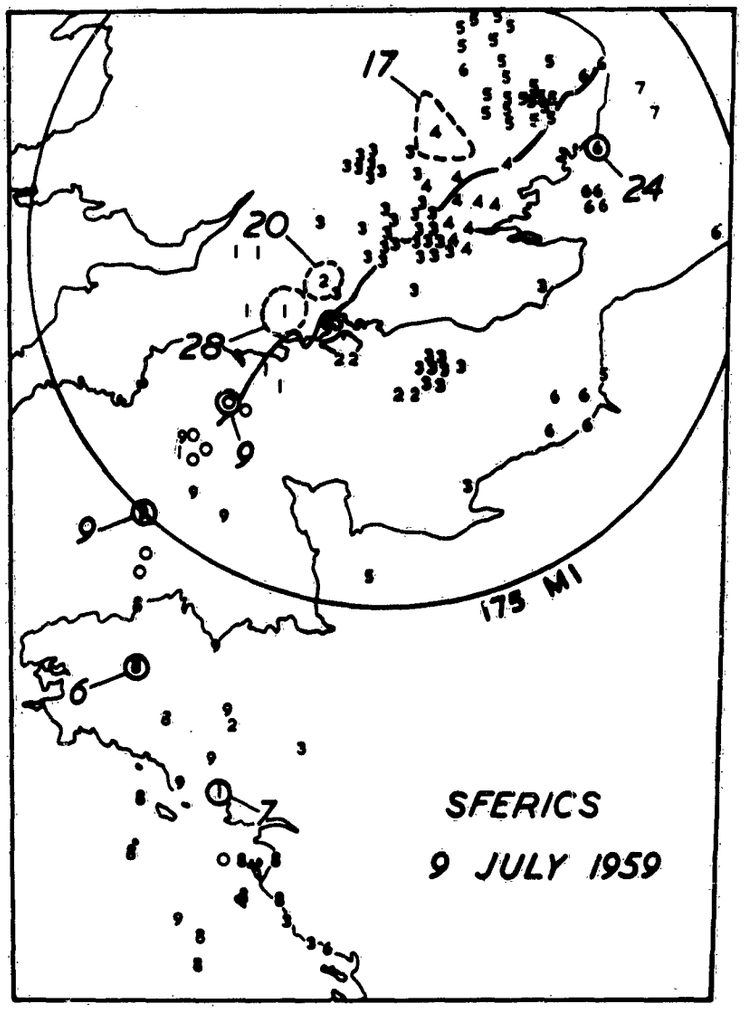

FIG. 2 Routine SFERICS observations, 0800-1700, 9 July 1959. The locations of lightning sources are shown by numbers representing the last figure of the hour of observation. Observations are made only during the 10 min preceding each hour so that a number '8' refers to the 10 min period prior to 0800 and '7' refers to the 10 min period before 1700. Where a number of sources were detected within a small area, the area is ringed and the total shown by large figures.

It appears that a storm which at 0800 had formed over the middle of the Brest peninsula moved into the Channel and then NE'ward into S. England where it was identified as Storm 1, giving the hail whose distribution is shown in Figs. 6a and 6b. The path of the right-hand edge of the radar echo of this main storm is shown; the extreme SW position is given by reports from the airfield control radar at Hurn and can be seen to be directly in the path of the storm indicated by SFERICS for 0900, 1000 and 1100.

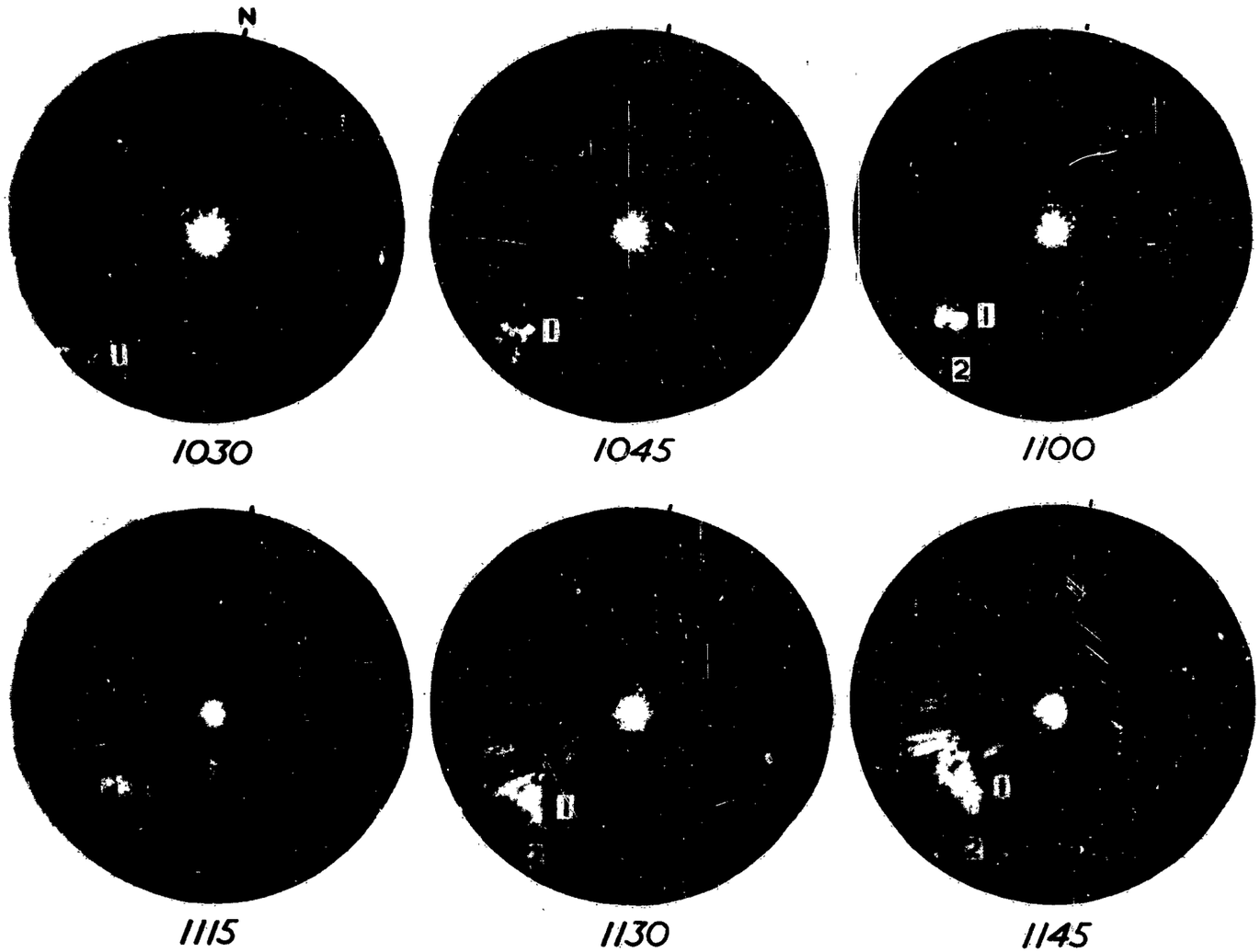

FIG. 3 Full gain 10 cm PPI photographs at 15 min intervals (with a 90 min break after 1300 owing to a power failure) showing the passage of the 7 separate storm areas across S.E. England.

The range markers are at intervals of 10 miles: azimuth markers are at 30° intervals from 010°.

Fig. 3

Fig. 3 cont.

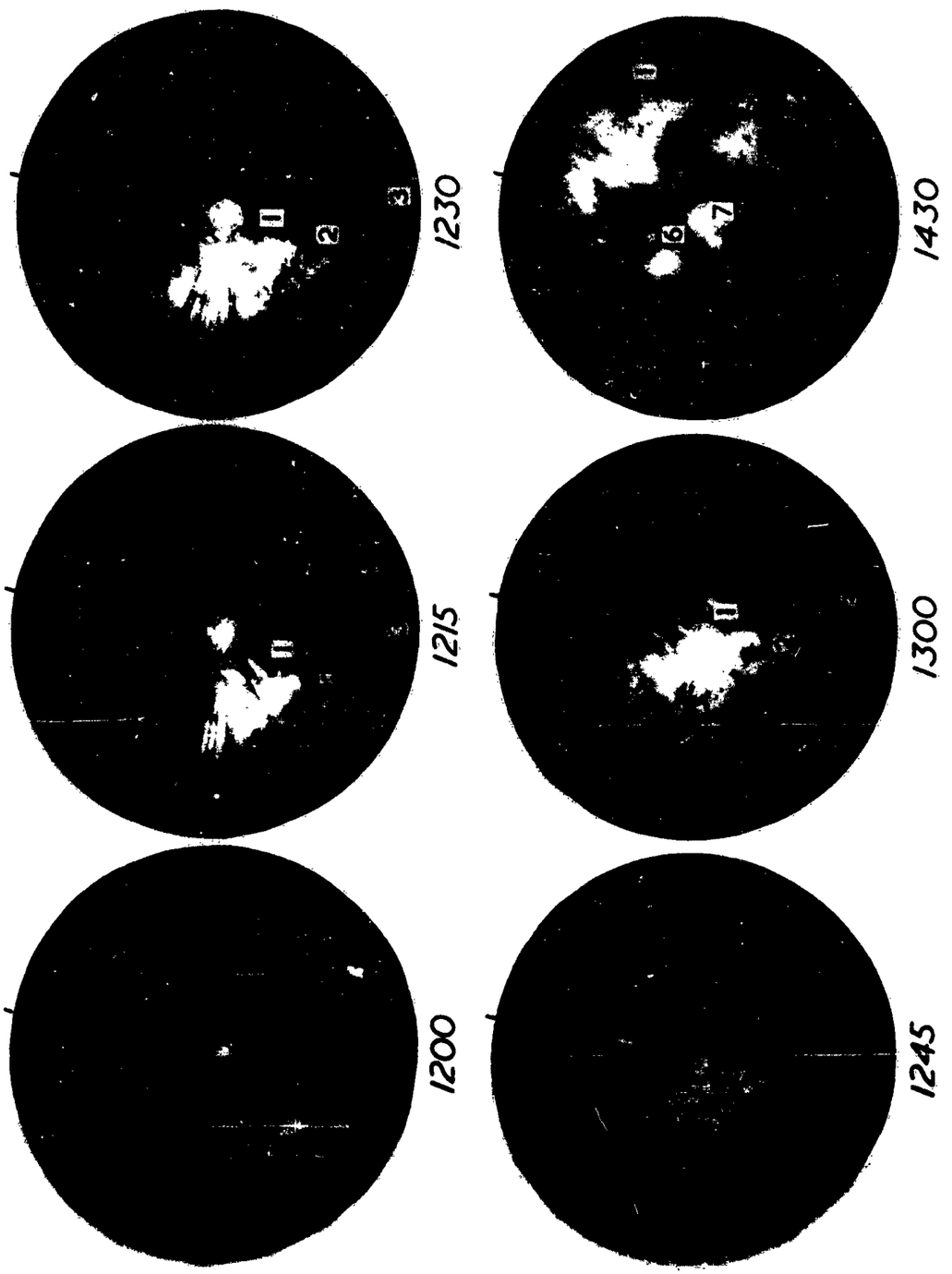

Fig. 3 cont.

Fig. 4

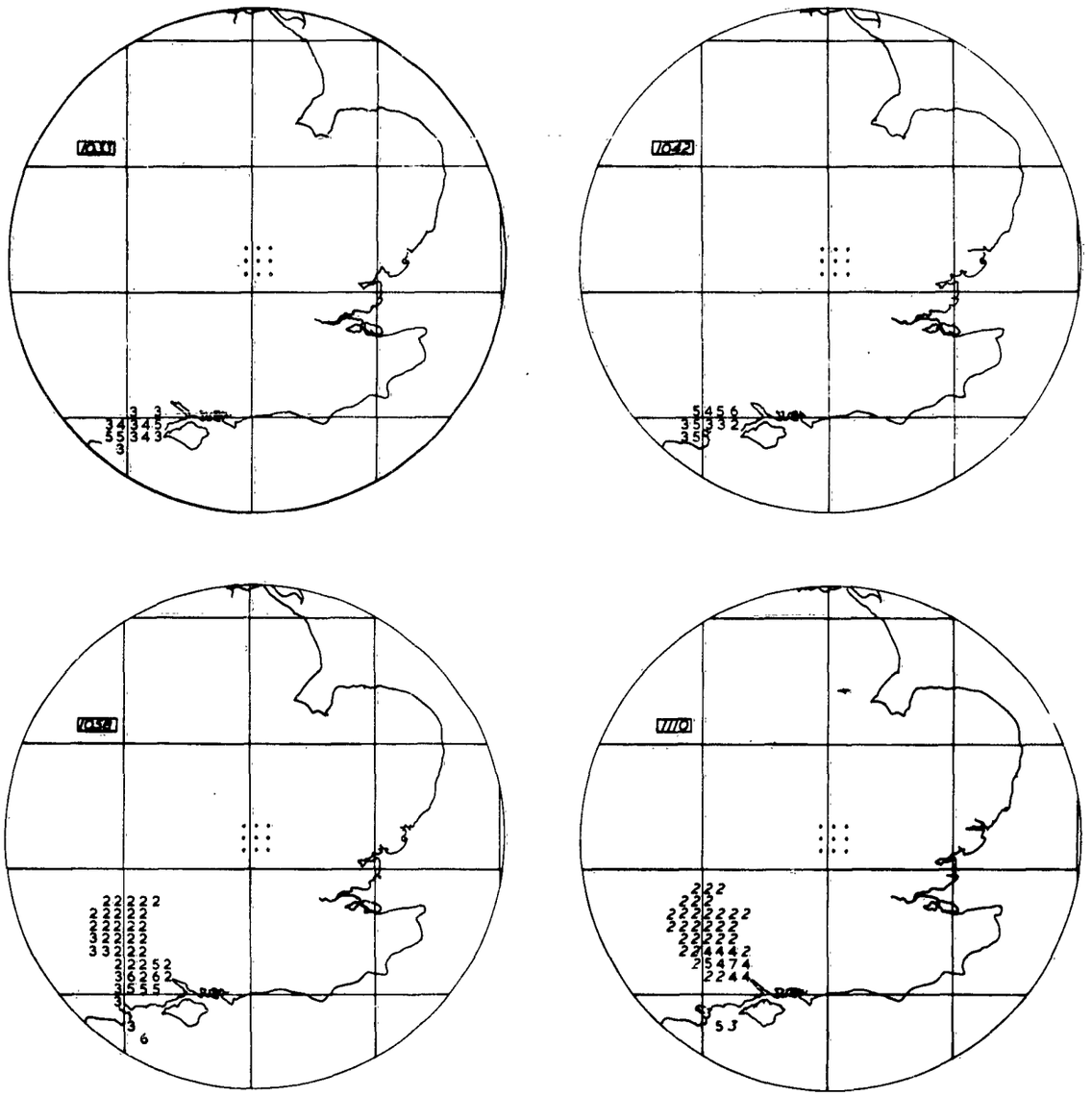

FIG. 4 The height-integrated echo-intensity distribution at roughly 20 min intervals (with a longer break during the power failure) over a region with the East Hill radar station as centre, deduced from the 10 cm PPI reduced gain series. The grid lines shown are those of the National grid and divide the area into squares of side 100 km. Each of these is sub-divided into 100 squares, which contain figures representing the greatest echo intensity present over any area of at least 4 km^2 according to the code of Table 1 (p. 4). (Where the figures are small their accuracy is poor, since they involve an arbitrary correction arising from the most intense region of echo occurring above the beam in intense storms at close ranges.

Where the figures are drawn sloping the correct intensity might correspond to the next higher figure: the ambiguity arises because of the omission of a step in the corresponding series of reduced gain photographs.)

The 9 dots in the centre of each diagram indicate those squares which are at least partly obliterated by echoes from ground objects.

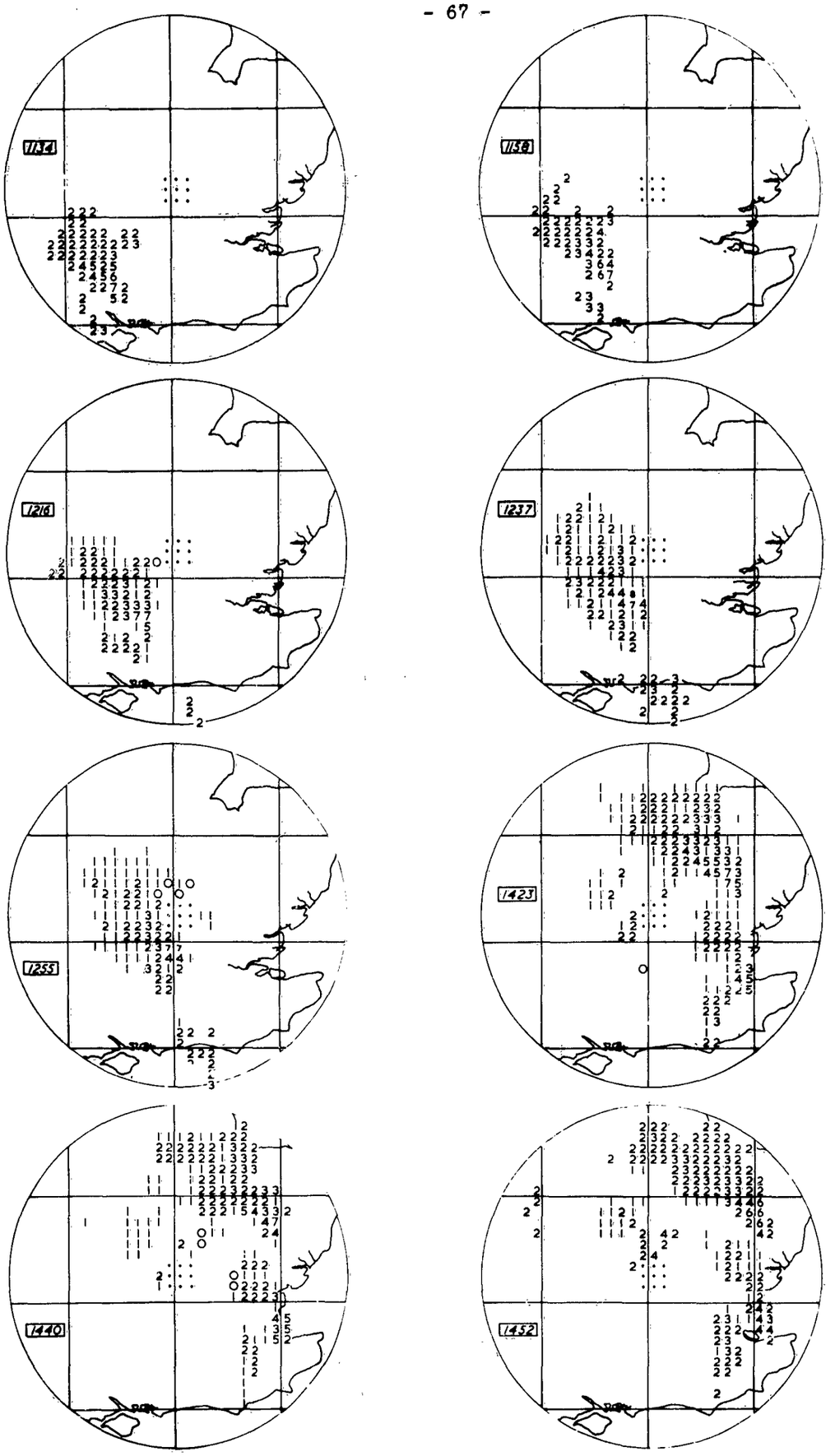

Fig. 4 cont.

Fig. 4 cont.

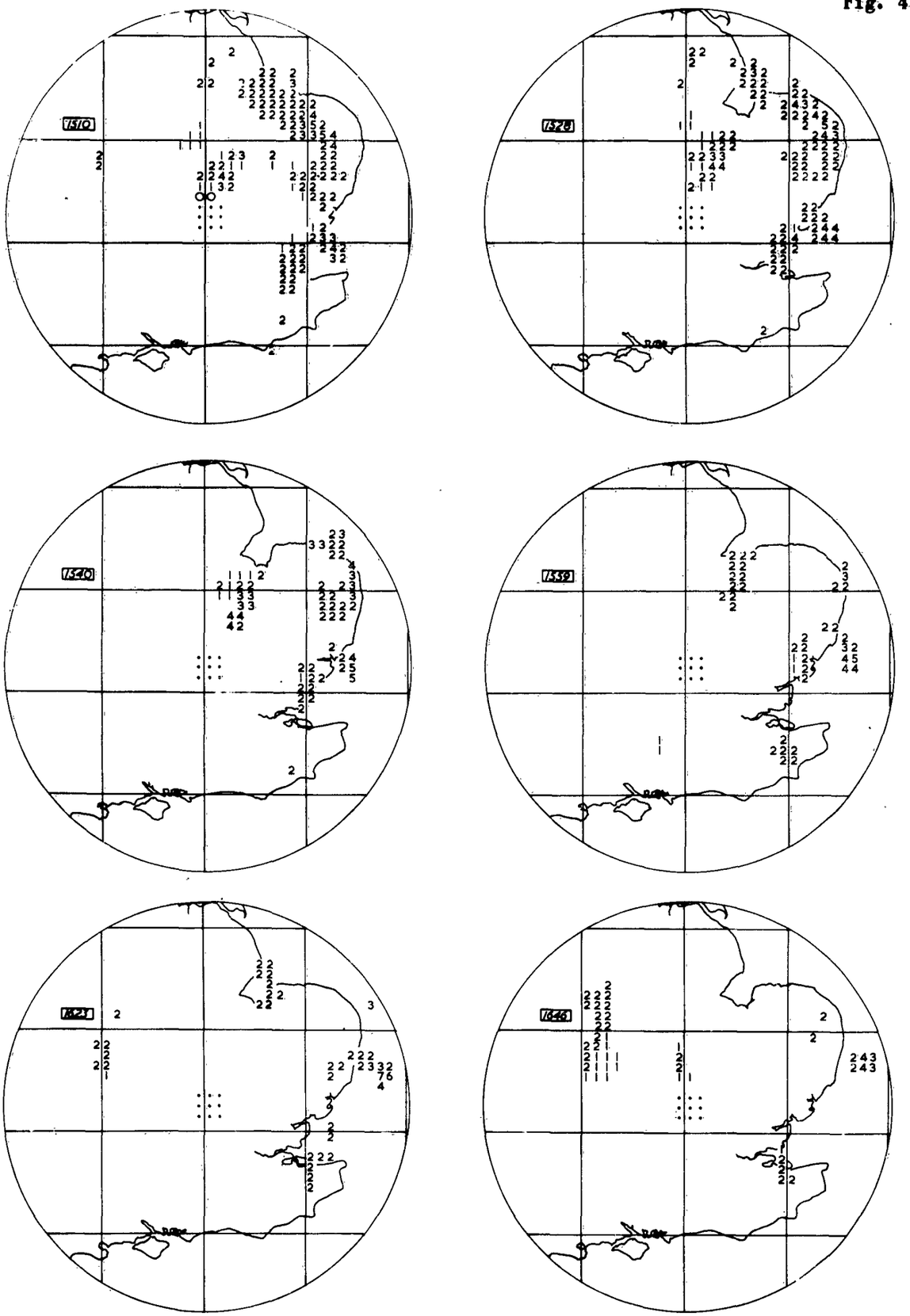

Fig. 5

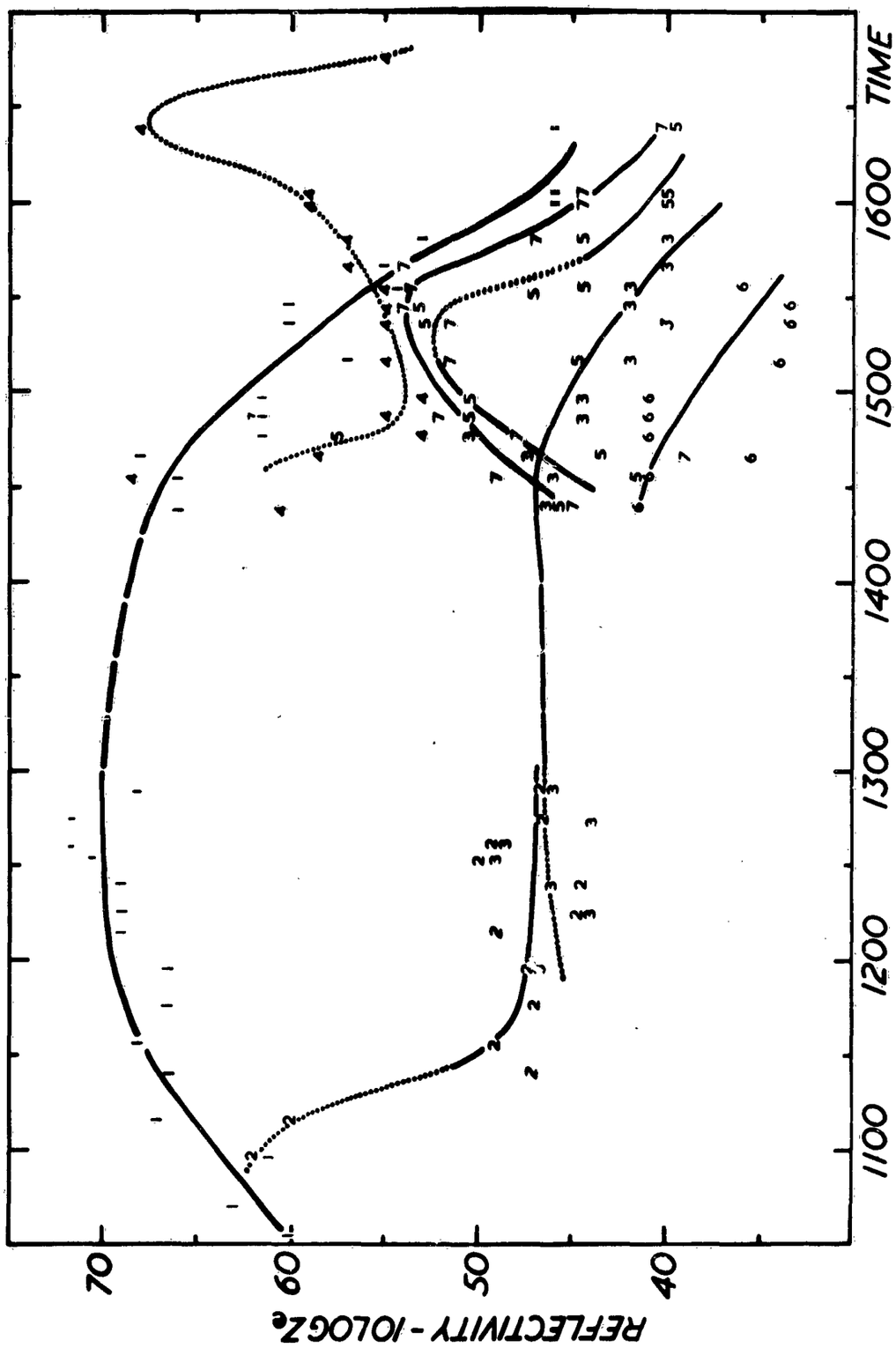

FIG. 5 The maximum intensity within each of the 7 storm areas as a function of time. The individual measurements have smooth curves drawn through them, which are dotted during periods when the storms were over the sea.

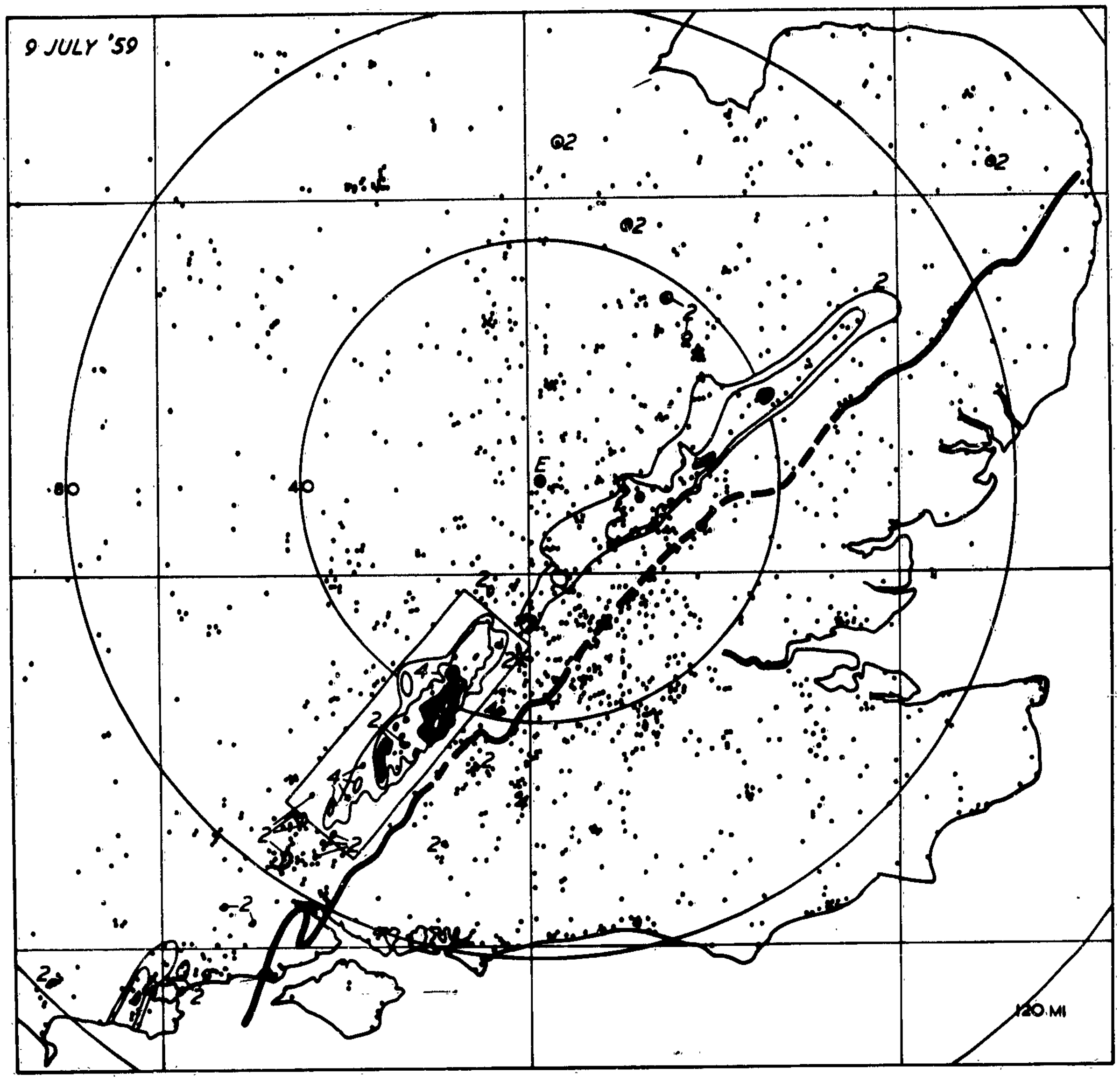

FIG. 6(a) Distribution of maximum hailstone size for 9 July 1959. The isopleths are for stones of sizes 2, 4, 6 and 8 (for scale see Table 2, p. 8).

The area between the size 6 and 8 isopleths is shown in black. Altogether there are 1935 observations whose positions are indicated. 442 of these lie within the rectangle surrounding the most severely affected area; their positions are indicated in the enlarged diagram in Fig. 6(b). The thick line is the path of the right flank of the main storm determined from the 10 cm PPI radar (continuous line) or the 4.7 cm PPI radar (dashed line); the rings are range markers drawn at distances of 40, 80, and 120 miles from East Hill radar station (E).

Fig. 6(b)

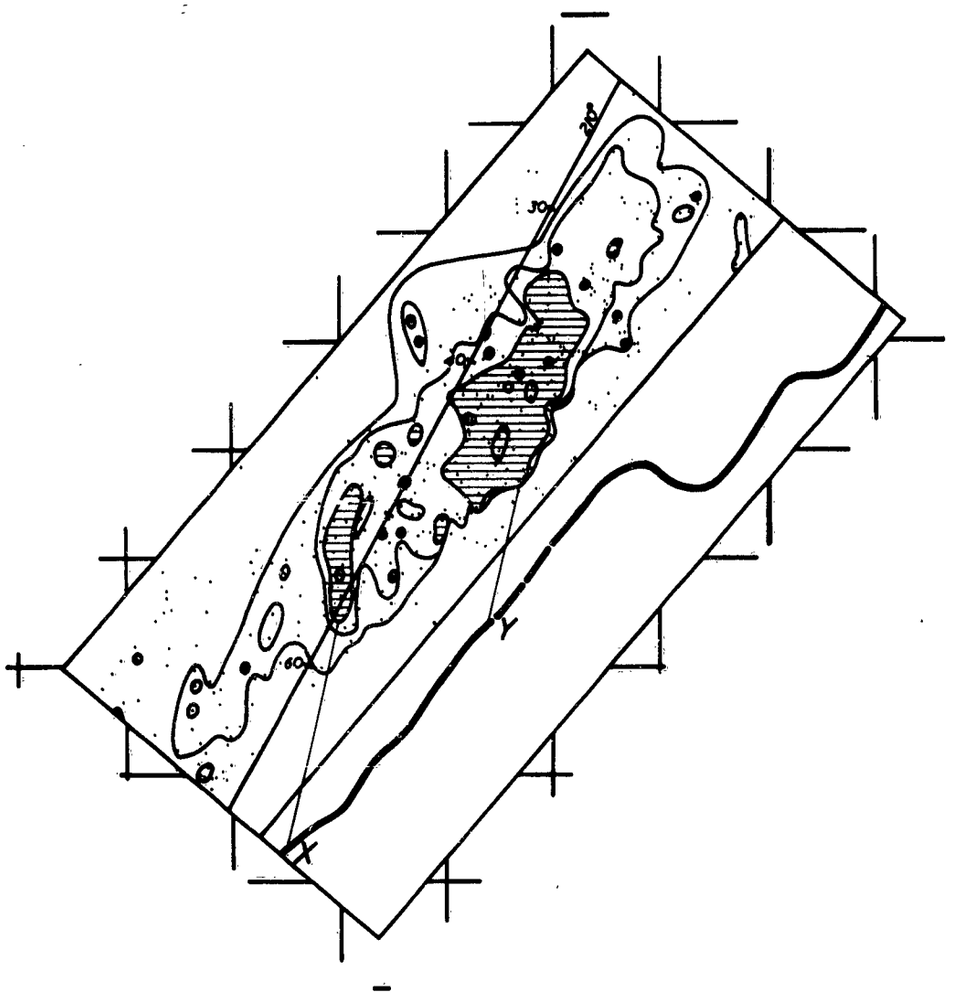

FIG. 6(b) Distribution of maximum hailstone size for 9 July 1959 within the rectangle shown in Fig. 6(a) containing the most severely affected area. The isopleths are for stones of sizes 2, 4, 6 and 8 (for scale see Table 2, p. 6).

The areas experiencing sizes greater or equal to 6 are shaded. The positions of the 442 observations within the rectangle are also indicated.

In addition, to the right of this rectangle is included the path of the right flank of the main storm determined from the 10 cm PPI radar. Two lines are drawn along a direction 195° indicating the likely displacements of those size 6 stones which fell nearest to the right flank at 2 different times. The lines leading from X and Y are shown in the text to imply periods of 760 and 1200 sec respectively for the growth of hail from a size which is just detectable to size 6.

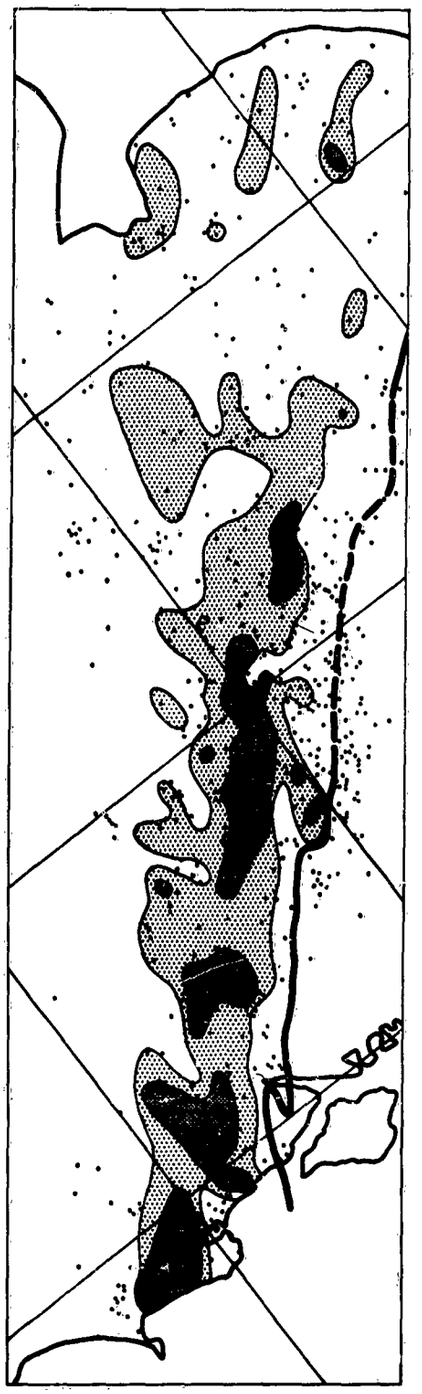

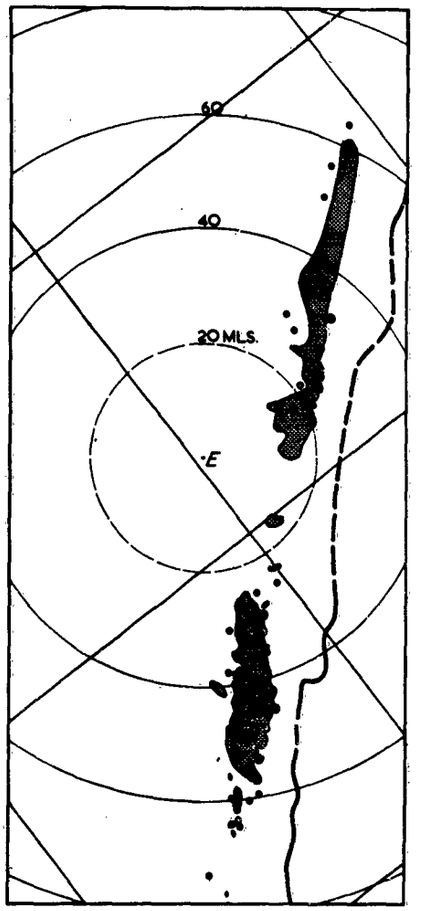

FIG. 8 The positions of highest echo tops and greatest echo intensities, as obtained by the 3.3 cm RHI radars, superimposed upon the region where the maximum hail size exceeded size 4 ($\geq \frac{1}{2}$ inch).

The small and large open circles denote observations of intensities which are equal to or exceed 65 and 70 respectively: the small and large filled circles denote the positions at which tops were observed at or higher than 40,000 ft and 43,000 ft respectively. (When a top exceeding 40,000 ft was followed for some time, only the position at which it reached its peak height is plotted.)

E denotes the position of the East Hill radar station. The thick line represents the path of the right flank of the main storm. Notice that tops above 43,000 ft occurred over an 8-mile-wide front at a range of 45 miles.

It was impossible to survey the tops within 20 miles because they were above the tops of the radar beams.

FIG. 7 Smoothed rainfall pattern in the vicinity of the path of the main storm (1); isopleths are for $\frac{1}{4}$, $\frac{1}{2}$, $\frac{3}{4}$, and 1 inch. Areas with more than $\frac{1}{4}$ in but less than $\frac{1}{2}$ in are shown lightly shaded: areas experiencing more than $\frac{1}{2}$ in are shown more heavily shaded.

The positions of the rainfall observations are also indicated. E denotes the location of the East Hill radar station. The thick line represents the path of the right flank of the main storm (1).

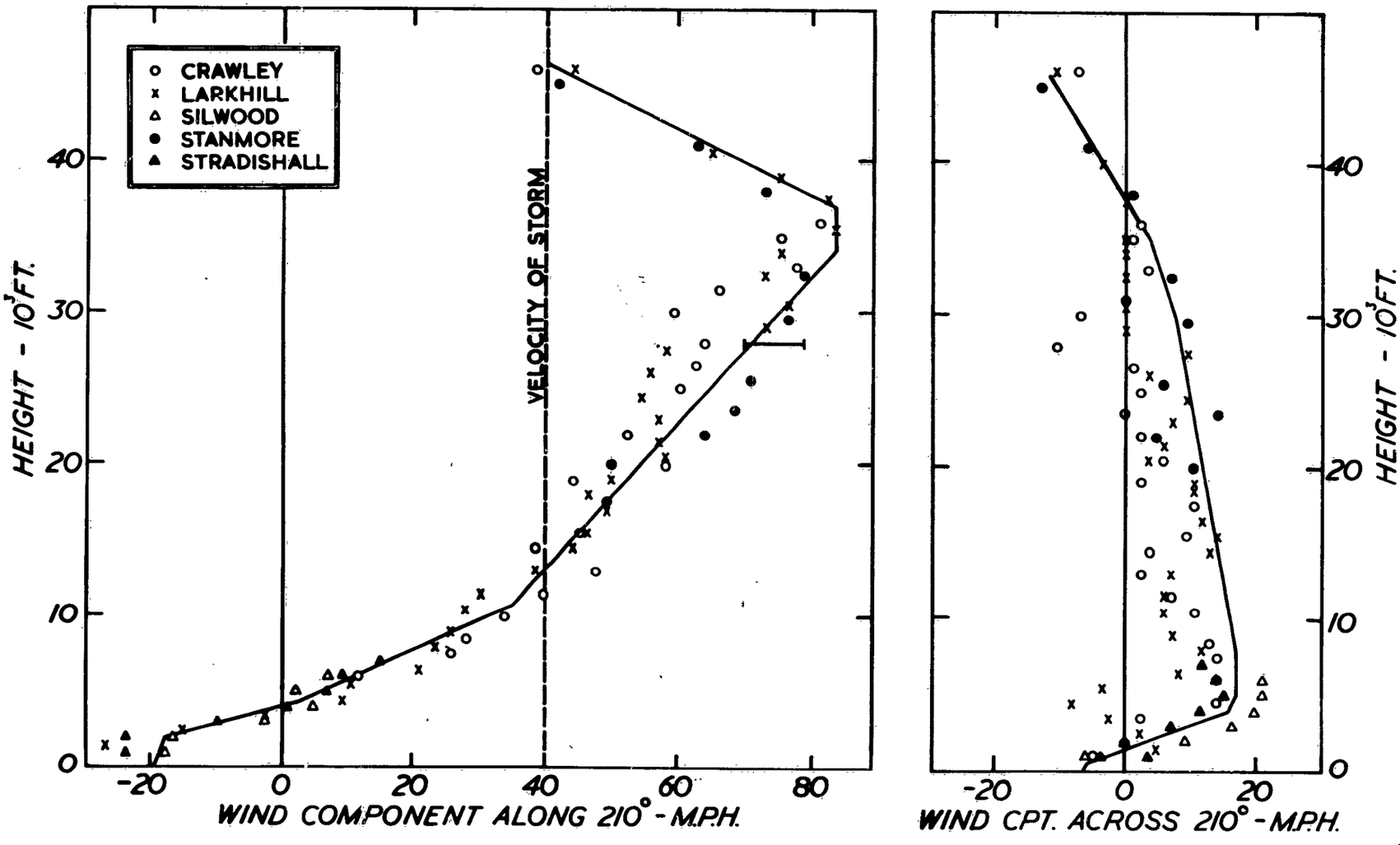

FIGS. 9(a) & (b) Wind components along and across the direction 210° as a function of height at 5 stations. The continuous line drawn through the points denotes the wind profile adopted for the winds around the main storm (1) during its intense phase.

The single additional observation of the component wind speed along 210° at 28,000 ft which is shown in Fig. 9(a) was derived by following 2 identifiable anvil echo elements for about 15 min. Notice the greater wind components across 210° below 6,000 ft observed at Silwood just ahead of the main storm (1).

Figs. 9(a & b)

Figs. 10(a,b,c,d,e,f & g)

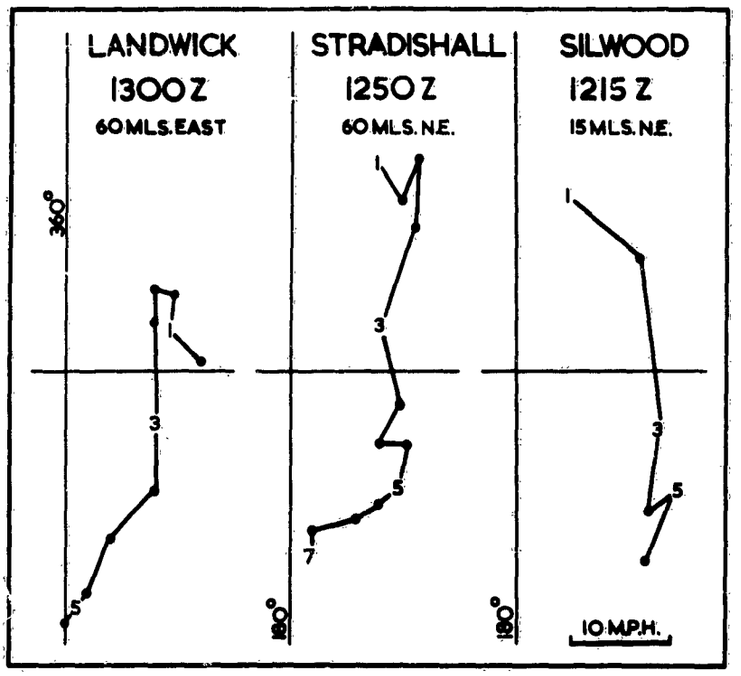

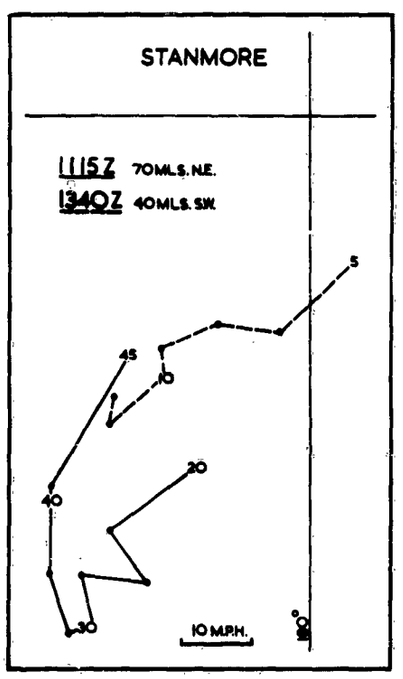

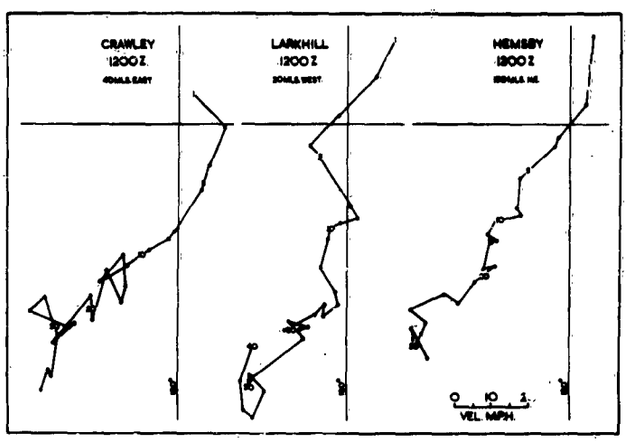

FIGS. 10(a,b,c,d,e,f and g)

Wind hodographs for 9 July 1959. (The small numbers denote height in thousands of feet.) Also indicated are the distance and direction of each sounding from the core of the main storm (1).

Notice that the Silwood sounding - which was the nearest to the leading edge of this storm - shows a greater wind component from the East in the lowest 6,000 ft.

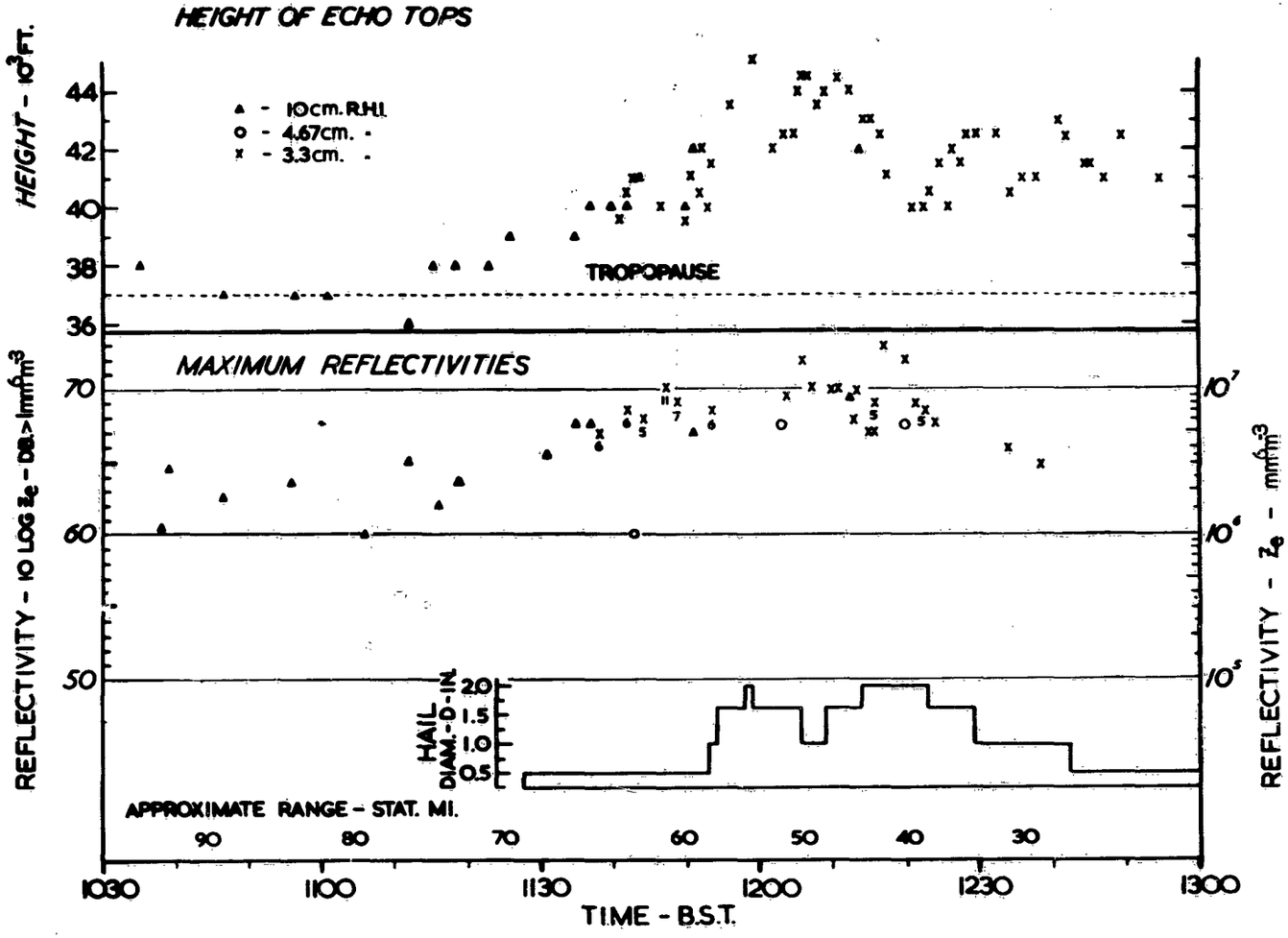

FIG. 11(a) Maximum observed reflectivities at 3 wavelengths, and maximum echo heights, as a function of time.

(The small numbers shown below the reflectivity measurements of the 3.3 cm set indicate the height interval in thousands of feet over which the intensity was observed.) An approximate range scale is indicated by which the maximum hailstone size at the ground is included. It can be seen that during the fall of the large hail there was a noticeable increase, on all radars, of the peak heights and intensities of the echoes.

Fig. 11(a)

Fig. 11(b)

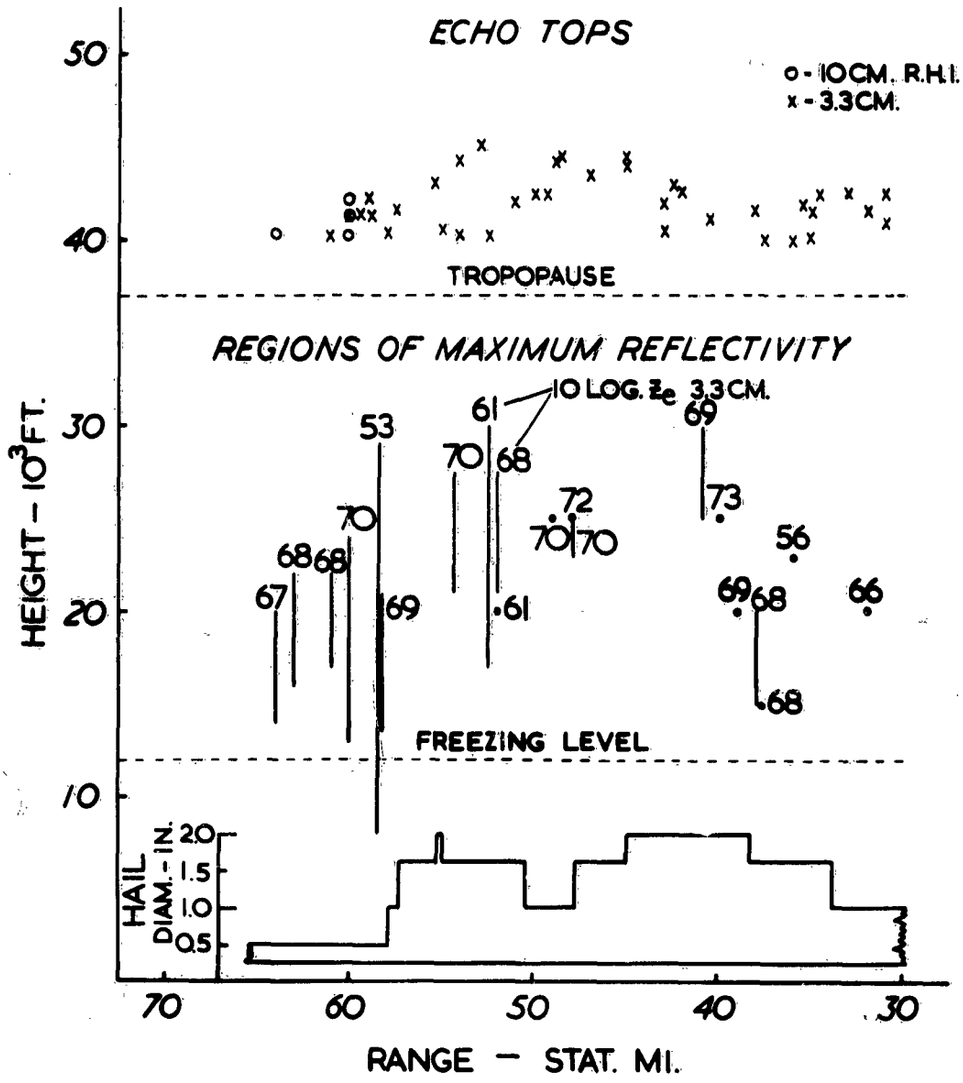

FIG. 11(b) Observed vertical extents of reflectivity maxima (vertical lines) and their values (expressed as 10 log Z_e), together with maximum echo heights and maximum hail sizes at the ground.

Fig. 12

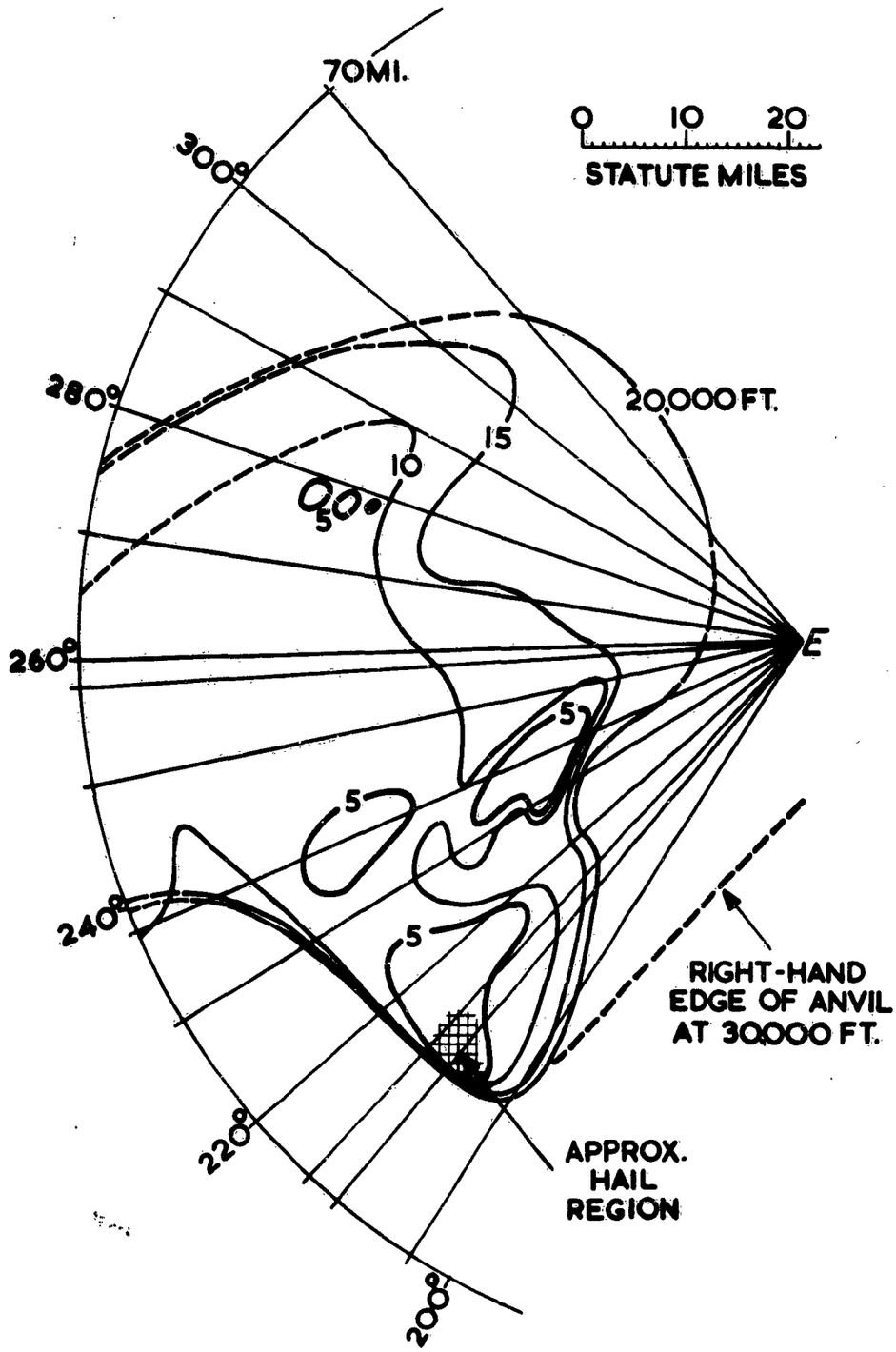

FIG. 12 General structure of the main storm (1) at 1900 as shown by contours of the height of the full gain echo base obtained from a series of 13 3.3 cm RHI sections along the azimuths indicated. The contours are drawn dashed at long ranges where they are rendered inaccurate owing to attenuation, and at short ranges where the base of the anvil 'cloud' lay above the top of the radar beam. The right-hand edge of the anvil at 30,000 ft was obtained from the MPS-4 data, and the approximate extent of the hail region was inferred from ground observations. E denotes the location of the East Hill radar station.

Fig. 13

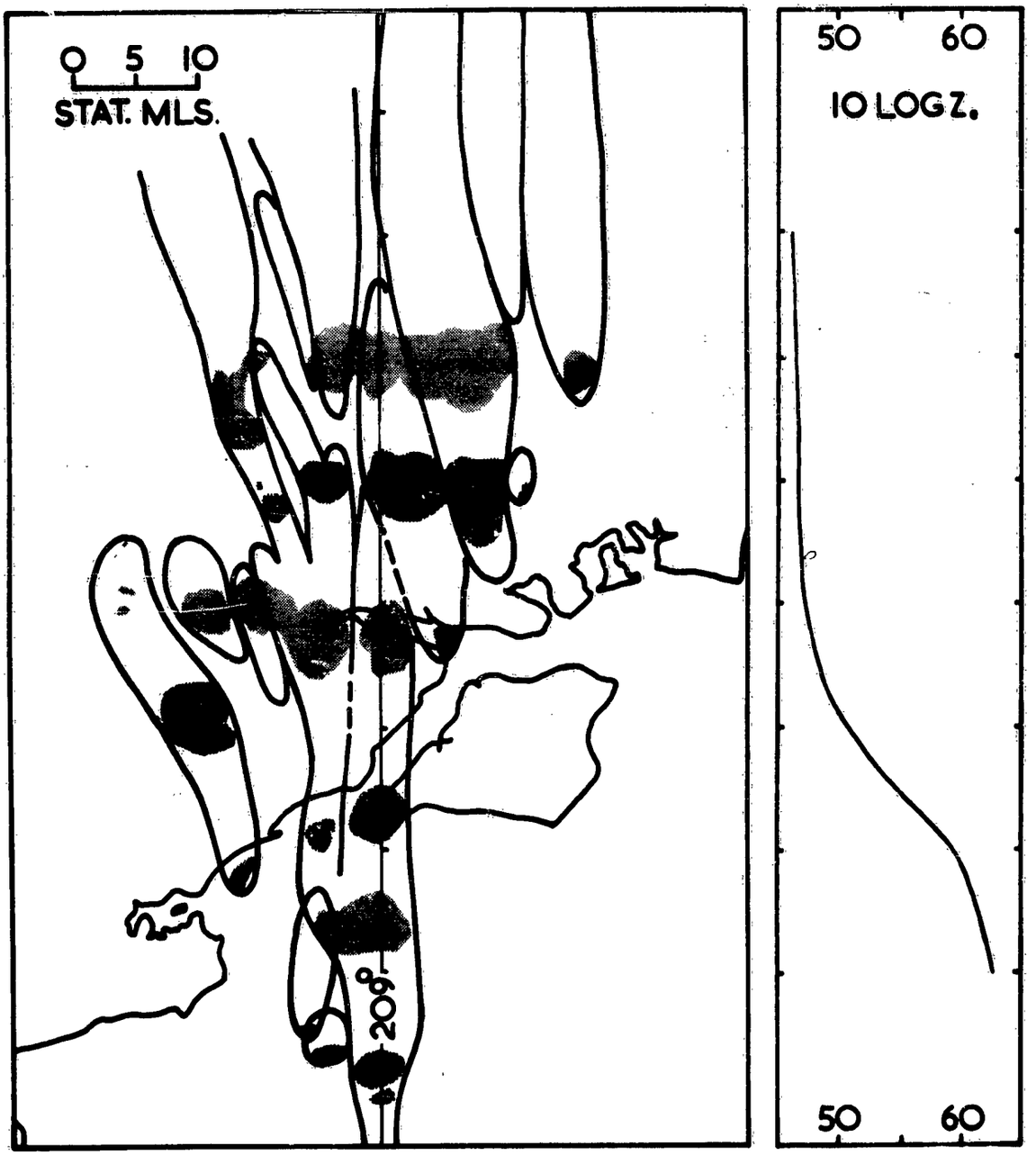

FIG. 13 Paths of echo-masses comprising storm 2. Their positions are indicated at times 1051, 1109, 1124, 1145, 1203 and 1218. Also included is the trend of the intensity of the most intense echo-mass within the storm.

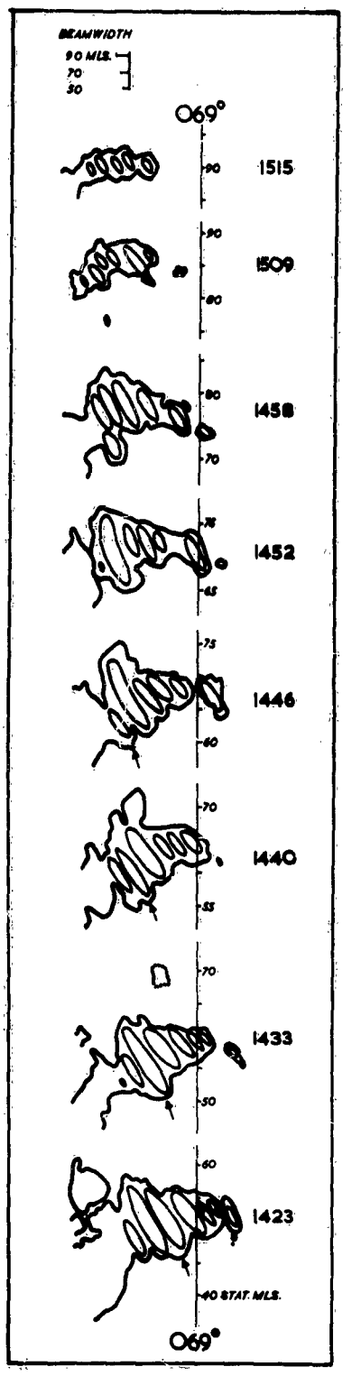

FIG. 14(a) Sketches of a series of 10 cm PPI photographs showing the core of the main storm (1). They refer to a period from 1422 to 1516 when the storm was moving away NE'wards from the radar site and weakening. Although 5 or 6 intensity contours are available, for the sake of clarity only one is shown in each diagram. This represents an intensity of [34] at 50 miles range increasing to [43] at 90 miles. The row structure within the echo-mass is indicated schematically by the inner contours. The arrow which is shown in the first 4 diagrams points to the rear of one of the rows which is particularly easily identifiable throughout. The dashed contour shown at 70 miles range at 1433 denotes an intensity of only [31]: it is included because this echo was subsequently overtaken by the principal echo-mass of the main storm (1) complicating the history of one of the rows.

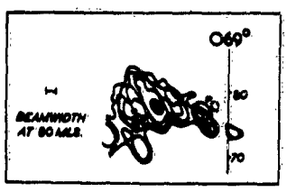

FIG. 14(b) Sketch of the outlines of 4 photographs of the 10 cm PPI displays at different gain reductions around 1458. The row structure is indicated by means of dotted lines.

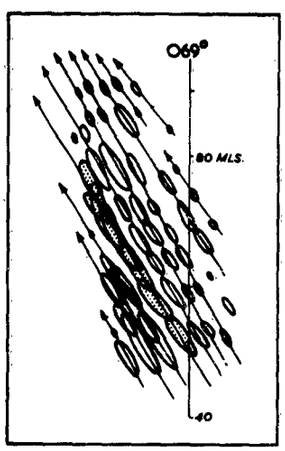

FIG. 14(c) Paths of the rows identified in Fig. 14a. They are straight and along the direction of the wind (whose direction was constant above 3,000 ft). The behaviour of the shaded row was complicated by amalgamation with a smaller echo which it overtook (cf. Fig. 14a)

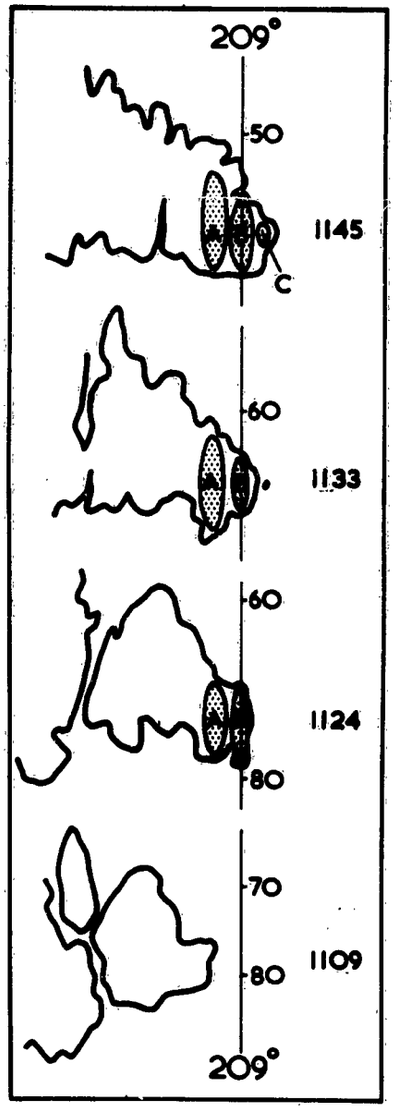

FIG. 16(a) Row structure within the core of the main storm (1) before it reached its peak intensity. For clarity only one intensity contour is shown; this corresponds to [38] at 60 miles range and [42] at 80 miles range. The echo to the left of row A was an amalgamation of a cluster of echoes which earlier had crossed the south coast; it possessed no discernible row structure.

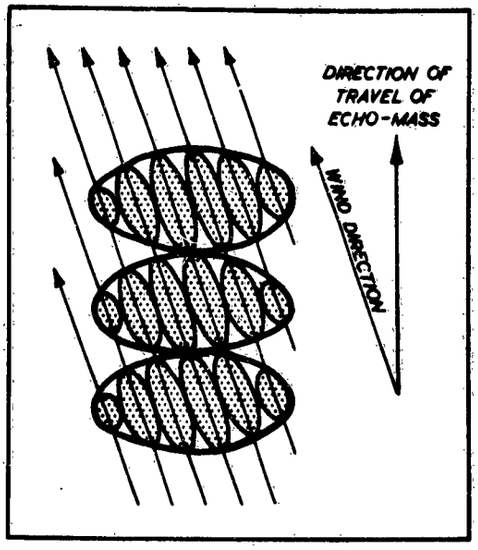

FIG. 15 Schematic diagram illustrating how the formation of new echoes at the right flank of the storm and their eventual decay on the left flank causes the movement of the echo-mass as a whole to the right of the winds.

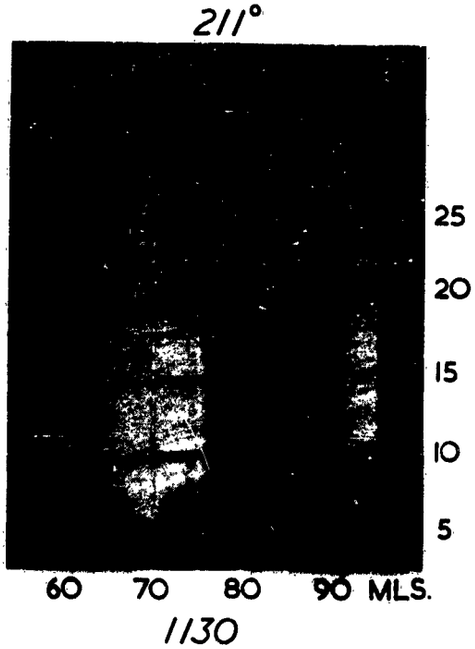

FIG. 16(b) 10 cm RHI photograph along the axis of row A at 1130. Storm 2 can be seen some 15 miles behind the main storm (1). Height markers are shown at intervals of 5,000 ft and range markers at intervals of 5 miles. Notice the great height of the radar horizon at these ranges.

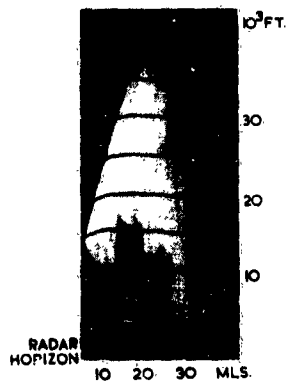

FIG. 17

Full gain 3.3 cm RHI photograph on azimuth 182° at 1247. It is typical of 13 such photographs taken between 1225 and 1255 in which the radar beams were directed obliquely across the leading edge of the echo mass, as shown in Fig. 18, in order to examine the rise of columns in the most recently formed row on its right flank.

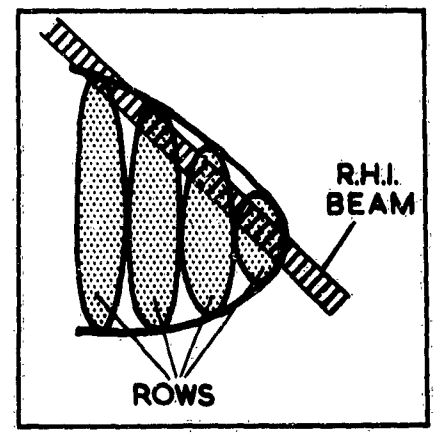

FIG. 18

Schematic diagram illustrating the manner in which photographs typified by Fig. 17 were obtained.

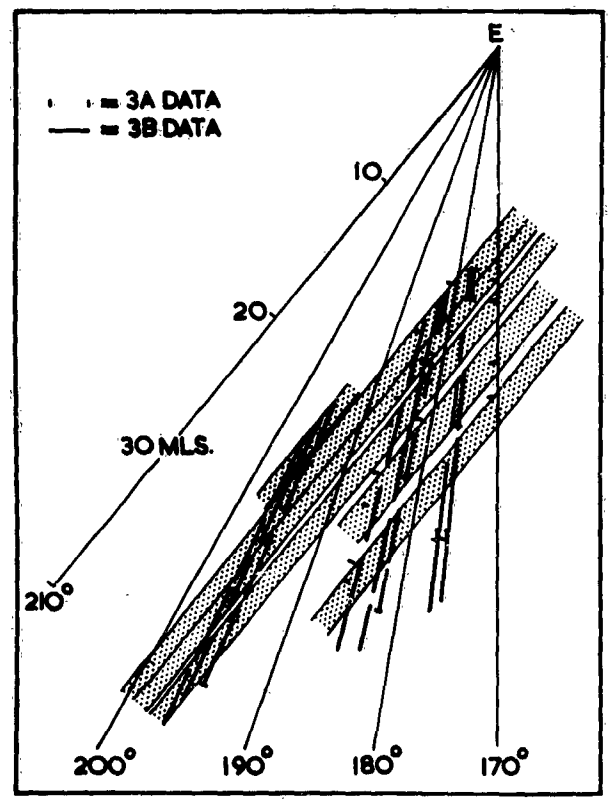

FIG. 19 Paths of rows deduced from the positions of the steps in the 13 3.3 cm RHI photographs which are typified by Fig. 17. E denotes the position of the East Hill radar station.

Fig. 20

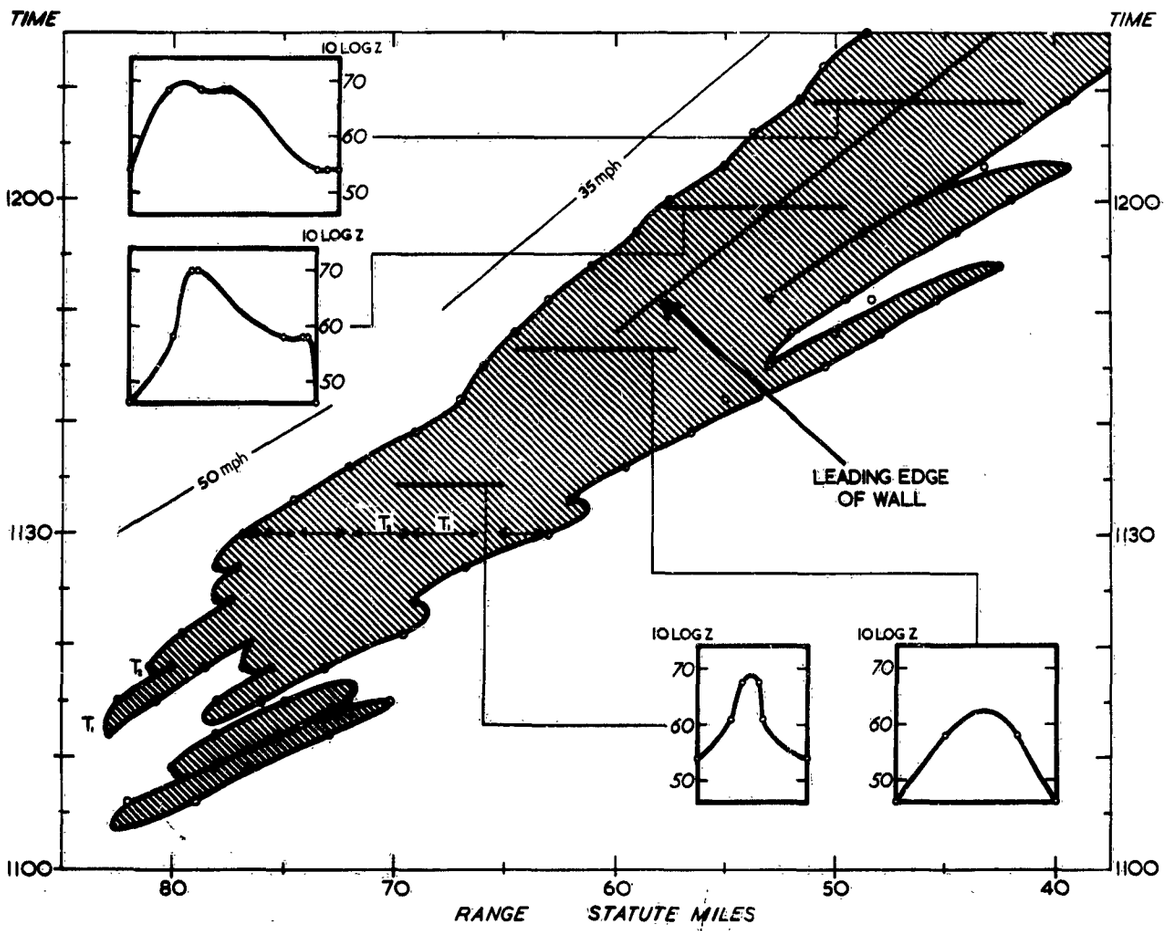

FIG. 20 Range of the rear and leading edges of the echo of row A as a function of time, determined from the full gain 10 cm PPI photographs taken at 3-min intervals. Also indicated is the position of the leading edge of the wall, which was deduced from the 3.3 cm RHI photographs. Profiles of intensity are given for times 1134, 1147, 1159 and 1209; these were deduced from series of reduced gain 10cm PPI photographs.

The approximate positions of the columns visible in the 10 cm RHI photograph of row A at 1130 (Fig. 16b) are shown, and the two towers T_1 and T_2 (which can be traced throughout the series of photographs in Fig. 21) are identified.

After 1147 the row structure ceased to be recognisable; thereafter Fig. 20 has been derived by considering that section of the echo-mass which corresponded to the continuation of row A.

Fig. 21

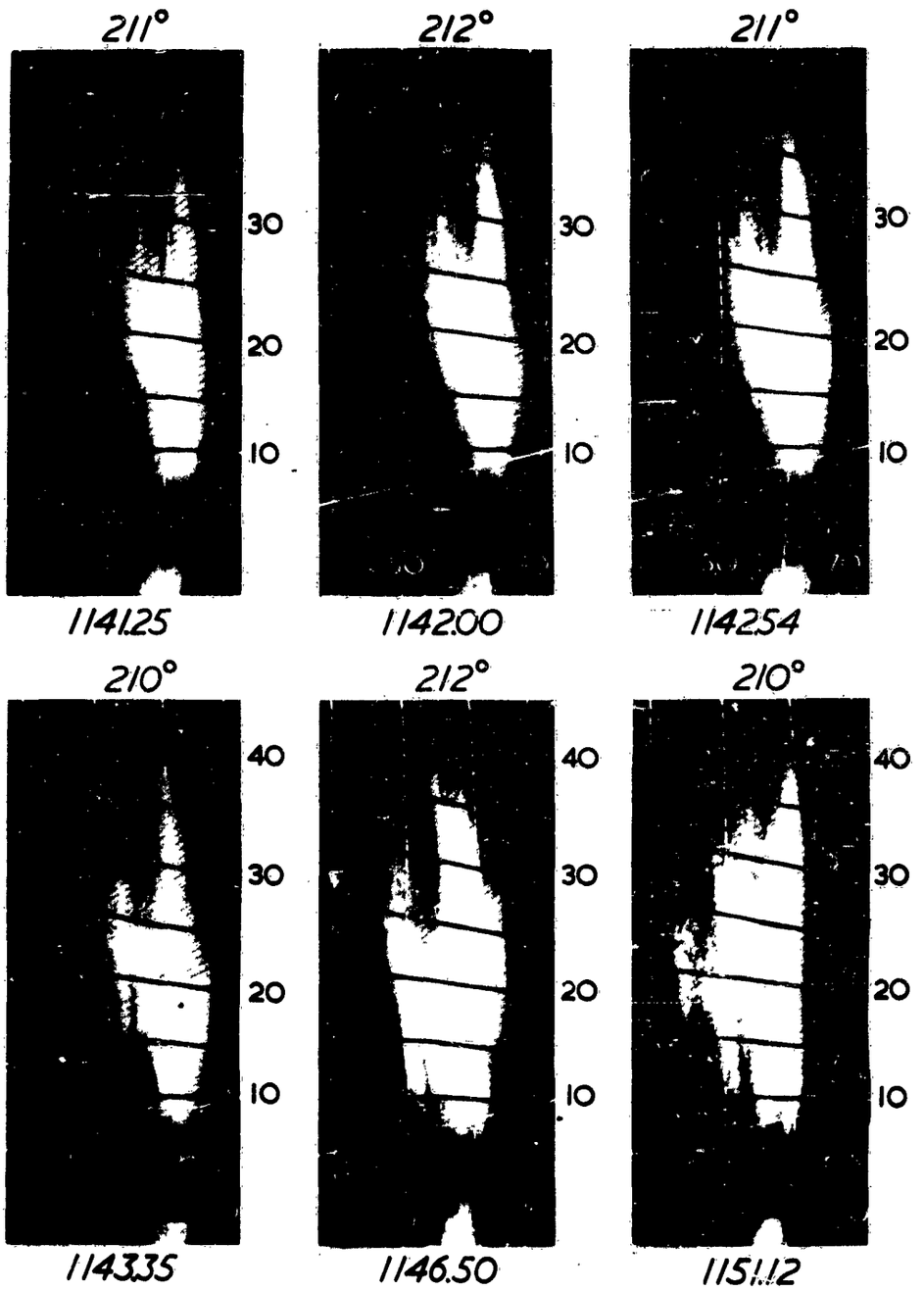

FIG. 21 Full gain 3.3 cm RHI photographs along the axis of row A. Two towers, T_1 and T_2, can be followed throughout the series as the storm approached the radar.

Height markers are at intervals of 5,000 ft and range markers at intervals of 10 miles. The radar horizon ($1\frac{1}{2}^0$) is indicated in each photograph.

Figs. 22 & 23

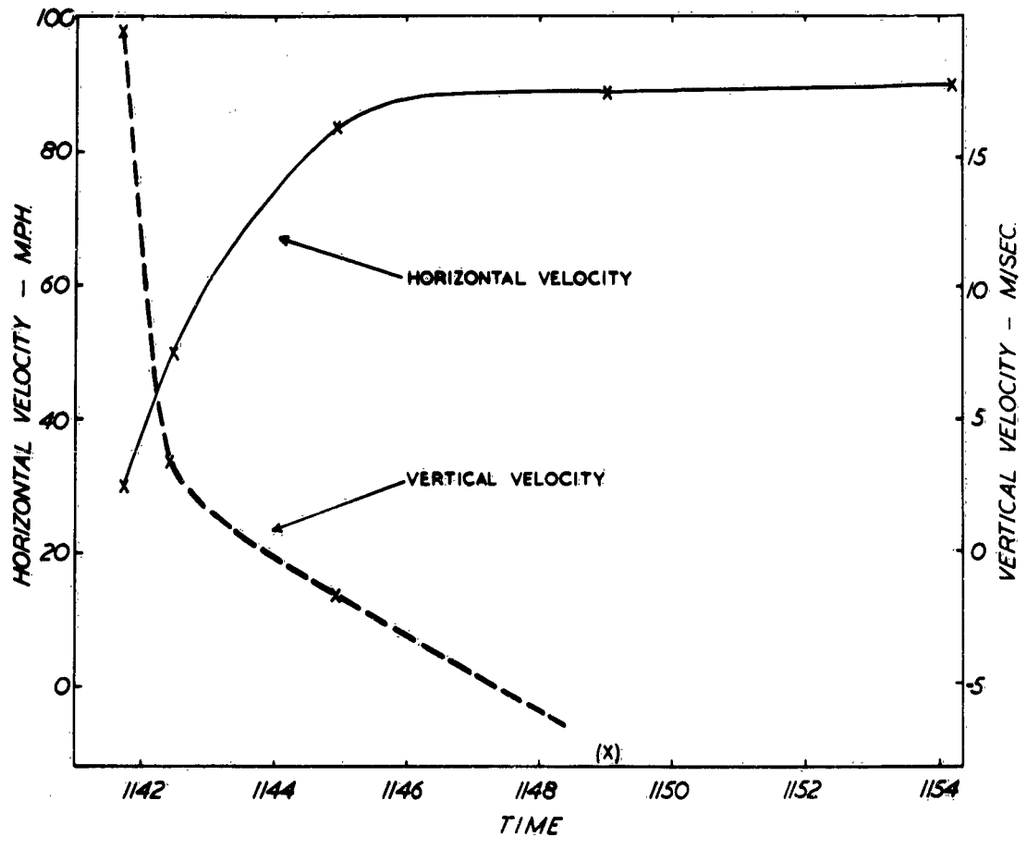

FIG. 22 Horizontal and vertical velocity of the top T_2 as a function of time: a part of the history of this top is shown in Fig. 21.

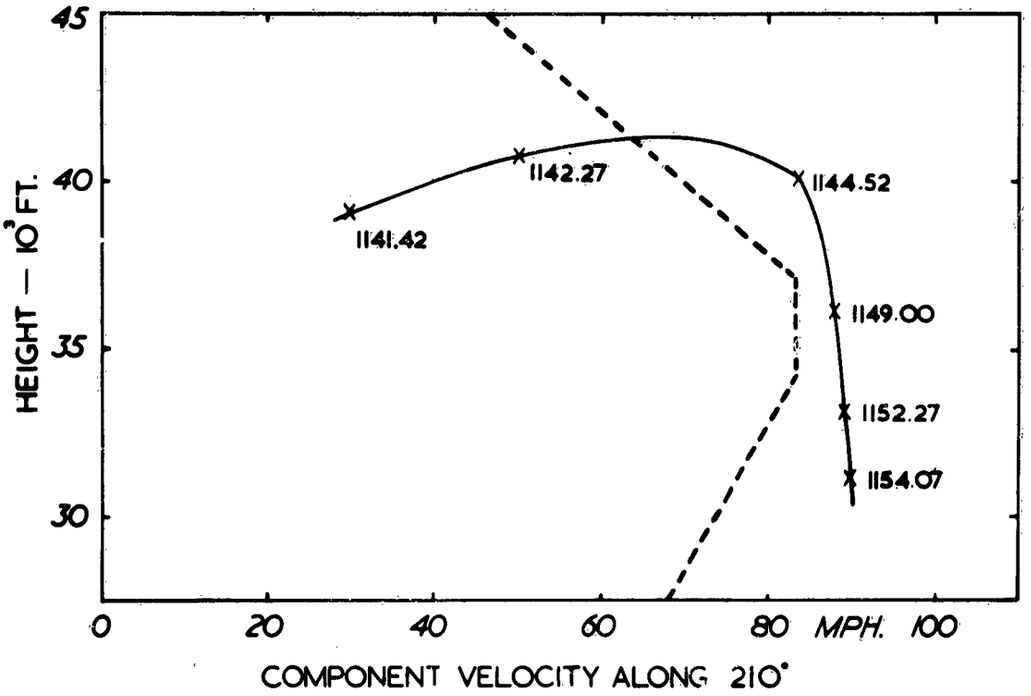

FIG. 23 Comparison of the horizontal velocity of top T_2 with that of the environment. Notice that the top reached a speed which was 5 mi/hr greater than the maximum speed of the environmental wind.

Fig. 24

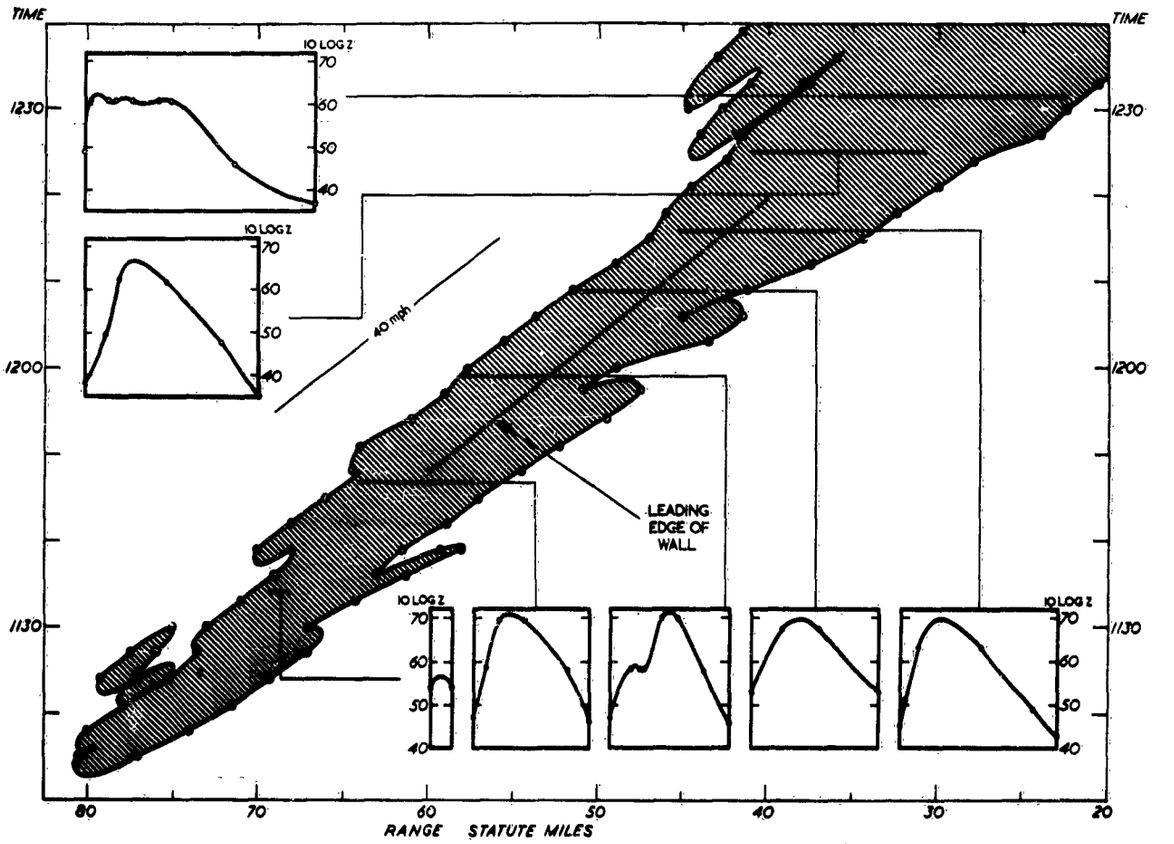

FIG. 24 Range of the rear and leading edges of the echo of row B as a function of time, determined from the full-gain 10 cm PPI photographs taken at 3-min intervals. Also indicated is the position of the leading edge of the wall, which was deduced from the 3.3 cm RHI photographs. Profiles of intensity are indicated for times 1134, 1147, 1159, 1209, 1216, 1225 and 1232; these were derived from series of reduced-gain 10 cm PPI photographs. After 1147 the row structure ceased to be recognisable; thereafter Fig. 24 has been derived by considering that section of the echo-mass which corresponded to the continuation of row B.

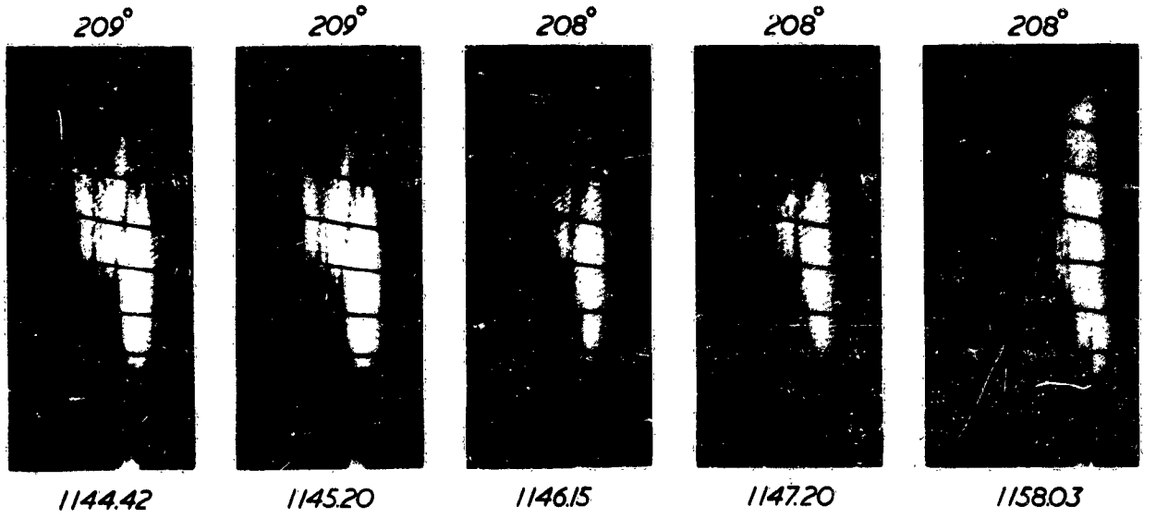

FIG. 25 Full-gain 3.3 cm RHI photographs along the axis of row B. The first 4 photographs in this series include the tops of the columns in row A which lay in the edge of the beam. The fifth photograph, taken some time later, is typical of the most intense phase and shows the characteristic forward overhang, echo-free vault and wall with the highest top vertically above it.

Height markers are at intervals of 5,000 ft, and range markers at intervals of 10 miles. The radar horizon (at 1½°) is indicated in each photograph.

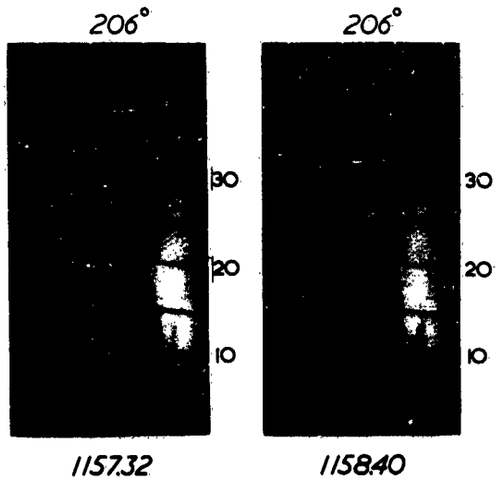

FIG. 26 Full-gain 3.3 cm RHI photographs along the axis of row C. Also visible are the (higher) tops of the columns in row B, which lay in the edge of the beam.

Height markers are at intervals of 5,000 ft, and range markers at intervals of 10 miles. The radar horizon (1½°) is indicated in both photographs.

Fig. 27(a & b)

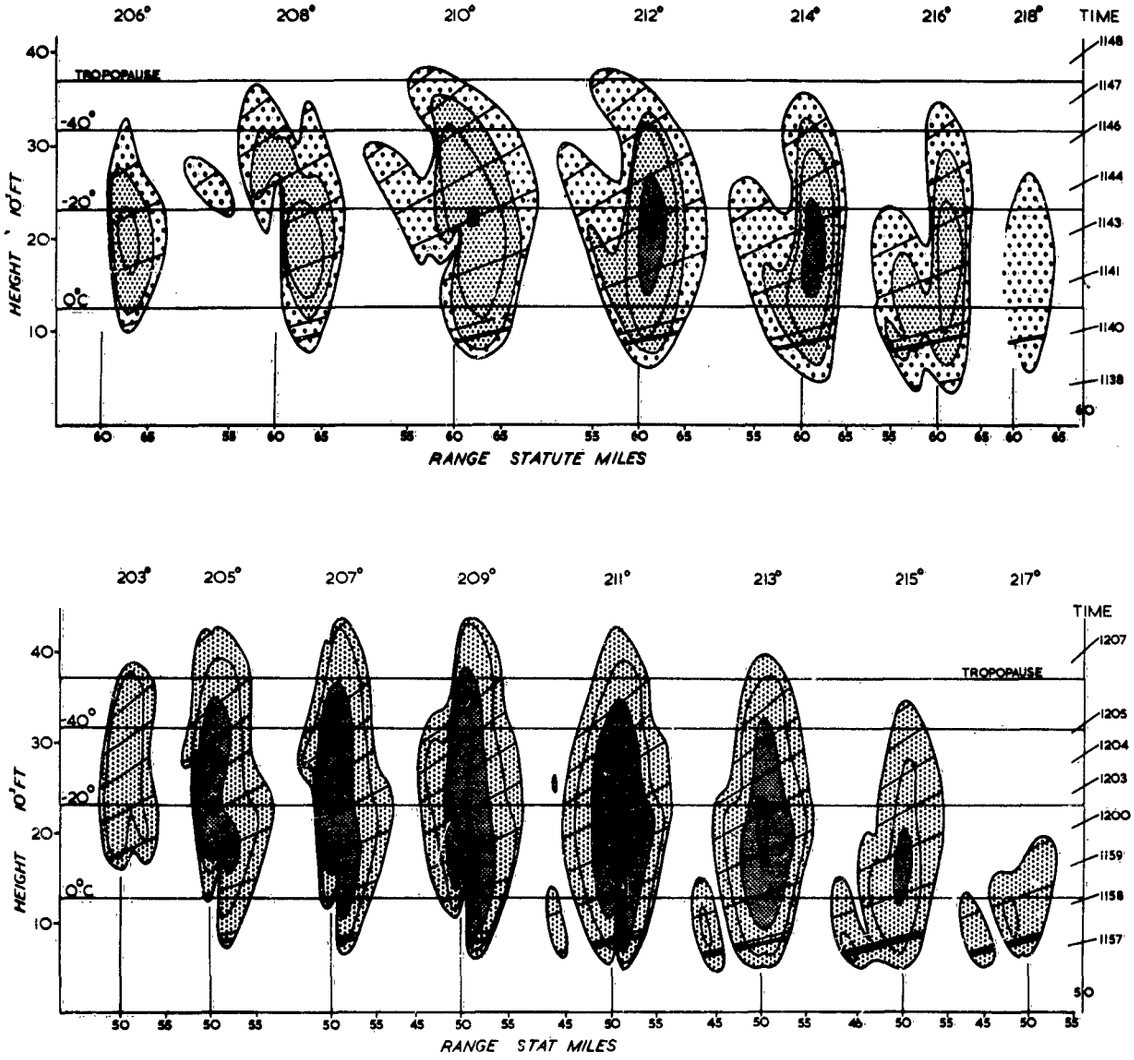

FIG. 27 (a, b & c) RHI sections at 2° intervals through the main storm approximately along its direction of movement for the 3 periods:

(a) 1137 - 1149 (during the development of the new organisation)
(b) 1156 - 1208
(c) 1213 - 1225

These have been derived from 4.7 cm PPI photographs taken at a series of gain steps at successive elevations. These photographs have been displaced assuming that the storm as a whole moved uniformly along 210° at 40 mi/hr to make the ranges indicated in Figs. (a), (b) & (c) applicable to the times 1142, 1202, and 1220 respectively. The times at which the photographs at the indicated elevations were obtained are shown to the right of each figure.

The radar horizon is shown as a thick line where it intersects each RHI section.

The contours refer to different gain steps, the intensities corresponding to which are listed below:

Range to which intensity is strictly applicable (mi)		Fig. (a) 60	Fig. (b) 50	Fig. (c) 40
Coarse stipple		(17)-(30)	-	-
Medium stipple		(30)-(39)	(29)-(38)	(27)-(36)
		(39)-(51)	(38)-(49)	(36)-(48)
Fine stipple		(51)-(58)	(49)-(58)	(48)-(56)
		> (58)	> (58)	(56)-(62)
		-	-	> (62)

Because of the large horizontal extent of intense echo, the small corrections for beam-width have not been applied to these values.

Fig. 27(c)

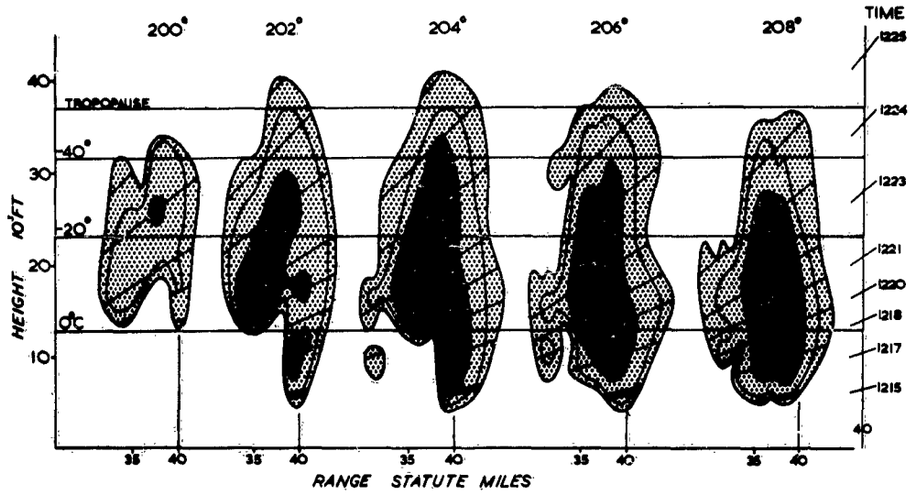
200°
202°
204°
206°
208°
TIME
1225
1234
1223
1221
1220
1218
1217
1215
40
TROPOPAUSE
-40°
-20°
0°C
HEIGHT 10'FT
40
30
20
10
35
40
RANGE STATUTE MILES

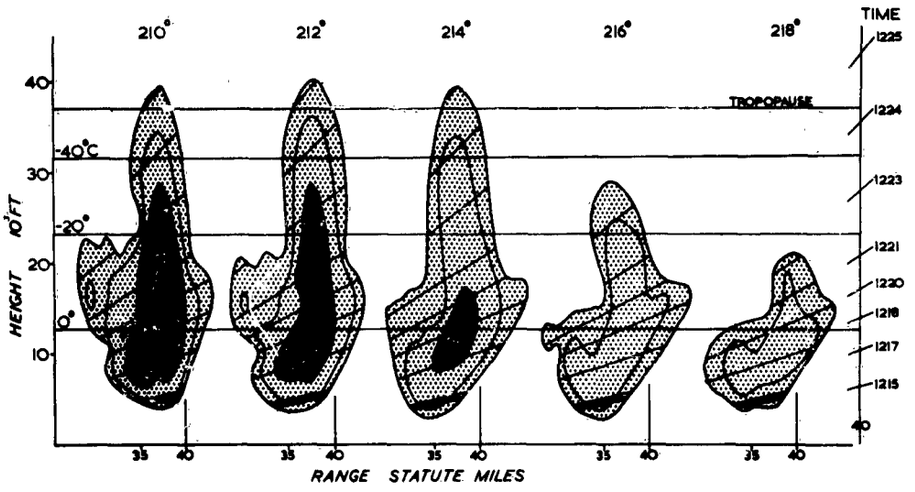
210°
212°
214°
216°
218°
TIME
1225
1234
1223
1221
1220
1218
1217
1215
40
TROPOPAUSE
-40°C
-20°
0°
HEIGHT 10'FT
40
30
20
10
35
40
RANGE STATUTE MILES

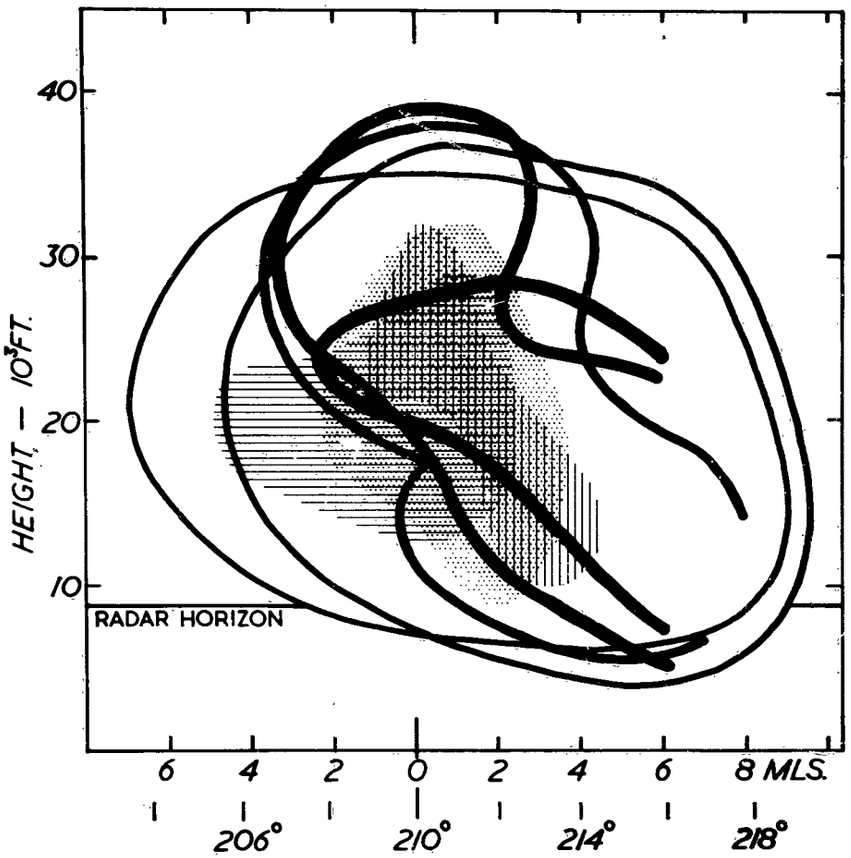

FIG. 28(a) Distance-height sections through the main storm at right angles to its direction of movement, applicable to the period 1137-1149 during the development of the new organisation. These are derived from Fig. 27(a). The contours represent the extent of intensity (17) at distances of 6 (thickest line), 4, 2, 0 and -2 (thinnest line) miles ahead of the wall. The vertical hatching, stippling, and horizontal hatching indicate the extent of intensity (39) at distances ahead of the wall of 2, 0, and -2 miles respectively. Sections at greater distances behind the wall are not shown because attenuation makes their interpretation difficult.

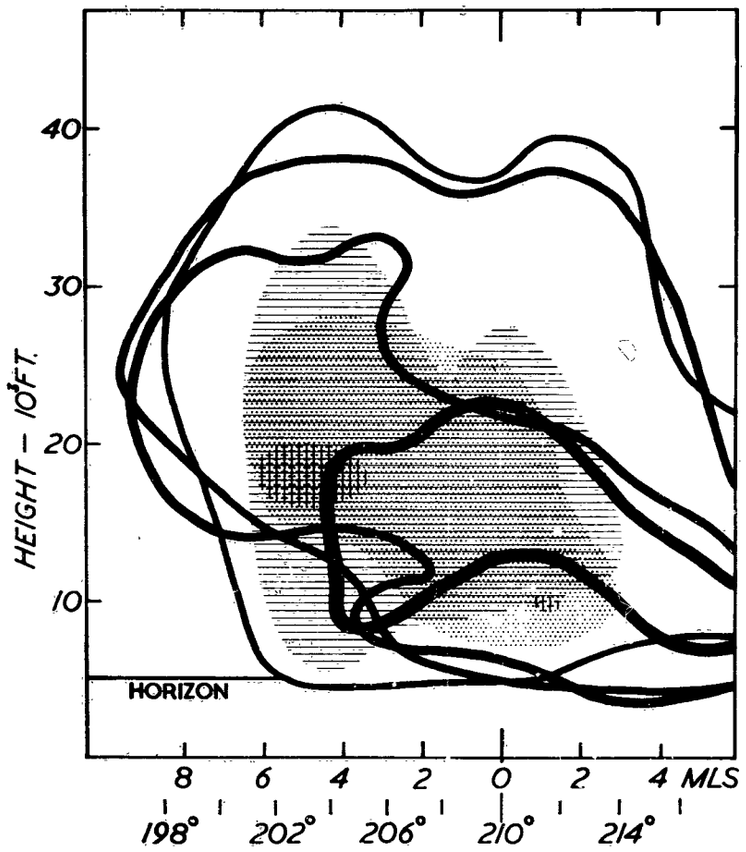

FIG. 28(c) Distance-height sections through the main storm at right angles to its direction of movement, applicable to the period 1213-1225. These are derived from Fig. 27(c). The contours represent the extent of intensity (26) at distances of 8 (thickest contour), 5, 2, and -1 (thinnest contour) miles ahead of the wall. The vertical hatching, stippling, and horizontal hatching indicate the extent of intensity (46) at distances ahead of the wall of 5, 2, and -1 miles respectively. Sections at greater distances behind the wall are not shown because they are distorted by the effect of attenuation.

This diagram shows the forward overhang just before it collapsed.

Figs. 28(a & c)

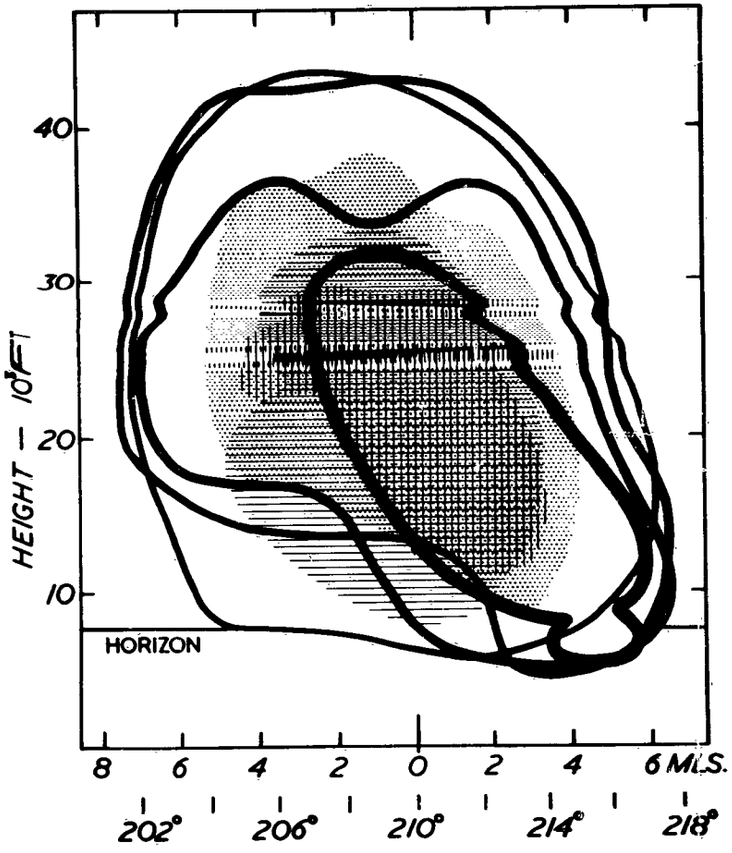

FIG. 28(b) Distance-height sections through the main storm at right angles to its direction of movement, applicable to the period 1156-1208. These are derived from Fig. 27(b). The contours represent the extent of intensity (29) at distances of 4½ (thickest contour), 2½, ½ and -1½ (thinnest contour) miles ahead of the wall. The vertical hatching, stippling, and horizontal hatching indicate the extent of intensity (49) at distances ahead of the wall of 2½, ½ and -1½ miles respectively. Sections at greater distances behind the wall are not shown because they are distorted by attenuation.

This diagram clearly shows the considerable horizontal extent of the forward overhang; it also shows that on the left front of the storm (right of diagram) precipitation was falling below the radar horizon (and presumably reaching the ground) more than 4 miles ahead of the wall.

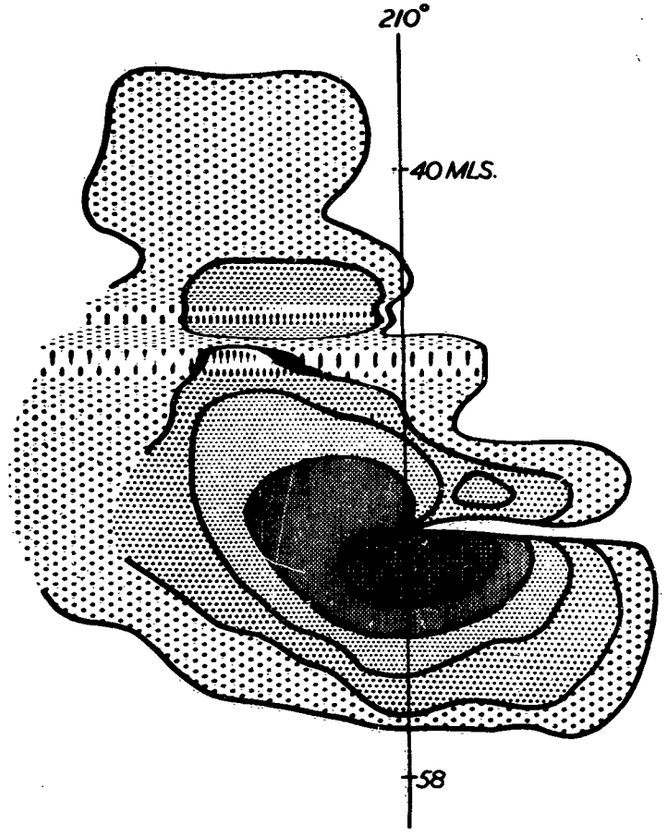

FIG. 28(d) Intensity contours in a nearly horizontal section through the storm at 13,500 ft (at 55 miles range) derived from the 4.7 cm radar data. Contours are for intensities (16), (29), (38), (49), and (58) (strictly, only at 55 miles range). Corrections for beam-width have not been applied to these values. This diagram demonstrates the extent of the wall and the echo-free vault (which appears as an echo-free notch in this presentation). The echo just ahead of the echo-free vault lies in the lower part of the forward overhang.

Figs. 28(b & d)

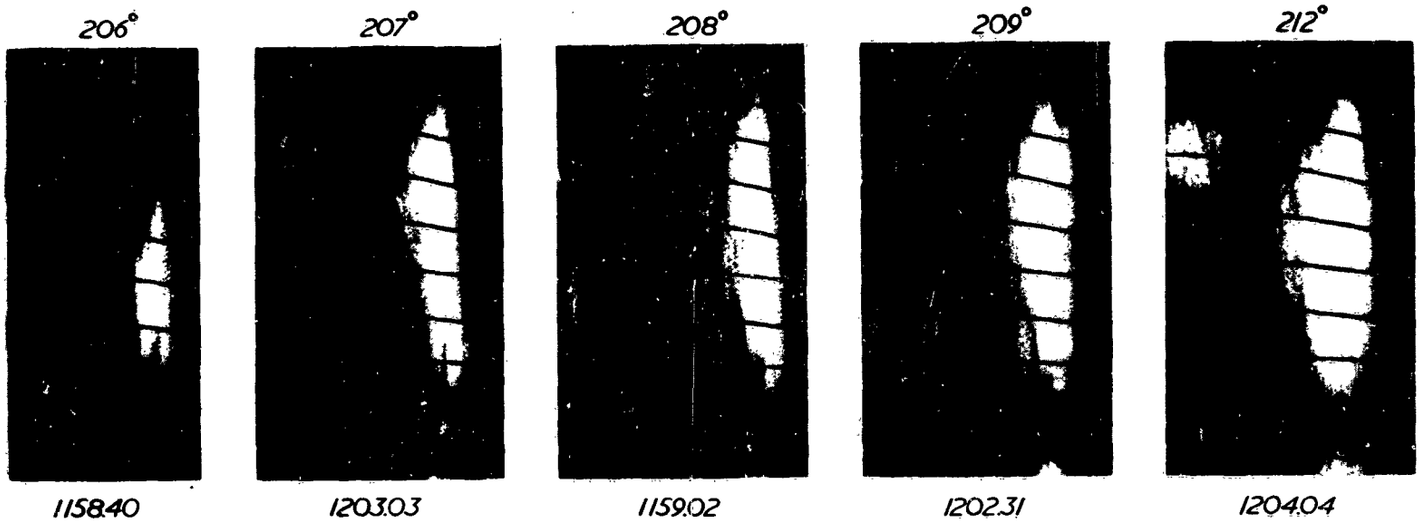

FIG. 29 Full-gain 3.3 cm RHI photographs of different sections through the main storm during the period to which Figs. 27(b) and 28(b) are applicable. Note the presence of the characteristic features of the new organisation - the forward overhang, and the wall with the highest top practically vertically above it (in the first 4 photographs), the echo-free vault (in the first two photographs), and the broader extent of the low-level echo on the left flank where precipitation reached the ground ahead of the wall (last photograph). The top in the centre photograph is practically at 45,000 ft and was the highest observed during the day.

Height markers are at intervals of 5,000 ft, and range markers at intervals of 10 miles. The radar horizon ($1\frac{1}{4}^{0}$) is indicated in each photograph.

Fig. 30(a)

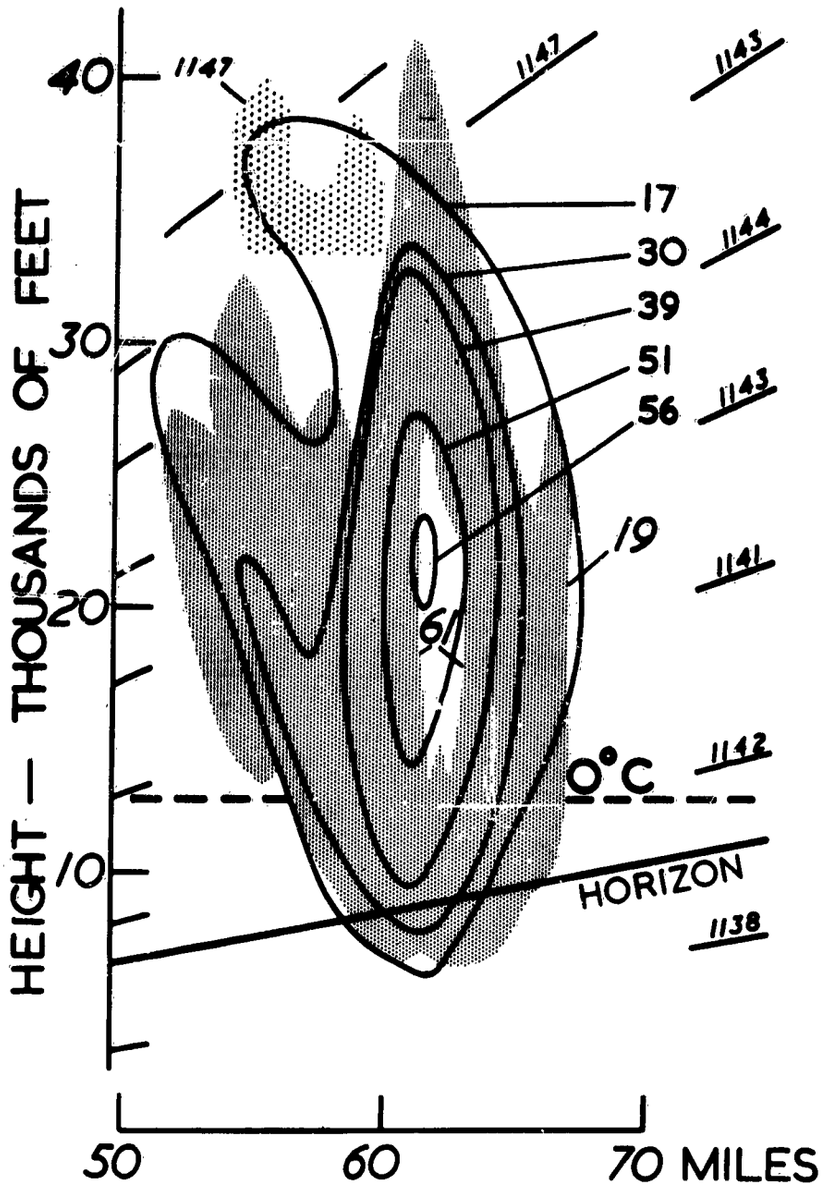

FIG. 30(a) Range-height sections through the main storm along azimuth 212°. The closely-stippled area denotes the region occupied by full-gain 3.3 cm echo at 1142.54: in the unshaded region inside it the intensity exceeds 61 according to a photograph at reduced gain at 1142.45. The contours represent the intensity distribution in the corresponding vertical section derived from the 4.7 cm data for the period 1137 to 1149. Corrections for beam-width have not been applied to these values. (This section has been displaced in range at 40 mi/hr along 210° in order that it should be comparable with the 3.3 cm pictures at 1143. The less densely stippled area represents the position of the full-gain 3.3 cm echo from the same column top 4 minutes later at 1146.50, and explains the distortion in the outer 4.7 cm contour.)

Fig. 30(b)

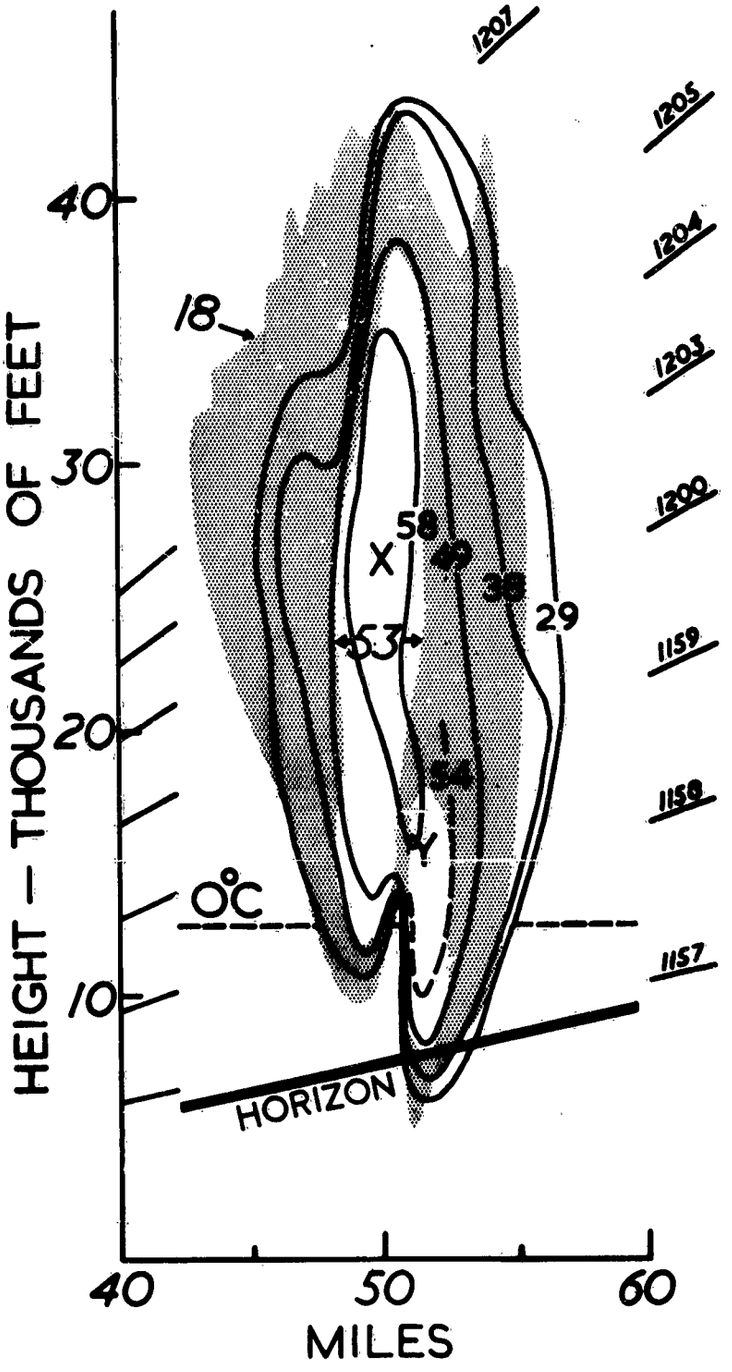

FIG. 30(b) Range-height sections through the main storm along azimuth 209°. The stippled area denotes the region occupied by full-gain 3.3 cm echo at 1202.31: in the unshaded regions in its interior the intensity exceeds 53, according to a photograph on reduced gain at 1203.40. The contours represent the intensity distribution in the corresponding vertical section derived from the 4.7 cm data for the period 1156-1208. Corrections for beam-width have not been applied to these values. (All three sections have been displaced in range at 40 mi/hr along 210° to make them applicable to the time 1203).

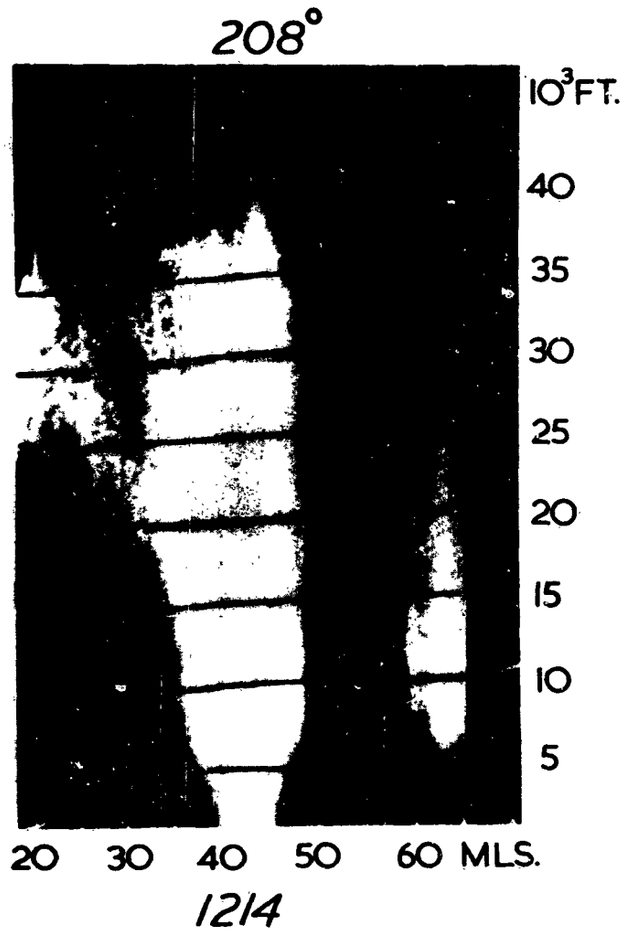

FIG. 31 10 cm RHI photograph showing the uprightness of the rear of the main storm. Storm 2 can be seen behind the main storm; it is comparatively small.

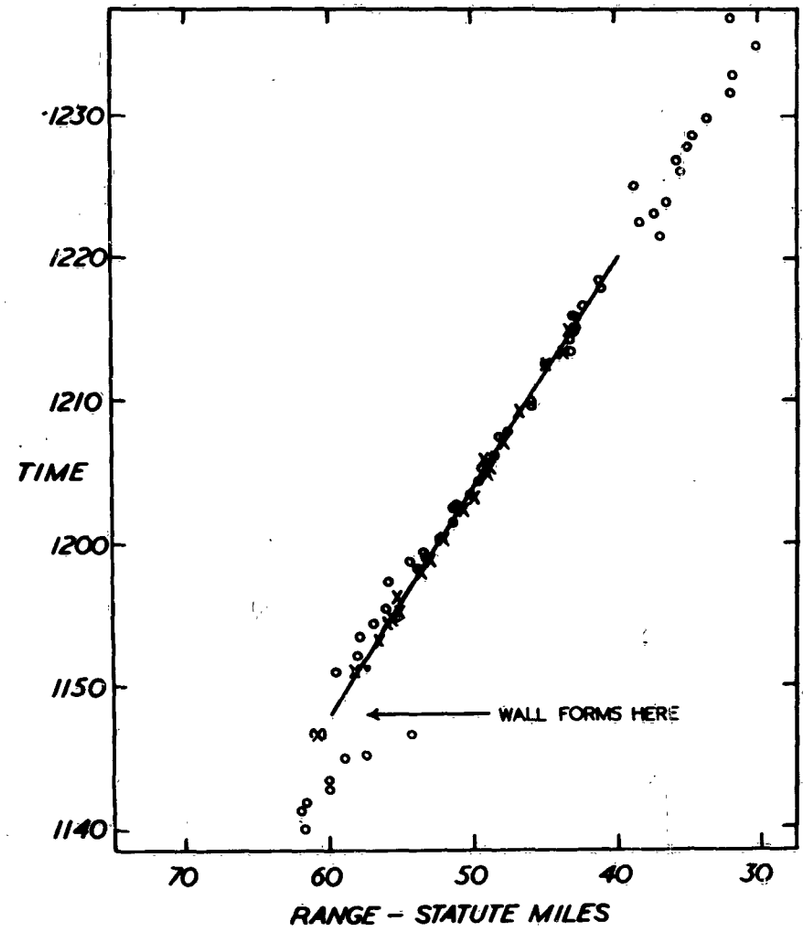

FIG. 32 The crosses (through which the straight line is drawn) represent the range of the wall as observed by the 3.3 cm radars. The circles represent the range of the highest top on each 3.3 cm photograph of the main storm. Notice that the highest tops were found vertically above the wall (within 1½ miles), but that before the formation of the wall and after its collapse their range was more variable.

Figs. 31 & 32

Fig. 33

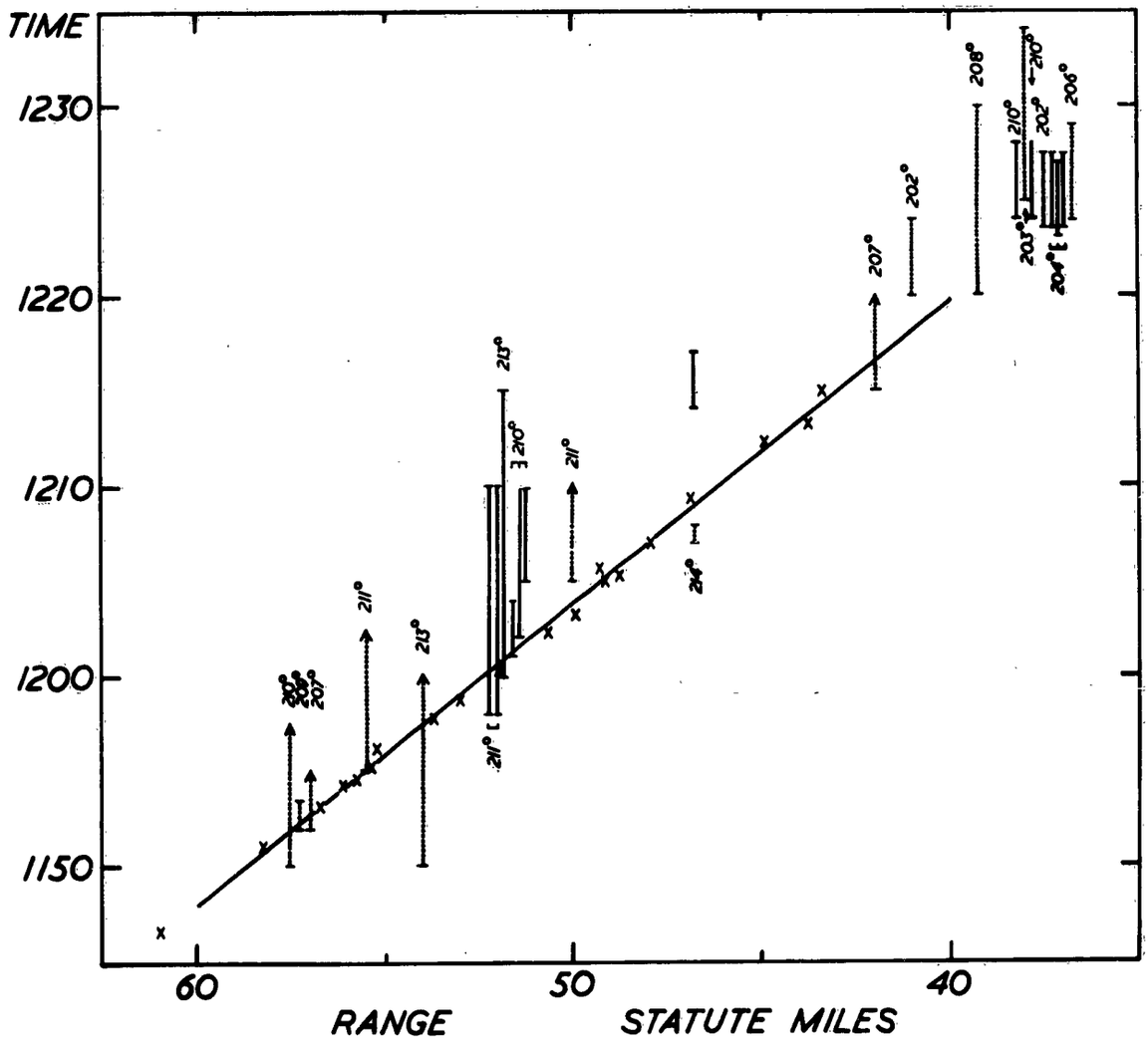

FIG. 33 Times of occurrence of hail and arrival of the wall. Crosses denote the position of the wall as ascertained from 3.3 cm RHI photographs. Vertical lines represent the period during which hail fell at the azimuths indicated: continuous or dotted lines are drawn according to whether the observations are accurate to within 1 min or 3 min. It can be seen that, except on the left flank of the storm (towards higher azimuths), the onset of the hail coincides within 2 or 3 min with the arrival of the wall.

Fig. 34

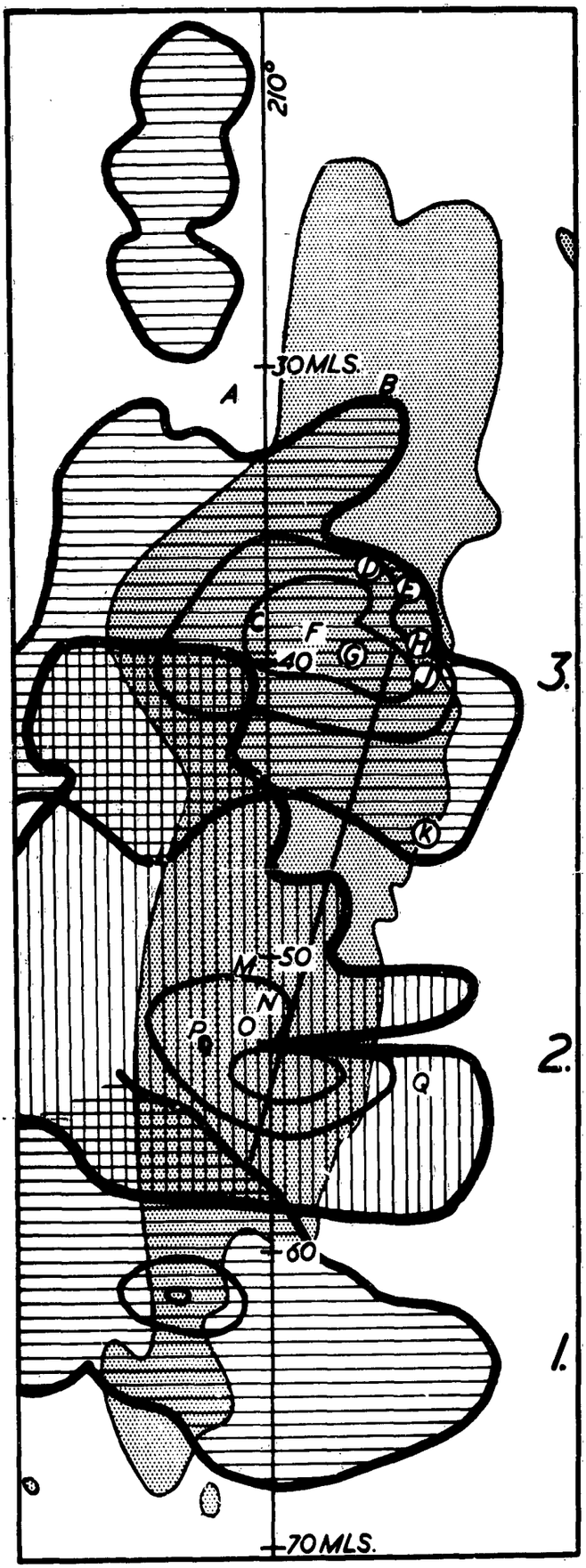

FIG. 34

The position of the ground observations (represented by letters and listed in Appendix 5) and of hail exceeding size 2 ($\geq \frac{1}{4}$ in) (denoted by stippled shading) with respect to the radar echo.

Three intensity contours of the 4.7 cm PPI radar echo at about the 14,000 ft level are shown for each of the three times 1141, 1158 and 1218

1. At 1141 contours indicate intensities of (17), (52) and (56) respectively (strictly only at 62 miles range)
2. At 1158 contours indicate intensities of (16), (50) and (55) respectively (strictly only at 55 miles range)
3. At 1218 contours indicate intensities of (27), (48) and (56) respectively (strictly only at 40 miles range)

Corrections for beam-width have not been applied to these values.

The straight line along the direction 225^0 - 045^0 represents the locus of the position to the left of which the tip of the (28) intensity contour of the forward overhang had dropped below 10,000ft, and can be regarded as the line followed by the left-hand end of the wall.

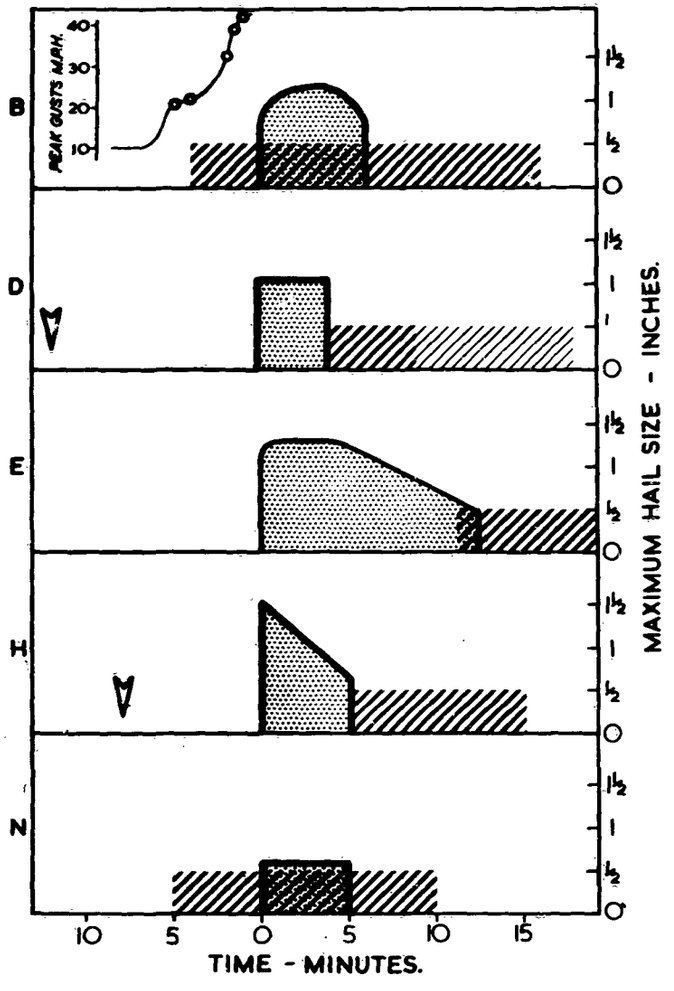

FIG. 35 Simplified representation of five of the more comprehensive ground observations, showing rainfall (diagonal hatching) maximum hail size (stippled shading) and (where reported) the passage of the nose of the gust front as a function of time from the onset of the hail.

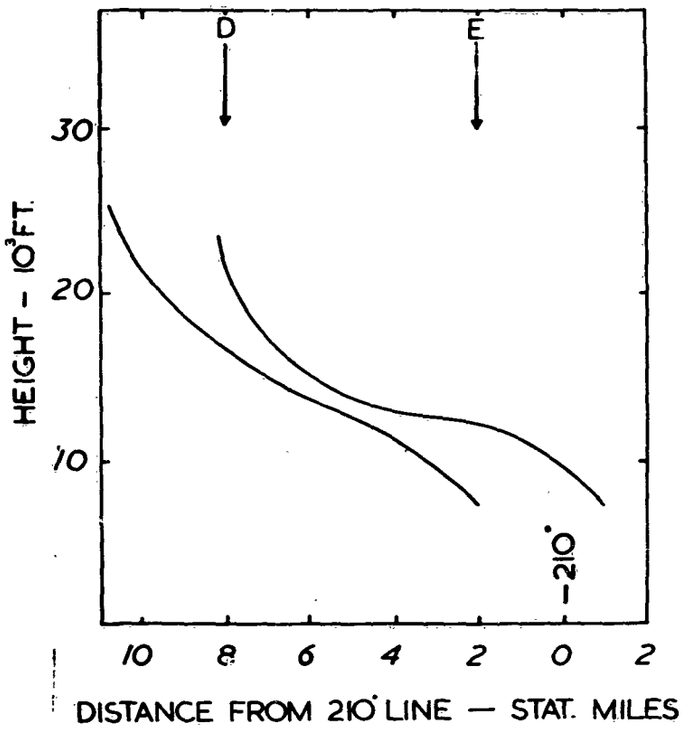

FIG. 36 Height of the lowest part of the forward overhang for which the intensity exceeded (28), as a function of distance from the 210° line at approximately 1158 (upper line) and 1218 (lower line).

Figs. 35 & 36

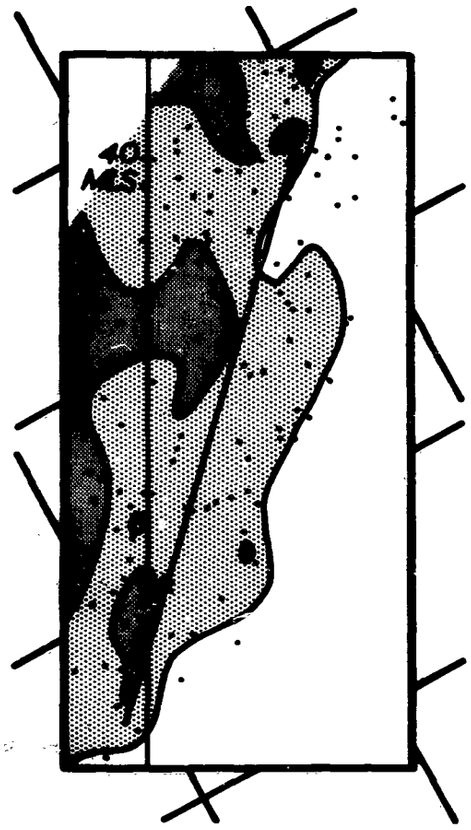

FIG. 37(a)

Duration of hail in the main storm during its intense phase. Areas shaded lightly had 5 min or more of hail; areas shaded heavily had 15 min or more of hail. The positions of the individual observations are also indicated. The straight line along the direction 225° - 045° represents the locus of the position to the left of which the (28) intensity contour within the forward overhang had dropped below 10,000 ft, and can be regarded as the path of the left-hand end of the wall.

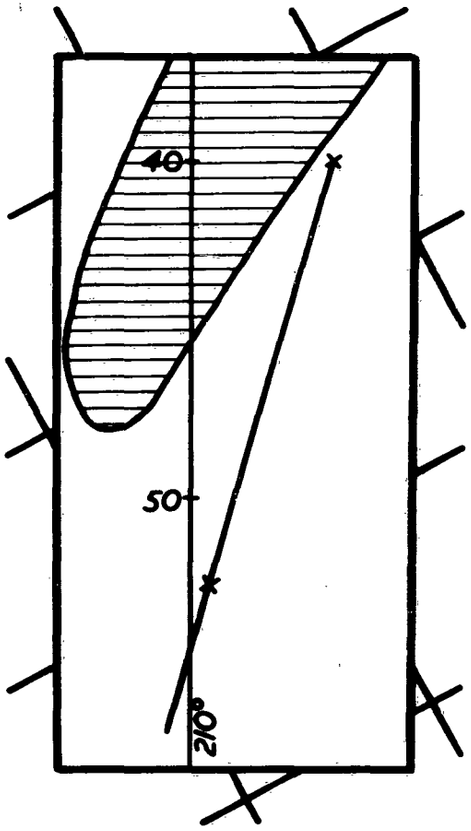

FIG. 37(b)

More than ½ in of rain fell in the shaded area, which lies entirely to the left of the line along which the (28) intensity contour within the forward overhang had fallen to below 10,000 ft.

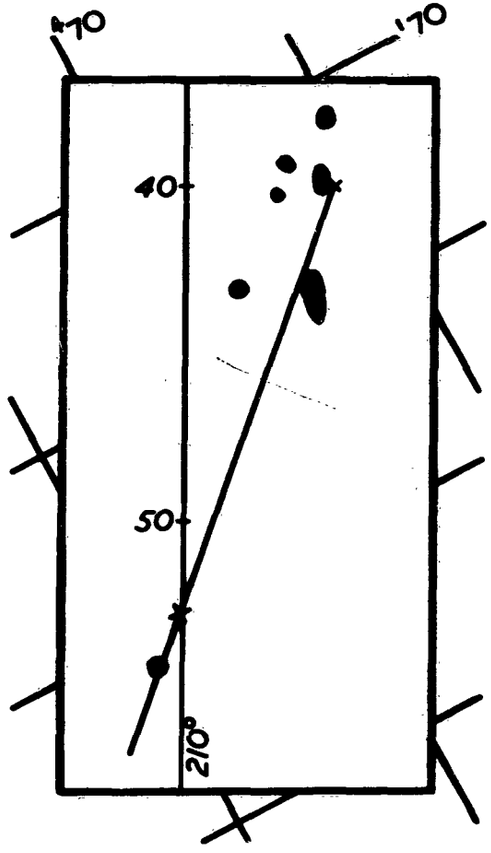

FIG. 37(c)

Areas experiencing giant hail. These are all within 2 miles of the position to the left of which the top of the echo-free vault was below 10,000ft.

Fig. 37(a, b & c)

Figs. 38 & 39

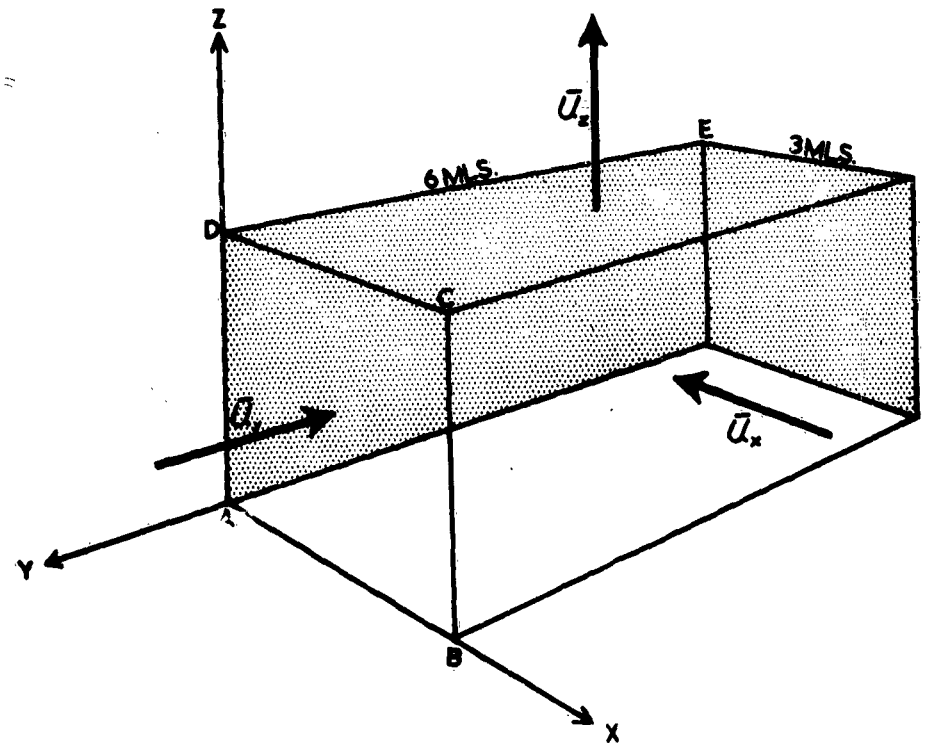

FIG. 38 Idealized representation of the volume beneath the forward overhang. The two shaded sides of the rectangular box represent the edges of the down-draught regions.

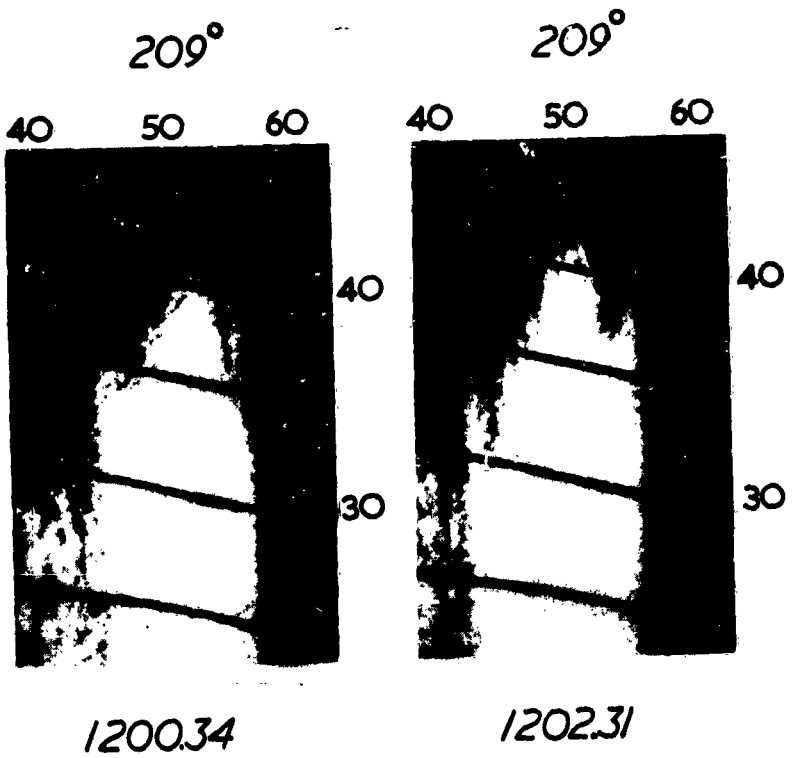

FIG. 39 Full-gain 3.3 cm RHI photographs along 209° at 1200.34 and 1202.31 to show a top at range 55 miles moving with a component velocity along this azimuth of only 15 mi/hr.

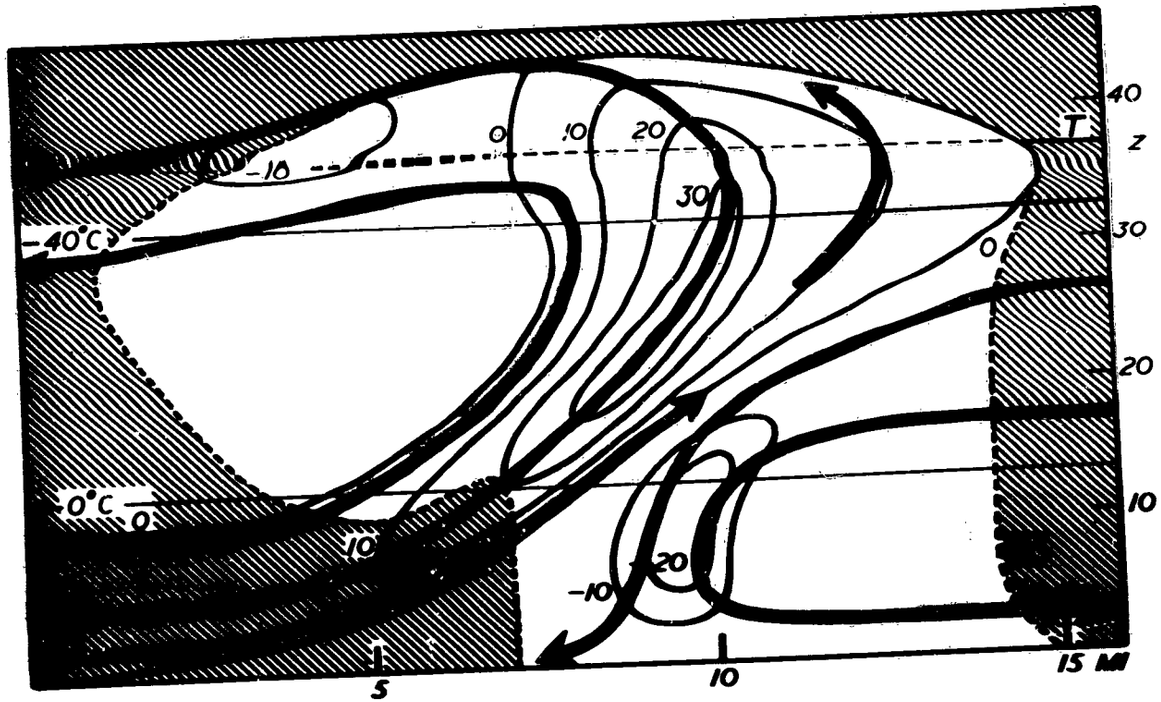

FIG. 40 Tentatively inferred streamlines and isopleths of vertical velocity (labelled in m/sec) within a range-height section along the direction of movement of the storm and intersecting the wall and forward overhang. Height Z is indicated in thousands of feet and range in miles. The unshaded area shows where the radar echo intensity exceeds about (30) (after rough correction for attenuation). The tropopause T is at 37,000 ft.

Fig. 40

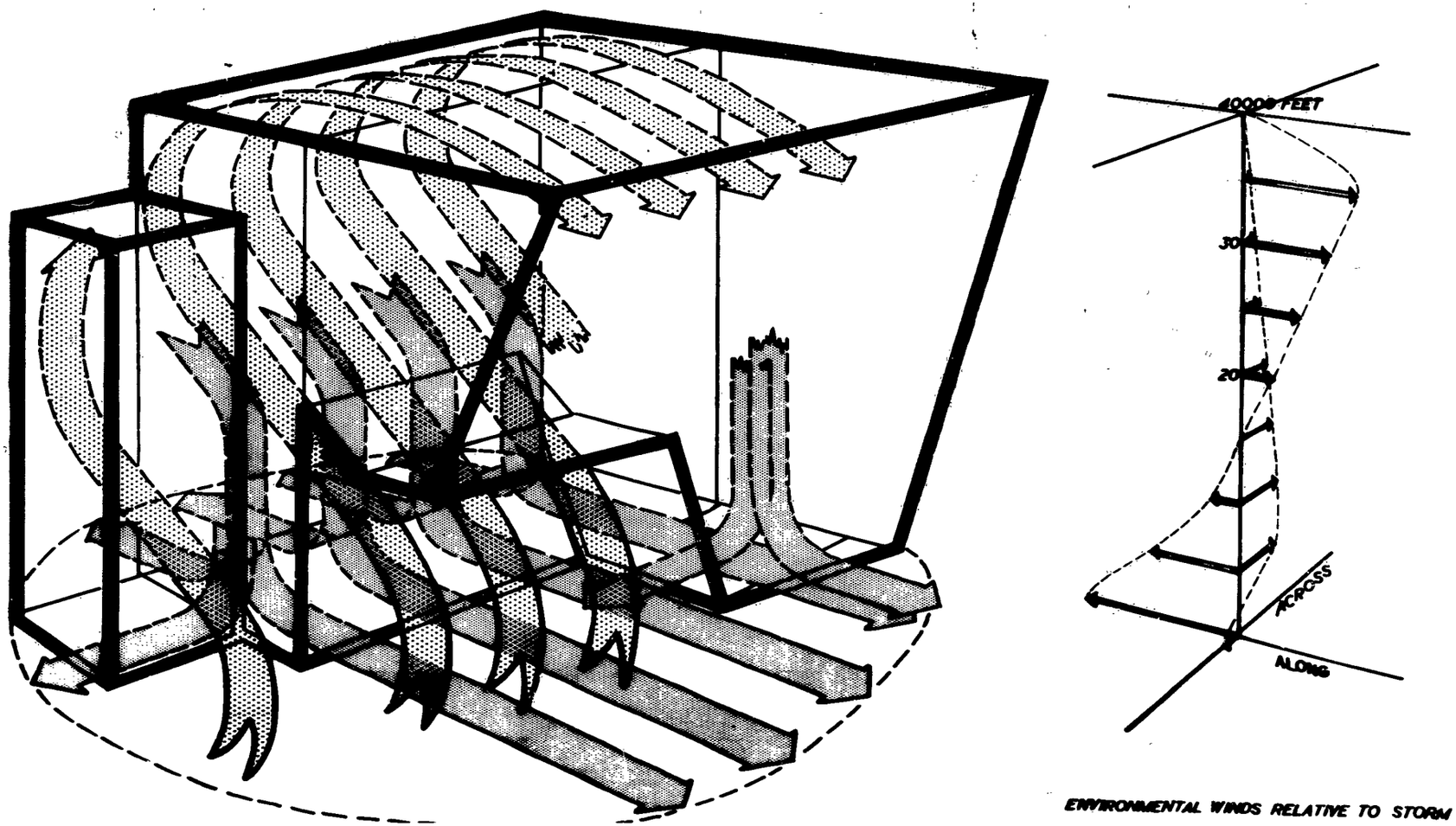

FIG. 41 Schematic three-dimensional model of the main storm during its intense phase, showing the approximate extent of echo of intensity exceeding 30 and the arrangement of the updraught and downdraughts.

Figs. 42, 43(a & b)

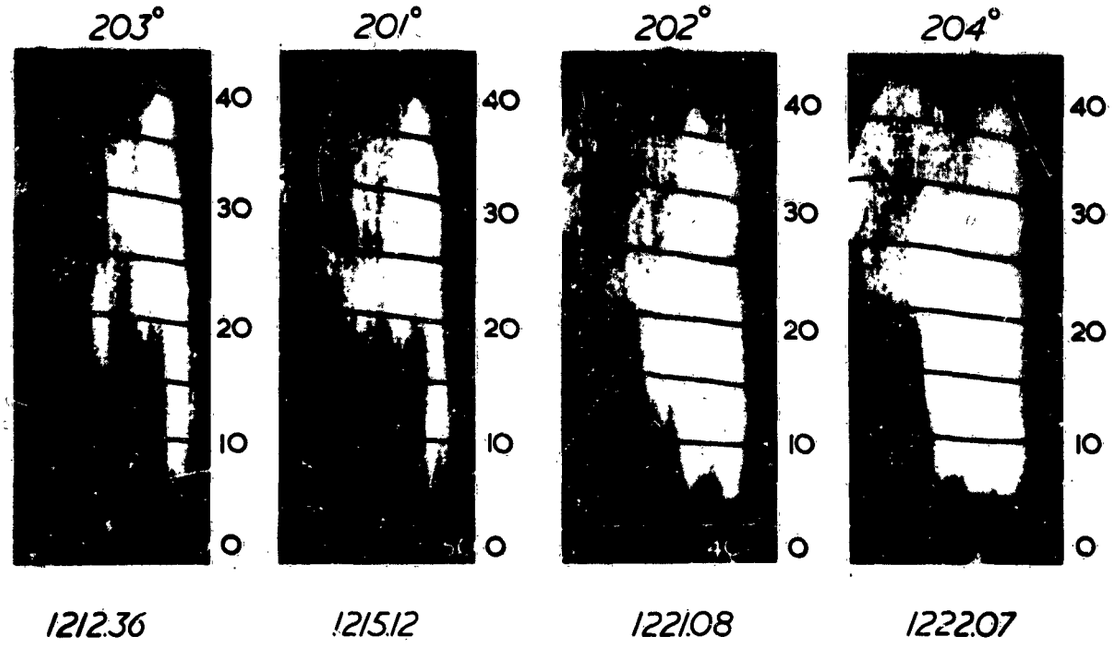

FIG. 42 Full-gain 3.3 cm RHI photographs just before and just after the bottom of the overhang dropped to the ground, in association with a 15 min fall of large hail in the Wokingham area. (See observation E in Figs. 34 and 35, and Appendix 5)

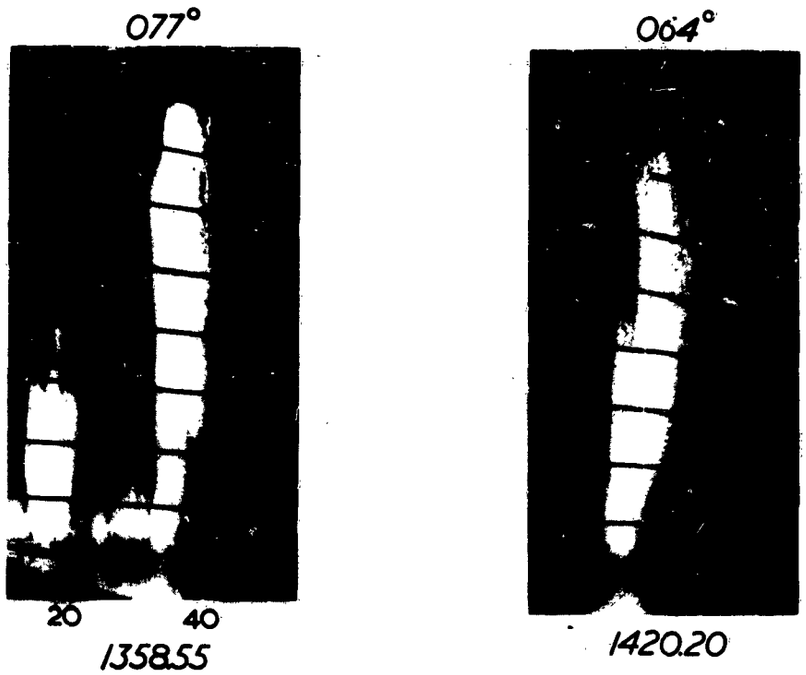

FIGS. 43 (a) and (b) Full-gain 3.3 cm RHI photographs showing (a) the characteristic forward overhang, echo-free vault, and wall with the highest top vertically above it, after the re-organisation of the storm; (b) the different appearance, with separate rising tops at the rear, during the final decline of the storm.

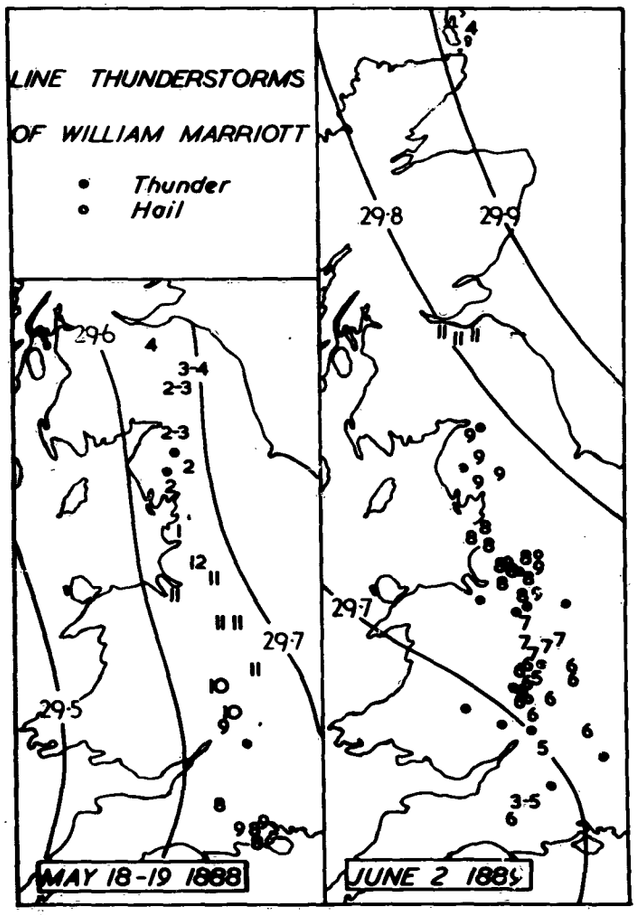

FIG. 44 Examples of the "line thunderstorms" of Marriott; the lines are sea-level isobars and the numbers show the last figure of the clock hour nearest to the time of the thunderstorm, according to the reports of voluntary observers.

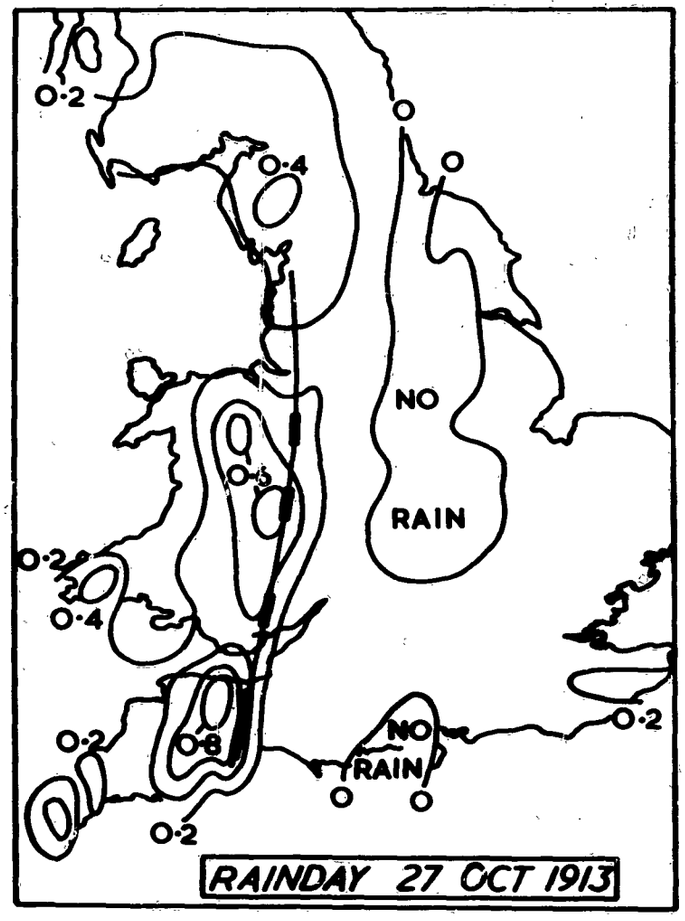

FIG. 45 24-hour rainfall on the occasion of the South Wales tornado, 27 October 1913. Isopleths are drawn at intervals of 0.2 inch and show that the principal falls characteristically occurred a little to the left of the line showing the path along which the storm was most severe. This line is thickened where tornadoes occurred, and also over Devon, where the storm was also particularly intense (adapted from Geophysical Memoir No. 11, Meteorological Office, London, 1914).

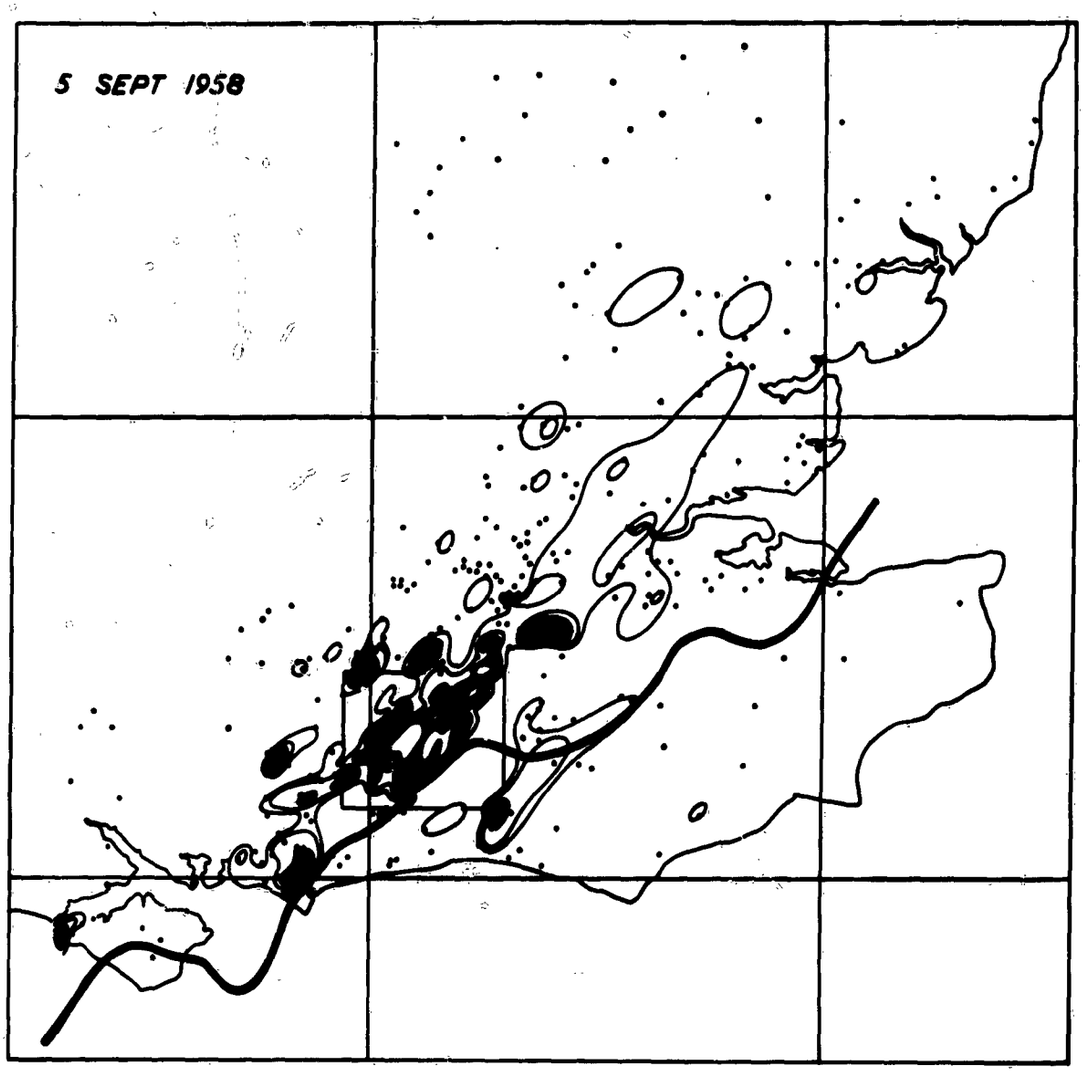

FIG. 46 Distribution of maximum hailstone size, storm of 5 September 1958. The isopleths are for stones of sizes 2, 4, 6, and 10, (the area between the latter two is shown in black: for scale see table 2).

The positions of the observations are shown by black dots: there are altogether 552, of which 299 lie within the small rectangle surrounding the most severely affected area.

The thick line is the locus of the right flank of the storm echo.

Fig. 1
Appendix 4

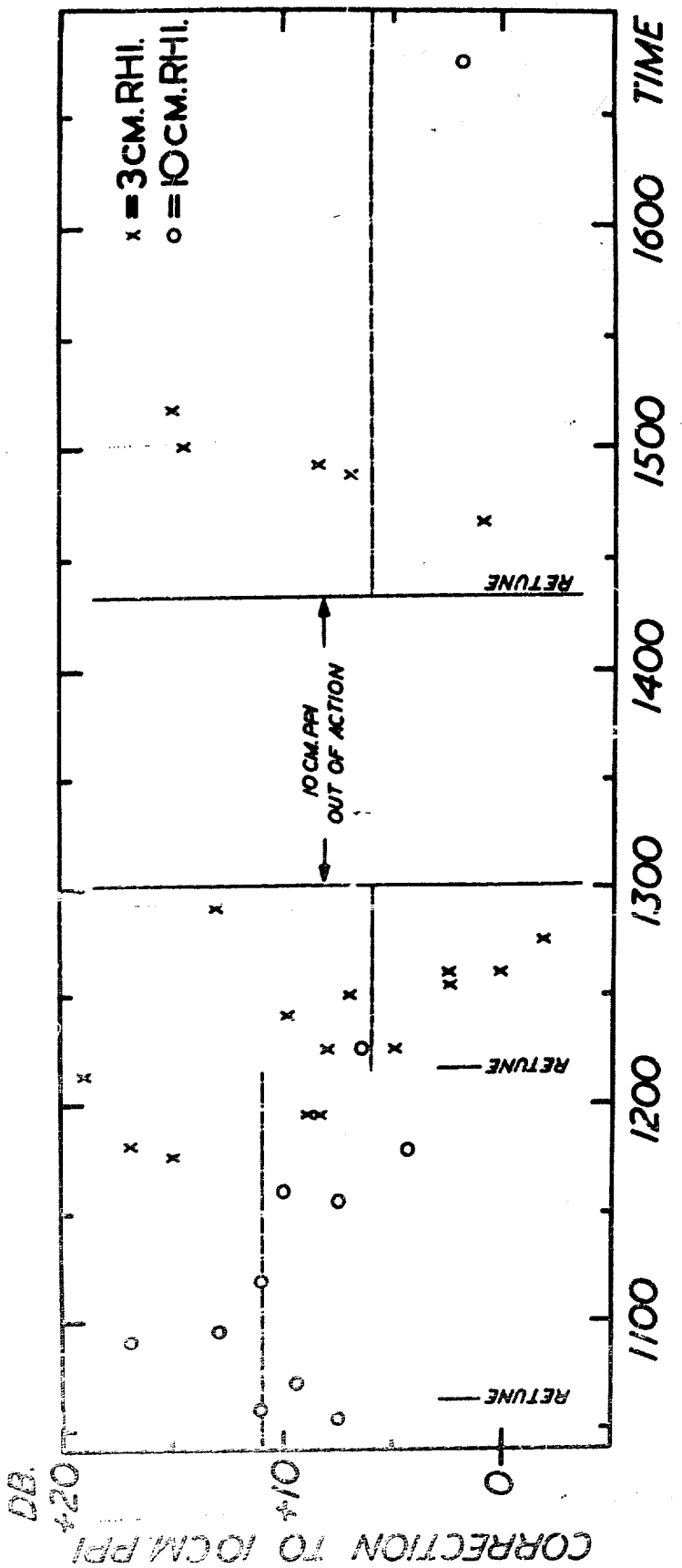

FIG. 1
Appendix 4

Corrections to 10 cm PPI intensity values to make them consistent with the intensity measurements of the other radars. Crosses and circles represent the number of db by which the intensity measurement made on a particular echo by the 10 cm PPI radar was less than that made on the same echo within 3 minutes by the 3.3 and 10 cm RHI radars respectively, after beam-width corrections had been applied. The horizontal dashed lines passing through the widely scattered points indicate the corrections which have been adopted.